Title

Haptic Feedback as an Information Channel Across Assistive and Robotic Systems

ISBN

9798191654188

Author

Hong, Kihun

Publication Date

2026-03-23

Peer reviewed|Thesis/dissertation

Haptic Feedback as an Information Channel Across Assistive and Robotic Systems

By

Kihun Hong
DISSERTATION

Submitted in partial satisfaction of the requirements for the degree of

DOCTOR OF PHILOSOPHY

in

Mechanical and Aerospace Engineering

in the

OFFICE OF GRADUATE STUDIES

of the

UNIVERSITY OF CALIFORNIA

DAVIS

Approved:

Jonathon S. Schofield, Chair

Wilsaan M. Joiner

Stephen K. Robinson

Committee in Charge

2026

Abstract

Human movements and perception of self-generated actions require the integration of multisensory information with motor commands to guide predictive control and error correction. Among the sensory channels that support movement, vision and haptics play distinct yet complementary roles. Vision provides broad spatial context and predictive information for planning and monitoring action, while haptic signals including tactile sensation and proprioception provide near-immediate, localized feedback about contact with external objects and body configuration. This integration is flexible and supports robust performance in the face of uncertainty: when one sensory modality becomes unreliable or unavailable, the nervous system can shift reliance toward alternative signals to better support state estimation and movement correction to maintain effective control under changing sensory conditions. As sensory information becomes more informative or reliable, control can also shift from deliberate, high-cognitive load control to fluent, largely automatic performance as learning strengthens internal models and improves predictive control. However, it remains unclear how multisensory integration supports the perception of one's action when sensory information is altered, reduced, or re-encoded through sensory substitution or augmentation, both in everyday human behavior and during interaction with robotic systems.

This dissertation examines how visual and haptic information jointly shape human motor control, and how these processes extend to interactions with assistive and robotic systems. It begins with an examination of how sensory feedback, when coupled with motor actions, influences perceptual integration and embodiment, such that a robotic prosthetic hand and its actions are experiences as part of the user's own body (**Chapter 2**). This chapter demonstrates that the degree to which an upper limb prosthesis is experienced as part of the body depends on sensorimotor contingencies, showing how changes in sensory feedback and action consequences reshape body representation and embodiment.

Next, this dissertation tactile snesory substitution for navigation (**Chapter 3**). This chapter shows how tactile cues can deliver spatial information when vision is reduced or absent, and it explains how this information is used to construct understanding while moving through an environment. Following this, multisensory integration through sensory substitution or augmentation extends to multi-limb coordination, a core for seamless interaction with external control systems (**Chapter 4**). Upon investigation, participants can adapt to extracting relevant patterns from haptic feedback, integrating them with vision, and progressively reducing reliance on visual monitoring while maintaining stable and effective motor performance.

Finally, teleoperated robotic control places perception and action under constrained and indirect feedback, where operators often rely heavily on vision to infer the remote task state and predict the consequences of their actions (**Chapter 5**). This chapter introduces a wearable haptic interface that conveys task relevant robotic information, and provides a foundational work that adding haptic feedback redistribute information away from vision, shape control strategies, and support skill acquisition during teleoperation.

Across these studies, the dissertation positions various forms of haptic feedback as complementary information channels that can be added to, or substituted for, vision. This dissertation shows how humans integrate augmentative haptic information with visions and motor commands to support bodily self-representation, understanding of the surrounding environment, and coordinated movement when interacting with external systems (***from the self to external systems***). Together, these findings bridge fundamental understanding of multisensory integration and motor control and clarify how augmentative haptic feedback can be structured usability, learning, and reliable performance in assistive and teleoperated robots.

Preface

The research presented within this dissertation is an original work by Kihun Hong, conducted within the Bionic Engineering and Assistive Robotics Laboratory at the University of California, Davis.

All data collection methods and study procedure performed on the participants herein received approval from University of California Davis Research Ethics Board. Written informed consent and assent were obtained from all participants and legal guardians.

This research was primarily supervised by Dr. Jonathon S. Schofield in collaboration with Dr. Wilsaan M. Joiner, Dr. Stephen K. Robinson, and Dr. Iman Soltani from the University of California, Davis. Additionally, this reserach received support from the National Science Foundation under award number 1934792 and the National Aeronautics and Space Administration under grant number 80NSSC21K1373.

The majority of Chapter 2 has been published and submitted as:

Hong, K., Trieu, P. H. D., & Schofield, J. S. (2023, August). Characterizing the sense of embodiment: the development of a sensorimotor robotic platform. In 2023 32nd IEEE International Conference on Robot and Human Interactive Communication (RO-MAN) (pp. 191-196). IEEE.

Hong, K., Gavrilov, M. G., Trieu, P. H. D., Waraich, S. A., Marasco, P. D., Weir, R. F., ... & Schofield, J. S. (In review 2026, March). Quantifying Prosthetic Embodiment: Interactions Between Agency, Ownership, and Peripersonal Space in a Closed-Loop Sensorimotor Task. In Journal of NeuroEngineering and Rehabilitation.

Contributions as the first author: Conducted the literature search, led manuscript writing and organization, synthesized data, generated figures and tables, authored draft manuscript, and performed revisions during peer review.

The majority of Chapter 3 has been in preparation for submission as:

Hong, K., I. Soltani Bozchalooi, & Schofield, J. S. (In preparation 2026, April). Tactile sensory substitution for path guidance and spatial localization across visual experience. Scientific Reports.

Contributions as the first author: Designed and fabricated the device, developed the experimental protocol, conducted data collection and analysis, generated figures and tables, led the writing and organization of the draft manuscript.

The majority of Chapter 4 has been published as:

Hong, K., Kanapskyte, A., Gowda, H. T., Joiner, W. M., Miller, L. M., Robinson, S. K., ... & Schofield, J. S. (2024, July). The Influence of Haptic Feedback and Visual Information on Multi-Limb Coordination. In 2024 16th International Conference on Human System Interaction (HSI) (pp. 1-6). IEEE.

Hong, K., Kanapskyte, A., Gowda, H. T., Joiner, W. M., Miller, L. M., Robinson, S. K., ... & Schofield, J. S. (Accepted 2026, February). From Sight to Touch: Haptic Sensory Substitution Can Facilitate Multi-Limb Coordination. In IEEE Transactions on Haptics (ToH).

Contributions as the first author: Designed experimental protocol, performed data collection and analysis, generated figures and tables, led the writing and organization of the draft manuscript, and performed revisions during peer review.

The majority of Chapter 5 has been published and submitted as:

Hong, K., Zhang, R., Lee, K. G., Young, P. R., Joiner, W. M., Robinson, S. K., ... & Schofield, J. S. (2024, October). A wearable haptic sleeve interface for spaceflight robotic arm operations. In Companion of the 2024 on ACM International Joint Conference on Pervasive and Ubiquitous Computing (pp. 318-322).

Hong, K., Syeda, Y. Z., Jeshurun, L., Brian, H., Weiwei, Z., Joiner, W. M., Robinson, S. K., ... & Schofield, J. S. (Submitted 2026, March). Effect of haptic feedback on skill learning and visual dependence for a robotic teleoperation. In IEEE International Conference on Robot and Human Interactive Communication (RO-MAN).

Contributions as the first author: Designed and fabricated the device, developed the experimental protocol, conducted data collection and analysis, generated figures and tables, led the writing and organization of the draft manuscript.

Acknowledgments

I would like to express my sincere gratitude to my advisors—Jonathon Schofield, Stephen Robinson, and Wilsaan Joiner. Each of you has been instrumental in my development as a young academic, offering unique perspectives and helping me cultivate a strong multidisciplinary foundation. I am especially grateful to my primary advisor, Jonathon Schofield, whose unwavering support has been invaluable throughout my journey toward becoming an independent researcher. I deeply appreciate how carefully you have listened to me, even when my thoughts were not yet fully formed, and the care you took to understand what I was trying to express. I am also thankful for your guidance early in my graduate career, when I needed it most. Reflecting on the time, care, and trust you invested in my growth has been deeply meaningful, and it has profoundly shaped me as a researcher. My graduate experience would not have been possible without you. Thank you for helping me turn my ideas into clear words and for encouraging me at every step. You are an exceptional advisor and mentor, and I could not have asked for a better one. I appreciate my lab mates for making a supportive and welcoming lab environment. I would like to acknowledge Peyton Young for helping me improve my English and feel more settled here, which has greatly shaped my graduate experience. I also thank Ada Kanapskyte for her dedication and patience while working on our project. I truly appreciated her thoughtful collaboration and the care she brought to our discussions and experiments. A big thanks to all the participants without whom this work would not be possible. I want to express my heartfelt thanks to my parents for their unconditional love and support. Without them, this dream would not have been possible. I am especially thankful that they have always believed in me and respected who I am, which gave me the confidence to pursue my goals. I would also like to express my love and appreciation to my niece, Leah, whose presence has been a quiet source of joy and motivation throughout this journey. Additionally, I sincerely thank my sister and brother-in-law for their constant support and encouragement throughout this journey. Finally, I would like to express my heartfelt thanks to my girlfriend, Heejee, for her unconditional support. Thank you for patiently standing by me through the final steps of graduate school. I am especially grateful for your understanding during the busiest times and for always being there for me. Without your love, encouragement, and patience, I could not have made it to this point. Although I have not listed individual names here, I would like to sincerely thank everyone who contributed to and supported this work.

Contents

List of Figures

List of Tables

Chapter 1 Introduction

1.1 Background

Human perception and action fundamentally rely on the brain's ability to integrate information from multiple sensory channels. In everyday behavior, humans continuously combine multiple sources of sensory information with motor commands to navigate space, manipulate tools, and coordinate complex movements. Within this frame, vision and haptics, including proprioception, play distinct yet complementary roles. Vision provides rich spatial and contextual information, allowing humans to anticipate movement outcomes and maintain precise control [**1**], [**2**], while haptic cues deliver immediate, localized information regarding contact, texture, force, and body configuration that is essential for refining movement in real time [**3**], [**4**].

Haptic definition: Specialized mechanoreceptors in the skin detect a variety of information that collectively contribute to somatosensation, the perception of touch (tactile sensation), as well as temperature, proprioception, and pain [**4**], [**3**]. Proprioception shapes our awareness of the body's position and movement in space, incorporating information related to forces, torques, movements, positions, and orientations of our body parts. Whereas tactile sensations encompass a variety of sensory experiences involving the mechanical interactions between objects and our skin, such as pressure, shear, and vibration are sensed by specialized mechanoreceptors and thermoreceptors embedded in both hairy and hairless skin [**5**]. Together, these proprioceptive and tactile cues provide continuous feedback about body configuration and interactions with the environment that the brain uses to plan, guide, and refine movement.

In natural human motor control, the brain seamlessly integrates continuous sensory feedback to refine movement and interact with the environment [**6**], [**7**], [**8**]. When visual and haptic cues are congruent and timely, individuals can transition from deliberate, high cognitive-load processing to fluid, automatic control, a hallmark of mastering natural motor skills. Crucially, as control becomes more fluent, the kinematics and dynamics of movement are delegated to fast, largely preconscious sensorimotor processes [**9**]. This delegation of low-level control to fast, largely preconscious processes is a hallmark of skilled motor behavior and contributes to the sense that our limbs are "transparent" tools of action, supporting bodily self-perception and embodiment [**10**].

Despite this understanding in natural human behavior, significant gaps remain in how multisensory integration supports human behavior under altered sensory conditions and interactions in human-robot systems. In many real-world scenarios such as navigating environments, operating assistive devices, or controlling remote robotic systems, visual information may be limited, unreliable, or cognitively demanding. Although haptic feedback has been proposed as alternative or supplementary sources of information, it remains unclear how such feedback contributes to shaping the seamless interaction with assistive robotic systems, spatial understanding, and reduces dependency on visual information during complex tasks including robot teleoperation.

1.2 Objectives

This dissertation focuses primarily on elucidating how visual and haptic information shape human motor control, support spatial understanding, and how these processes extend to human-robot interactions. Thus, we investigate how multisensory integration supports fluent or adaptive control of both biological and artificial effectors.

Specifically, this work investigates how haptic feedback can be used to (1) support embodiment over non-biological limbs, (2) facilitate spatial understanding when vision is reduced or absent, (3) enable the coordination of multiple limbs under altered sensory conditions, and (4) reduce reliance on visual feedback during the learning of robotic teleoperation. By systematically examining these processes across increasingly complex interaction scenarios, this dissertation seeks to establish a holistic understanding of haptic feedback to enhance human capability in assistive and robotic systems.

1.3 Dissertation outline

This dissertation is organized to progressively examine multisensory integration across natural and human-robot contexts, moving from embodiment of artificial limbs to spatial navigation, multi-limb coordination, and robotic teleoperation. Each chapter builds on the previous ones to develop a cohesive understanding of how visual and haptic information shape perception - action coupling.

Chapter 2. Sensorimotor integration to shape embodiment over upper limb prostheses.

This chapter investigates how the integration of visual and haptic information supports the perceptual experience of owning and controlling an upper-limb prosthesis; that is, the sense of embodiment over a non-corporeal effector. Despite advances in prosthetic mechanics and control, many users still report that prosthetic devices feel like external tools rather than natural body parts, limiting long-term acceptance and functional benefit. A systematic methodology was developed to examine how changes in sensorimotor contingencies affect perceived embodiment. By leveraging this experimental paradigm, this chapter characterized a more complete understanding of the dynamic nature of the sense of embodiment under factors reflective of advanced upper-limb prosthetic use.

Chapter 3. Tactile and visual information to support spatial navigation.

Within this chapter, we recruited sighted individuals and individuals with visual impairments to explore how tactile information can support spatial understanding and navigation within an external environment. While tactile information has shown promise as substitutes for visual information to support independent navigation, it remains unclear how such cues can contribute to the construction of cognitive maps that support wayfinding and object localization, critical for independent navigation. This work marks a significant step toward a comprehensive understanding of how spatial representation can be shaped through touch sensation, providing foundational insights for the design of sensory substitution systems for navigation.

Chapter 4. Sensory substitution and augmentation to coordinate multiple limbs.

This chapter extends multisensory integration to tasks requiring the coordination of multiple limbs. By integrating multimodal (visual and haptic information) sensory information with motor outputs, the nervous system constructs internal models that support predictive and adaptive motor control. However, the extent to which haptic feedback can compensate for reduced visual information or unreliable visual information and how such compensation emerges through learning remains unclear. This chapter aims to provide a deeper understanding of how the integration of visual and haptic feedback adapts, and how this integration influences the coordination of multiple limbs, particularly under conditions of altered sensory availability, with implications for complex human-robot interaction tasks.

Chapter 5. Sensory substitution and augmentation for robotic teleoperation.

Although haptic feedback has been used to supplement visual information in teleoperated robotic systems, the coupling between multisensory perception (i.e., the integration of visual and haptic information) and motion execution remains poorly understood in human-robot systems mediated by teleoperation interfaces. Effective and natural motor behavior relies on the integration of sensorimotor information, yet it is still unclear how users' reliance on visual information evolves during skill acquisition when haptic feedback is introduced into teleoperation interfaces. Within this chapter, a haptic-enabled teleoperation framework is presented and examined through two tightly coupled studies. **First**, a wearable haptic interface was developed to convey task-relevant robotic information. The design of this interface focuses on delivering spatial and directional information in an interpretable and scalable manner, enabling users to perceive robotic state information. **Second**, the developed haptic interface was employed in a teleoperation training study to examine how haptic feedback influences learning progression, task performance, and users' reliance on visual information over time. This chapter provides a framework applied to a teleoperation task to assess the feasibility of integrating haptic feedback into training with emphasis on whether users can effectively utilize the feedback during task execution and adapt to the interface over practice.

Conclusions and future directions.

This chapter synthesizes the presented work and outlines future directions to enhance our understanding of multisensory integration across various applications.

References

[1] J. T. Fisher, J. R. Keene, R. Huskey, and R. Weber, “The limited capacity model of motivated mediated message processing: taking stock of the past,” *Annals of the International Communication Association*, vol. 42, no. 4, pp. 270–290, 2018.

[2] E. D. Ragan, D. A. Bowman, R. Kopper, C. Stinson, S. Scerbo, and R. P. McMahan, “Effects of field of view and visual complexity on virtual reality training effectiveness for a visual scanning task,” *IEEE Transactions on Visualization and Computer Graphics*, vol. 21, no. 7, pp. 794–807, 2015.

[3] H. Culbertson, S. B. Schorr, and A. M. Okamura, “Haptics: The present and future of artificial touch sensation,” *Annual Review of Control, Robotics, and Autonomous Systems*, vol. 1, no. 1, pp. 385–409, 2018.

[4] S. J. Lederman and R. L. Klatzky, “Haptic perception: A tutorial,” *Attention, Perception & Psychophysics*, vol. 71, no. 7, pp. 1439–1459, 2009.

[5] F. Iheanacho and A. R. Vellipuram, “Physiology, mechanoreceptors,” in *StatPearls*, StatPearls Publishing, 2019.

[6] G. Desmarais, M. Meade, T. Wells, and M. Nadeau, “Visuo-haptic integration in object identification using novel objects,” *Attention, Perception, & Psychophysics*, vol. 79, no. 8, pp. 2478–2498, 2017.

[7] T. L. Gibo, W. Mugge, and D. A. Abbink, “Trust in haptic assistance: weighting visual and haptic cues based on error history,” *Experimental Brain Research*, vol. 235, no. 8, pp. 2533–2546, 2017.

[8] C. Bozzacchi, R. Volcic, and F. Domini, “Grasping in absence of feedback: systematic biases endure extensive training,” *Experimental Brain Research*, vol. 234, no. 1, pp. 255–265, 2016.

[9] D. M. Wolpert, Z. Ghahramani, and M. I. Jordan, “An internal model for sensorimotor integration,” *Science*, vol. 269, no. 5232, pp. 1880–1882, 1995.

[10] U. Proske and S. C. Gandevia, “The proprioceptive senses: Their roles in signaling body shape, body position and movement, and muscle force,” *Physiological Reviews*, vol. 92, no. 4, pp. 1651–1697, 2012.

Chapter 2 Sensorimotor integration to shape embodiment over upper-limb prostheses

The majority of this chapter has been published and submitted as:

1. ***Hong, K.****, P. H. D. Trieu and J. S. Schofield, ”Characterizing the Sense of Embodiment: the Development of a Sensorimotor Robotic Platform,” 2023 32nd IEEE International Conference on Robot and Human Interactive Communication (RO-MAN), pp. 191-196.*

2. ***Hong, K.****, Gavrilov, M. G., Trieu, P. H. D., Waraich, S. A., Marasco, P. D., Weir, R. F., ... & Schofield, J. S. (In review 2026, March) Quantifying Prosthetic Embodiment: Interactions Between Agency, Ownership, and Peripersonal Space in a Closed-Loop Sensorimotor Task. In Journal of NeuroEngineering and Rehabilitation.*

2.1 Chapter preface

This chapter identifies critical gaps in our understanding that continue to limit the long-term acceptance of upper-limb prostheses and explores how these limitations may be addressed through the integration of sensorimotor information. Building on our previous work, the chapter provides deeper insight into the dynamic nature of embodiment when interacting with upper-limb prosthesis simulator under altered sensorimotor conditions. Finally, future directions are discussed with the goal of reducing barriers to device adoption and effectively translating dexterous devices to individuals with limb loss.

2.2 Introduction

Advancements in mechatronic upper-limb prostheses now offer sophisticated control, dexterity, and sensory feedback, with significant potential to improve independence and quality of life for individuals with limb amputation [**1**], [**2**], [**3**], [**4**]. Despite these recent technological strides, users often continue to experience frustration when interacting with these devices, which can hinder both acceptance and sustained use of emerging prosthetic technologies [**5**], [**6**]. As upper-limb prostheses continue to evolve, modern mechatronic design goals are expanding beyond functional performance to include seamless user integration, enabling the prosthesis to respond naturally, precisely, and in line with their intentions. Understanding how users perceive, interpret, and relate to their prostheses is increasingly essential. In this context, prosthetic embodiment has become a central objective: enabling users to experience the device and its actions as part of their own body [**1**], [**3**], [**7**].

The sense of embodiment, the perceptual experience of owning and controlling a body or non-corporeal objects in space, has been understood to arise from three key perceptual components: sense of ownership (SoO), sense of agency (SoA), and peripersonal space (PPS), also referred to as self-location [**8**].

Sense of Ownership: SoO refers to the feeling that a body part belongs to oneself and is believed to be modulated by congruent multisensory feedback, most commonly the alignment of visual and tactile cues [**9**], [**10**], [**11**], [**12**].

Sense of Agency: SoA is the experience of initiating and controlling one's actions and their consequences, shaped by the match between motor intentions, internal predictions of action outcomes, and the sensory feedback that follows (e.g., feeling the movement of a limb in response to one's intention to move it) [**13**], [**11**], [**14**], [**15**], [**16**].

Peripersonal space: PPS is defined as the dynamic envelope of space surrounding the body within which interaction with the environment is possible, and it can adapt based on context, tool use, and multisensory experience [**9**], [**17**], [**18**], [**19**], [**20**].

Recent experimental approaches have demonstrated that the sense of embodiment over artificial limbs or objects is underpinned by multisensory integration and motor-related mechanisms. Many of these approaches stem back to the rubber hand illusion (RHI), which provided empirical evidence that individuals can develop ownership over a rubber hand when synchronous visuotactile stimulation is applied to both the real and rubber hands [**9**]. Later adaptations of the paradigm incorporated voluntary movements, showing that the perception of authorship over intended movements can also arise through congruent sensorimotor engagement [**13**], [**21**], [**22**]. Together, these findings indicate that this experience is highly malleable and can extend beyond the biological body [**23**], [**9**], [**24**], [**25**], [**10**], [**26**], [**27**], [**28**], laying the groundwork for prosthesis embodiment [**29**], [**30**].

Understanding how the components shaping embodiment interact, and how they can be modulated through a device's motor behaviors and sensory feedback, may offer a critical pathway for assistive systems to promote a seamless, coherent integration within users' sensorimotor control loops [**6**], [**31**], [**23**], [**32**], [**33**], [**34**]. Although embodiment is widely viewed as important for effective integration with upper-limb prostheses, there is still limited consistency in how it is measured, and a variety of disparate techniques are employed across studies [**1**], [**3**], [**7**]. Broadly, these measures fall into two categories. Explicit measures use validated questionnaires to capture conscious perceptions of an artificial limb. Implicit measures instead quantify behavioral, autonomic, or perceptual changes that occur behind conscious awareness when a limb is embodied.

Explicit measure of SoO and SoA: It can be measured by having participants report on their conscious feeling (e.g., perceiving the device as their own body parts, or control over experimental events) using Embodiment Likert scale questionnaires.

Implicit measure of PPS and SoA: Intentional binding, one of implicit indices for SoA, is to quantify distortions in time perception between self-generated actions and their sensory outcomes; and PPS assessed through proprioceptive drift, a non-conscious change in which perceived limb position shifts toward an embodied inanimate object [**27**], [**35**], [**36**], [**37**], [**38**], [**39**]. Although PPS-related measures are often discussed as implicit correlates of SoO, evidence for this link is mixed and not consistently replicated across studies [**37**], [**38**], [**40**], [**41**].

In various domains, including advanced prostheses, explicit and implicit measures of embodiment are applied inconsistently across studies, and there is continued debate over whether they tap the same underlying construct or instead reflect distinct facets of embodiment [**1**], [**42**], [**7**]. This lack of conceptual clarity complicates the interpretation and comparison of findings [**1**], [**3**]. These difficulties are compounded by the fact that there are relationships between SoO, SoA, and PPS; however, how they influence one another remains poorly understood and inconsistently defined. For example, ownership and agency often emerge together when individuals engage with non-biological objects under congruent multisensory and sensorimotor contingencies [**13**], [**21**], [**36**]. On the other hand, they can appear dissociable, with one present in the absence of the other [**13**], [**43**], [**44**]. Similarly, proprioceptive drift is often interpreted as an implicit measure of SoO. However, recent studies have questioned the reliability of this association, suggesting that proprioceptive drift may instead reflect changes in peripersonal space (PPS) rather than ownership [**9**], [**18**], [**19**], [**37**], [**38**], [**40**]. Similarly, the relationship between explicit SoA and intentional binding as an implicit behavioral marker of SoA, remains contentious [**35**], [**45**], [**46**], [**47**], [**48**], [**49**].

These ambiguities are further compounded by the fact that most embodiment theories and assessment paradigms have been primarily developed from studies involving healthy individuals with intact limbs and no sensorimotor impairments. Thus, relatively few studies have systematically tested whether these measures are psychometrically valid in affected populations, such as users of modern upper-limb prostheses. For example, sensory feedback that closely matches the stimulation of missing hands in sensory modality, somatotopic mapping, and timing can promote a strong SoO over a prosthetic limb [**50**]. However, most commercial systems still lack biological-level fidelity, and users commonly experience response delays that can disrupt natural movement timing [**51**], control inaccuracies that can compromise the execution of intended movements [**52**], and dependence on predefined grasp patterns that restrict functional flexibility [**53**], all of which may alter or reduce SoA over the prosthesis.

Moreover, sensory feedback in prosthetic systems remains largely experimental, and often depends on sensory substitution (e.g., vibrotactile cues on the residual limb) that does not align with the natural somatotopy or sensory modalities of the missing limb [**54**]. Although direct peripheral nerve stimulation can evoke somatotopically appropriate sensations, these are often described as buzzing, tingling, or other sensations rather than natural touch or associated contact forces [**55**]. Such mismatch in feedback quality and location can result in an artificial feeling, which can impede the development of SoO. Thus, without validation efforts, it remains unclear how embodiment emerges and presents in modern prosthetic systems, given these current differences from the biological control and sensory experience of a biological limb.

In our previous work [**56**], we developed and validated an experimental paradigm using an upper-limb prosthesis simulator capable of strategically manipulating sensorimotor variables to perturb the SoO, SoA, and PPS. Building on this framework, the objective of this work was to develop a more complete understanding of the dynamic nature of the sense of embodiment by jointly examining explicit measures of agency and ownership alongside implicit indices under conditions that reflect key features of advanced upper-limb prosthesis use. Specifically, We investigated which factors selectively elicited or suppressed components of the sense of embodiment, either independently or in combination and used these results to characterize how SoO, SoA, and PPS relate to one another in shaping cohesive embodiment over the upper-limb prosthetic simulator.

2.3 Methods

2.3.1 Participants

We recruited a cohort of able-bodied participants (N= 23) aged 18-30 years (mean age: 21.3 years; 53% male). All participants provided written informed consent prior to participation, and protocols were approved by the UC Davis Institutional Review Board. All participants were right-handed as verified by the Edinburgh Handedness Inventory [**57**]. Exclusion criteria included cognitive deficits, limited hand movement due to acute or chronic injury or disease, and neurological or musculoskeletal conditions affecting biological motor control and/or sensory perception.

2.3.2 Experimental setup

Participants were seated at a dual-layered table, with a robotic right hand positioned on the upper layer of the table, while their own right hand remained hidden on the lower layer of the table [**56**]. Following the classic rubber hand illusion paradigm [**9**], a cloth was draped over the participant's shoulders to occlude the real arm and enhance the visual impression that the visible robotic hand belonged to their body. Participants were instructed to keep their left hand resting on the upper layer of the table while maintaining their right hand in a fixed position under the table throughout the experiment.

The experimental setup was designed to manipulate three key sensorimotor variables, enabling us to test how spatial congruency, intentions over movement, and tactile feedback contribute - independently and jointly - to embodiment-related experiences: (1) position of the robotic hand, (2) the level of control that participants had over the hand, and (3) the presence of tactile feedback they received.

The setup included the following components, as illustrated in 2.1a: (1) A custom-built robotic hand capable of open/close grasping movements, (2) Capacitive force sensors (SingelTact, Glasogow, UK) embedded in the robotic hand's digits (index, middle, and thumb) to detect object contact during grasping, (3) A wearable electromyography (EMG) armband (Thalmic Labs, Waterloo, Canada) used to read participants' muscle activity and translated it into a single degree of freedom (open/close) for robotic control, (4) A sensory feedback system comprising: a custom-built tactile vibration feedback glove delivering to relevant fingertips [**9**], [**18**], [**58**], an LED light indicating voluntary grasping actions as a visual feedback, and a piezoelectric speaker to emit auditory feedback corresponding to the subsequent sensory event, (5) Headphones to dampen background noise and present an auditory tone, as well as (6) A 'light box' placed on the upper layer, geometrically identical to a 'blank box' on the lower layer, allowing participants to perform grasping tasks with both the robotic and their actual hand respectively. This setup ensured precise control over sensory and motor conditions and was previously validated as capable of perturbing SoO, SoA, and PPS [**56**].

TABLE 2.1. Overview of manipulated sensorimotor conditions and time delays.

	Factor	**Level**	**Description**
Manipulated sensorimotor conditions (9 conditions)	Sensorimotor feedback	BUZ	VIB[1] on + Active control
		NB	VIB[1] off + Active control
		WAT	VIB[1] off + Passive control
	Robotic hand position	C	No offset from the actual hand
		M	200 mm offset
		F	400 mm offset
Time delay of auditory tone (ms)		300	Randomized and evenly distributed across experimental blocks
		500	
		700	

[1] VIB: tactile vibration feedback.

2.3.3 Experimental procedure

In each trial, participants either actively grasped the 'blank box' on the lower layer of the table with their hidden right hand while the EMG armband detected the resulting muscle activity and actuated the robotic hand to synchronously grasp the "light box" on the upper layer or passively observed the robotic hand's movement. As shown in Fig. 2.1a, when the 'light box' was grasped, its LED illuminated immediately. An auditory tone then presented after a variable time delay (0 1 second). This LED-auditory tone sequence was designed to quantify the implicit SoA through intentional binding (see outcome measurements below). Together, this setup enabled perturbation of the SoO, SoA, and PPS by manipulating the following factors listed in Table 2.1.

The experiment consisted of 9 blocks, each corresponding to one of the 9 combinations of sensorimotor feedback (3 levels) and robotic hand position (3 levels). Within each block, participants completed 18 trials: 6 repetitions of each of the three time delay of auditory tone conditions, presented in a randomized order to minimize bias in interval estimation. Block order was randomized across participants (totaling 18 trials per block and 162 trials per participant), as illustrated in Fig. 2.1b and Table 2.1.

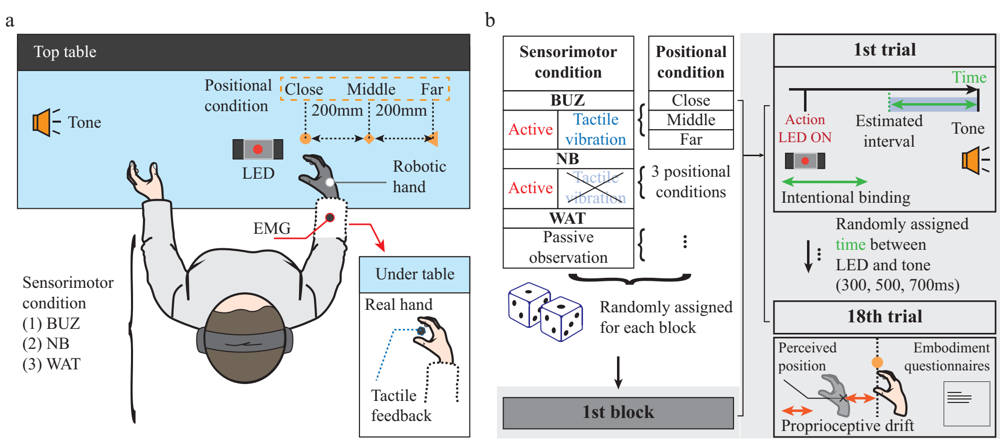

FIGURE 2.1. Schematic design of the experimental setup and process. **a**. Overview of the experimental setup used to systematically investigate how visual, tactile, and motor cues shape the sense of embodiment through sensorimotor integration. Participants interacted with a robotic hand positioned at one of three positions (close, middle, far) on the upper layer of a dual-layer table. The experiment involved three sensorimotor conditions: BUZ (active control with tactile feedback), NB (active control without tactile feedback), and WAT (passive observation without control) **b**. Participants experienced nine conditions, combining three sensorimotor conditions (BUZ, NB, WAT) with three hand positions (close, middle, far). These combinations were randomly assigned to blocks. Within each block, trials included randomized time intervals (300ms, 500ms, 700ms), with each interval repeated six times. During each trial, participants reported intentional binding by estimating the perceived time interval between LED activation and the auditory tone. At the end of each block, they completed embodiment questionnaires (Appendix A, Supplementary Table 1) and proprioceptive drift measurements by indicating the perceived location of their right hand to assess changes in the perceived position of their hand.

2.3.4 Outcome measures

Fig. 2.1b illustrates the procedure used to measure each component of the sense of embodiment, including explicit SoA, SoO, intentional binding, and peripersonal space.

Explicit measure of SoO and SoA: As an evaluation of the subjective sense of embodiment, we implemented a 16-statement ownership and agency questionnaire, which included questionnaires to control for task compliance, suggestibility, and expectancy effects (Appendix A, Supplementary Table 1). These statements were adapted from established questionnaires used in traditional rubber hand illusion experiments [**9**], [**8**]. At the end of each block, participants rated the statements on a Likert-scale ranging from -3 (totally disagree) to +3 (totally agree), with randomized question order.

Implicit measure of SoA and PPS: (1) Intentional binding: Participants verbally estimated the temporal interval between LED illumination (representing the active action) and the auditory feedback (the subsequent sensory outcome). On each trial, participants reported the perceived time interval in milliseconds (0 1000 milliseconds), following procedures validated in previous studies on intentional binding [**47**], [**59**], [**60**], [**61**], [**62**]. A shorter perceived duration of this interval indicates stronger SoA [**45**], [**63**], [**64**]. (2) Proprioceptive drift: At the end of each block, participants closed their eyes and used their left index finger to indicate the perceived position of their right hand. The indicated location was marked on the upper layer. Proprioceptive drift was then quantified as the displacement between the indicated and actual hand positions [**65**], with positive drift defined as a shift in perceived hand location toward the robotic hand.

2.3.5 Statistical analysis

The goals of our analysis were to investigate how sensorimotor cues - spatial alignment, tactile feedback, and level of control (active/passive)- shape a cohesive sense of embodiment, and to examine how implicit and explicit measures of SoO, SoA, and PPS relate to one another. This multi-metric approach allowed us to disentangle their respective contributions, assess how they are modulated by experimental conditions, and explore their potential interrelationships within participants.

Data for each component of the sense of embodiment (SoO, SoA, and PPS) were collected using repeated measures across conditions, yielding a hierarchical dataset with observations nested within participants. Accordingly, we modeled the effects of (1) <u>position of the robotic hand</u>, (2) <u>level of control</u>, and (3) <u>presence of tactile feedback</u> using generalized linear mixed-effects models (GLMMs). Three-factor GLMMs were fitted using maximum likelihood estimation with adaptive Gauss-Hermite quadrature [**66**] to estimate the effects of these categorical independent and their interactions. To account for within-subject correlations across repeated measurements, participant was included as a random intercept in all models. Intentional binding values were approximately normally distributed; therefore, we used a Gaussian family with an identity link function (i.e., the expected value of the outcome variable μ is given by $\mu = \eta$, where η represents the linear predictor). Distributions of agency and ownership scores, as well as proprioceptive drift, showed deviations from normality, exhibiting heavy tails with potential outliers. For these outcomes, models for these outcomes were specified using a t-family distribution with an identity link function. The t-distribution was chosen for its robustness to non-normality and its ability to accommodate extreme values without disproportionately influencing parameter estimates.

Model comparisons were conducted using an information-theoretic approach based on Akaike Information Criterion (AIC) [**67**], to identify the best-fitting model for each outcome. For the selected models, residual diagnostics plots were visually inspected, and Levene's test was used to evaluate homoscedasticity. Model-based estimates (from the linear predictor) were then used to generate fitted curves for each outcome. Full model summaries are provided in theAppendix B, Supplementary Tables 1–6.

To assess correlations among outcome variables within participants, each outcome was standardized using a z-score transformation, ensuring comparability across scales by subtracting the mean and dividing by the standard deviation. This standardization allowed direct comparisons of effect sizes. A linear mixed-effects model (LMM) was then constructed to examine the effects of independent variables on these standardized outcomes while accounting for inter-individual variability. The model included fixed effects for the interaction between outcomes, positional conditions, feedback status, and activity status, while also incorporating a random intercept for each outcome within participants to capture inter-individual variability.

To further investigate within participant associations between outcomes, the variance covariance matrix of the random effects was extracted and transformed into a correlation matrix. This transformation enabled standardized estimates of within-participant relations: positive correlations indicate outcomes that tend to increase together, negative correlations indicate inverse relationships, and values near zero implied minimal correlation.

All statistical analyses were conducted using R version 4.3.3 via RStudio, and plots were generated with the ggplot2 package. GLMMs and LMMs were implemented using the glmmTMB function from the glmmTMB package [**68**] and the lmer function from the lme4 package [**69**], respectively. The DHARMa package was used for diagnostic assessment [**70**]. Variance-covariance matrices were calculated using the VarCorr function from the nlme package [**71**] and converted to correlations using the cov2cor function. Adjusted means and contrasts were calculated using the emmeans package, with Tukey's Honest Significant Difference (HSD) correction for multiple comparisons, with a significance level set at $\alpha = 0.05$ (two-sided) [**72**].

2.4 Results

2.4.1 Explicit sense of agency

Using the fitted generalized linear mixed-effects model, we found that agency questionnaire scores were significantly higher than control questionnaire scores when averaged across all levels of the independent variables. The estimated difference was 1.44 (SE= 0.0262; z.ratio = 55.04; $p < 0.001$ with Tukey's adjustment; Fig. 2.2a). Fig. 2.2 shows the estimated marginal means of SoA ratings across conditions, with 95% confidence interval.

The effects of three categorical independent variables on explicit SoA were also assessed. It showed significant effects of active control (level of control), tactile vibration feedback (presence of tactile feedback), and position of the robotic hand ($\chi^2 = 17437.61$; df = 1, $p < 0.001$ for active control, $\chi^2 = 51.91$; df = 1, $p < 0.001$ for the presence of tactile vibration feedback, and $\chi^2 = 39.07$; df = 2, $p < 0.001$ for robotic hand positions), Table 2.2.

Participants reported a significantly higher sense of agency when tactile vibration feedback was provided during active control (BUZ; score: 2.07 ± 0.04), compared to when no feedback was given (NB; score: 1.87 ± 0.03) (Fig. 2.2a). This difference was statistically significant (Tukey-corrected post-hoc analysis 95% CI [0.29,0.40], $p < 0.001$). Furthermore, active control had a significant positive influence on agency scores across all hand-position levels relative to the passive observation (WAT) conditions ($p < 0.001$), which produced the lowest scores, ranging from -0.49 ± 0.09 to -1.14 ± 0.07 across positions.

To test whether spatial alignment modulated the effects of sensorimotor feedback, we performed pairwise comparisons between hand-position levels within the BUZ and NB conditions (Fig. 2.2b). In the BUZ condition, placing the prosthetic hand farther from the participant's body significantly reduced explicit SoA ($p < 0.001$). Specifically, the agency score decreased from 2.07 ± 0.04 at the close position to 1.86 ± 0.04 at the far position, with a statistically significant difference (95% CI [0.24,0.35], $p < 0.001$). In contrast, in the

NB condition, hand position also affected explicit SoA, but the pattern was not monotonic ($p < 0.001$).

2.4.2 Explicit sense of ownership

To examine how participants perceive the feeling of "mine" toward their own body part (SoO), we fitted a generalized mixed-effects model that included question type and the independent variables .We compared ownership (Q1–Q4) to control items (Q5–Q8) which were included to check compliance and suggestibility, confirming that participants selectively endorsed ownership-related statements rather than indiscriminately agreeing with all items. A significant difference indicates participants specifically endorsed ownership-related statements

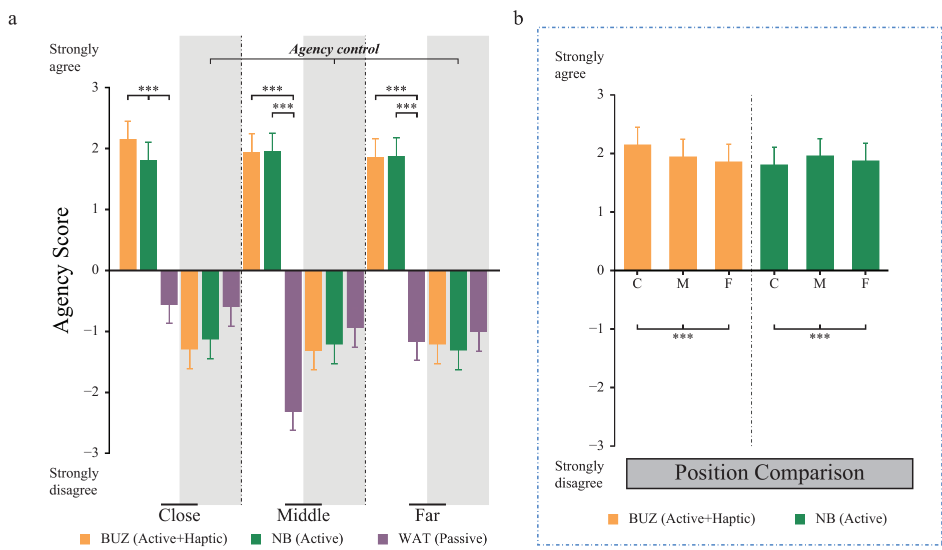

FIGURE 2.2. Measure of explicit sense of agency depending on sensorimotor conditions. Estimated marginal mean values of agency scores across participants, with error bars indicating the 95% confidence intervals. Values were obtained from a generalized mixed-effects model that included robotic hand position, active control, and tactile vibration feedback (BUZ: active control with tactile vibration feedback, NB: active control without tactile vibration feedback, WAT: passive control) as fixed effects, and participant (N=23) as a random intercept to capture variation among individuals. The cut-off for the sense of agency score is 1, indicated by the horizontal dashed line [**73**], [**74**]. **a**. Changes in explicit sense of agency questionnaire ratings and control questionnaire ratings (gray-shaded rectangles) across experimental conditions (combinations of robotic hand position and sensorimotor conditions: BUZ, NB, and WAT) **b**. Comparisons between different robotic hand positions within BUZ and NB. Asterisks indicate statistically significant pairwise differences ($p < 0.001$, Tukey-corrected post-hoc test) between conditions sharing the same prosthetic hand position and sensorimotor condition.

rather than uniformly agreeing with all items. Averaged across all levels of the independent variables, ownership ratings were significantly higher than control ratings (Tukey-adjusted pairwise comparison: mean difference = 0.89; SE = 0.02; $p < 0.001$), as shown in Fig. 2.3a.

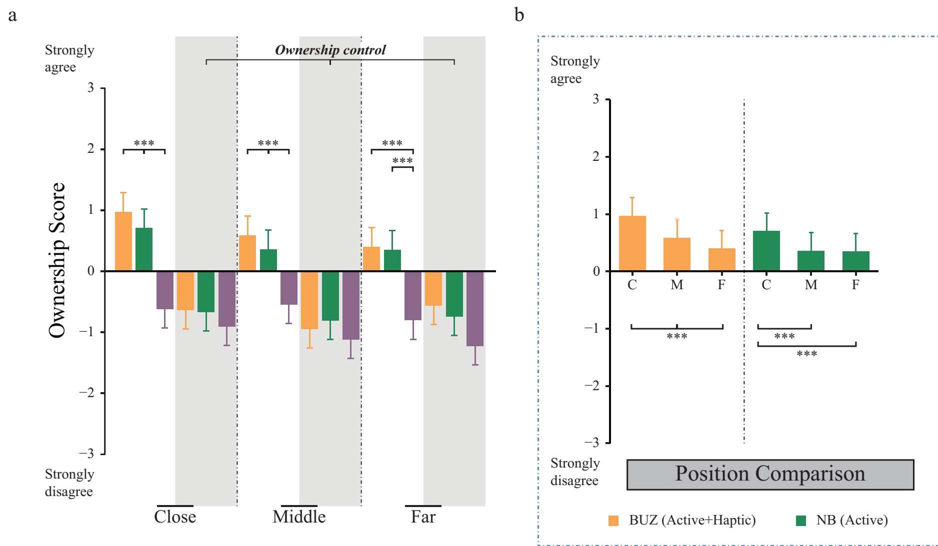

FIGURE 2.3. Measure of explicit sense of ownership depending on sensorimotor conditions. Estimated marginal mean values of ownership scores across participants, with error bars indicating the 95% confidence intervals. Values were obtained from a generalized mixed-effects model including robotic hand's position, active control, and tactile vibration feedback (BUZ: active control with tactile vibration feedback, NB: active control without tactile vibration feedback, WAT: passive control) as fixed effects and participant (N=23) as a random intercept to capture variation among individuals. The cut-off for the sense of ownership score is 1, indicated by the horizontal dashed line [**73**], [**74**]. **a**. Changes in explicit sense of ownership questionnaire ratings and control questionnaire ratings (gray-shaded rectangles) across experimental conditions (combinations of robotic hand position and sensorimotor feedback condition: BUZ, NB, and WAT) **b**. Comparisons between different robotic hand positions within BUZ and NB. Asterisks indicate statistically significant pairwise differences ($p < 0.001$, Tukey-corrected post-hoc test) between conditions sharing the same position of the prosthetic hand and sensorimotor condition.

Responses to the explicit SoO (Q1-Q4) generally indicated uncertainty, with scores falling in the 0 - 1 range, where a score of 1 serves as the cut-off for a definitive sense of ownership [**73**], [**74**]. At the close position, the estimated explicit ownership scores were 0.98 ± 0.05 for BUZ and 0.71 ± 0.05 for NB. Both values were slightly below the cut-off score of 1, with no significant difference (z.ratio = -0.18; $p = 0.858 > 0.05$ for BUZ; z.ratio = -1.83; $p = 0.0674 > 0.05$ for NB)based on Wald tests with post-hoc comparisons using Sidak adjustment (see

Fig. 2.3a). Although ownership ratings remained in the positive uncertainty region, Fig. 2.3a shows that the explicit ownership was significantly modulated by the presence of active control ($\chi^2 = 1027.00$; df = 1, $p < 0.001$), the presence of tactile vibration feedback ($\chi^2 = 20.85$; df = 1, $p < 0.001$), and robotic hand positions ($\chi^2 = 110.90$; df = 2, $p < 0.001$), Table 2.2.

Ownership scores were lower in NB than in BUZ, indicating reduced ownership over the robotic hand in the absence of tactile vibration feedback, particularly at the close and middle positions. These differences were statistically significant (95% CI [0.15,0.38], $p < 0.001$ for close position; 95% CI [0.09,0.36], $p < 0.001$ for medium position). Similarly, when participants actively controlled the robotic hand without tactile vibration feedback (NB), they reported a higher sense of ownership than in the WAT condition (estimated marginal mean difference between NB and WAT: 95% CI [1.20,1.44], $p < 0.001$ for the close position; 95% CI [0.78,1.02], $p < 0.001$ for the medium position; 95% CI [1.03,1.27], $p < 0.001$ for the far position), as shown in Fig. 2.3a.

We next assessed the effect of position levels within the BUZ and NB conditions. As Fig. 2.3b shows, placing the robotic hand farther from the participant's real hand significantly reduced the ownership score. For example, in the BUZ condition, the score decreased from 0.98 ± 0.05 at the close position to 0.40 ± 0.05 at the far position, with a statistically significant difference (95% CI [0.45,0.69], $p < 0.001$). But, in the NB condition, the score at the close position was significantly greater at the middle and far positions, whereas other two positions did not differ significantly from each other.

2.4.3 Intentional binding

Fig. 2.4 illustrates how spatial alignment and sensorimotor factors influence intentional binding, indexed by perceived time compression between the action-related LED onset (intention) and the subsequent tone (sensory outcome). The figure indicates the estimated marginal means of perceived time delay (ms) with 95% confidence intervals across experimental conditions. Fitted model results indicate that presence of tactile vibration feedback had a significant effect on intentional binding responses ($\chi^2 = 61.44$; df = 1, $p < 0.001$), while the presence of active control also had a significant but weaker effect ($\chi^2 = 4.75$; df = 1, $p = 0.03$), summarized in Table 2.2. Pairwise comparisons revealed that tactile vibration feedback produced shorter perceived intervals (i.e., stronger intentional binding) than the NB condition at all robotic hand positions (close: -82.61 ± 9.59 ms; medium: -75.48 ± 10.82 ms; far: -97.83 ± 10.17 ms), exhibiting a significant difference compared to the NB condition (95% CI's: [33.53,84.58], [24.59,75.65], and [42.11,93.16] for close, medium and far respectively, $p < 0.001$), as shown in Fig. 2.4.

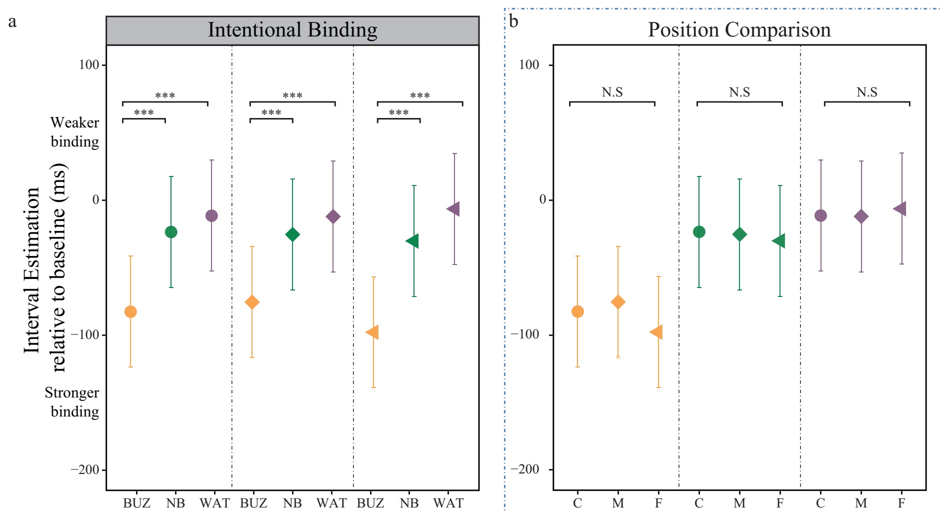

FIGURE 2.4. Intentional binding across sensorimotor conditions. Participants estimated the perceived time interval between an action (LED illumination) and its sensory outcome (auditory tone). After subtracting the actual time delay from the estimated time, the time interval was used to capture the effects of the independent variables. Marginal mean values with 95% confidence intervals were derived from a generalized mixed-effects model, which had prosthetic hand position, active control, and tactile feedback as fixed effects, and participant (N=23) as a random intercept to capture variation among individuals. Asterisks indicate statistically significant differences between pairwise comparisons between conditions with the same prosthetic hand position ($p < 0.001$, Tukey-corrected post hoc test).

Although participants actively controlled the prosthetic hand without tactile vibration feedback (NB), Fig. 2.4 suggests slightly weaker intentional binding than in the involuntary (WAT) condition. However, NB and WAT did not differ significantly at any position (95% CI [-13.45,37.60], $p = 0.35$ for the close position; 95% CI [-12.24,38.81], $p = 0.31$ for the middle position; and 95% CI [-1.73,49.32], $p = 0.06$ for the far position). Moreover, robotic hand positions alone did not significantly affect intentional binding across conditions ($p > 0.05$).

2.4.4 Peripersonal space

We examined how body-self representation expanded toward the robotic hand by manipulating spatial alignment and sensorimotor factors. Fig. 2.5 illustrates the estimated proprioceptive drift (spatial expansion relative to the robotic hand's position) with 95% confidence intervals. Likelihood-ratio tests (ANOVA on the fitted model) revealed significant main effects of tactile vibration feedback ($\chi^2 = 69.35$; df = 1, $p < 0.001$) and position ($\chi^2 = 777.77$; df = 2, $p < 0.001$), while active control did not significantly affect proprioceptive drift ($\chi^2 = 0.81$; df = 1, $p = 0.37$), summarized in Table 2.2.

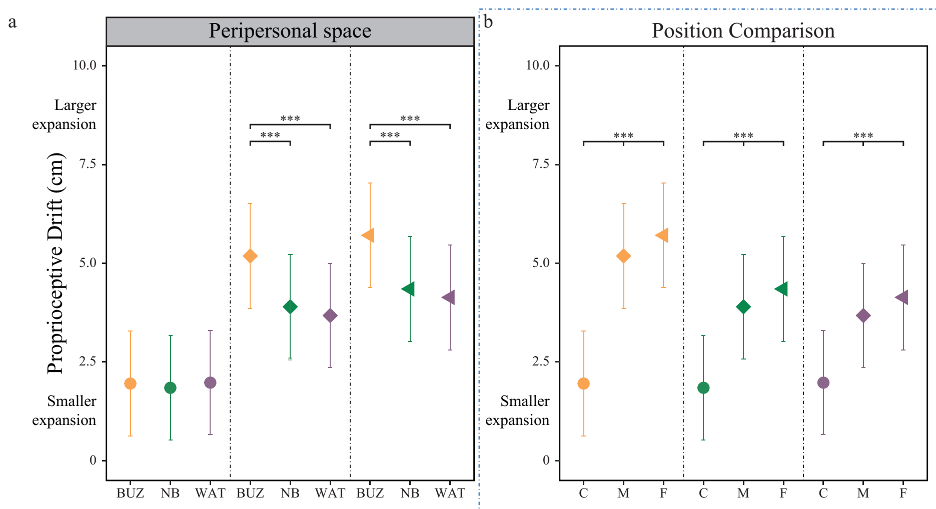

FIGURE 2.5. Proprioceptive drift depending on sensorimotor conditions. Participants estimated the perceived location of their right hand; proprioceptive drift (unit: cm) was defined as the distance between the perceived and actual hand locations. Estimated marginal mean values with 95% confidence interval from the generalized mixed-effects model, which included robotic hand's position, active control, and tactile vibration feedback (BUZ: active control with tactile vibration feedback, NB: active control without tactile vibration feedback, WAT: passive control) as fixed effects, and participant (N=23) as a random intercept to capture variation among individuals. a. Changes in proprioceptive drift depending on varied independent variables (different robotic hand positions along with BUZ, NB, and WAT) b. Comparisons between different prosthetic hand positions within the BUZ and NB. Asterisks indicate significant pairwise comparisons ($p < 0.001$, Tukey-corrected post hoc test) between conditions sharing the same prosthetic hand position and sensorimotor condition.

To assess how each factor influenced PPS, we conducted Tukey-adjusted post-hoc pairwise comparisons. Across conditions, participants' perceived hand location generally remained near the actual hand position. However, tactile vibration feedback (BUZ) produced a significantly greater PPS expansion toward the robotic hand than the absence of feedback (NB), as shown in Fig. 2.5a (mean difference between BUZ and NB: 95% CI [0.94,1.63], $p < 0.001$ at the middle position; 95% CI [0.98,1.74], $p < 0.001$ at the far position). Within the BUZ condition, increasing the distance of the robotic hand further increased PPS expansion (Fig. 2.5b). Relative to the close position, drift was significantly higher at the middle position (95% CI [2.86,3.60], $p < 0.001$) and at the far position (95% CI [3.39,4.12], $p < 0.001$). In the other sensorimotor conditions (NB and WAT), a similar position-dependent pattern was observed with significantly greater drift at the far position than at the close position ($p < 0.001$).

TABLE 2.2. Summary of main effects of sensorimotor conditions on each outcome measure.

Factor	**Explicit SoA**	**Intentional binding**	**Explicit SoO**	**Peripersonal space**
Active control	17437.61	4.75	1027.00	0.81
Tactile vibration feedback	51.91	61.44	20.85	69.35
Robotic hand position	39.07	1.00[a]	110.90	777.77

2.4.5 Relationships between explicit and implicit sense of agency and sense of ownership

Fig. 2.6 summarizes the relationships among embodiment-related measures by combining explicit and implicit indices of SoA and SoO. We observed an overall positive association between the implicit and explicit SoA measures: stronger intentional binding (i.e., shorter reported time intervals) was linked to greater explicit SoA ratings (Fig. 2.6). This pattern is consistent with individual component-level results, where voluntary control (BUZ and NB) increased both explicit SoA and intentional binding relative to passive observation (see Fig. 2.2a and 2.4). Furthermore, the BUZ condition (active control with tactile vibration feedback) led to greater explicit SoO and an PPS expansion toward the robotic hand (see

Fig. 2.3a and 2.5a). Although differences in explicit SoO were observed between the NB and WAT conditions, PPS did not show a corresponding difference. These condition-dependent patterns are captured in Fig. 2.6 while also showing that two measures can dissociate under some sensorimotor conditions.

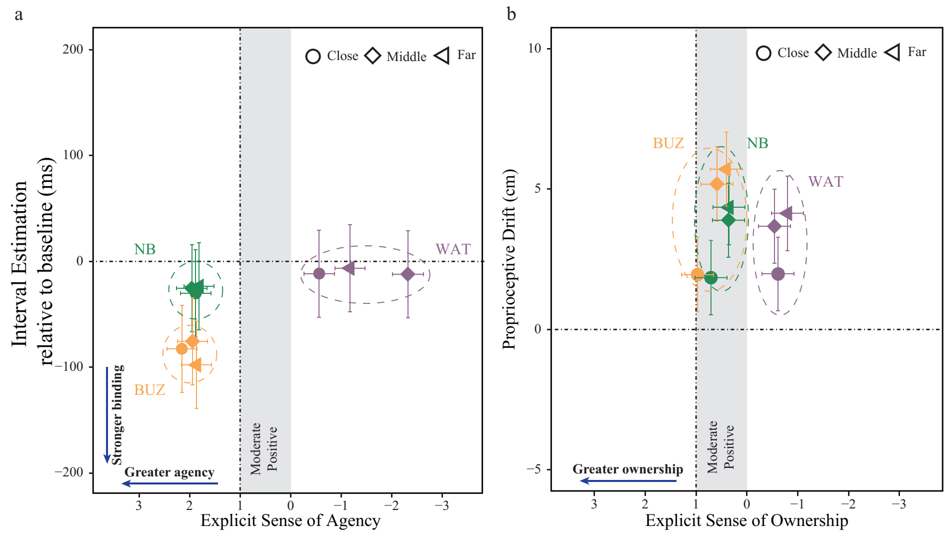

FIGURE 2.6. Relationships between components of sense of embodiment. Estimated marginal means values with 95% confidence intervals are plotted for each measure to illustrate the relationships between different components. **a**. Relationship between explicit and implicit sense of agency. The horizontal dashed line denotes no deviation in time interval estimation from baseline, and the vertical dashed line indicates the cut-off score of +1, denoting the threshold for an experience of agency. **b**. Relationship between explicit and implicit sense of ownership, with the vertical dashed line indicating the cut-off score of 1 for an experience of ownership, and the gray-shaded rectangle highlighting the moderate positive region (where explicit ownership scores range between 0 and 1).

2.4.6 Relationships between each component of the sense of embodiment

To enable comparisons between embodiment outcomes, all outcomes were scaled using z-score transformation. A linear mixed-effects model was applied to account for inter-individual variability. The variance-covariance matrix of its random effects was extracted and converted into a correlation matrix to quantify within-participant associations between outcomes, as shown in Fig. 2.7.

It revealed a moderate positive correlation (r = 0.48) between explicit agency and intentional binding, an implicit measure of agency. Explicit ownership was strongly correlated with explicit agency (r = 0.70) and moderately correlated with implicit agency (r = 0.56), indicating that agency and ownership covaried closely across participants. However, we observed that peripersonal space showed no relationship with explicit ownership (r = -0.03), and only weak negative correlations with explicit agency (r = -0.29) and intentional binding (r = -0.11). Together, these results suggest that agency and ownership are tightly coupled, whereas PPS may be relatively independent of explicit ownership and only weakly related to agency.

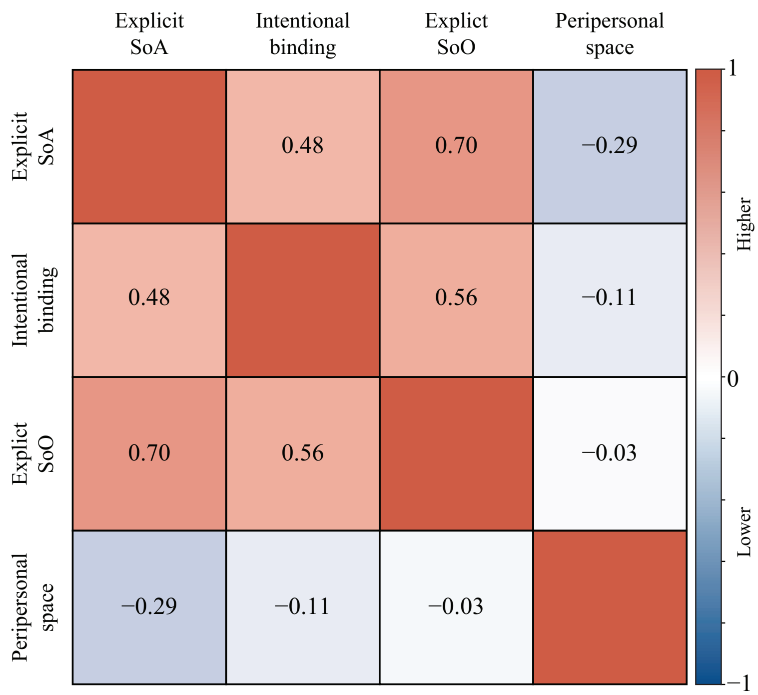

Figure 2.7. Correlation matrix among measures of explicit ownership, explicit agency, intentional binding, and peripersonal space. The covariance matrix was transformed into a correlation matrix to standardize the relationships between components of the sense of embodiment. Positive correlation (shown in red) indicates that outcomes increased together, while negative correlations (shown in blue) indicate an inverse relationship.

2.5 Discussion

Our findings underscore the importance of understanding the complex and dynamic nature of the sense of embodiment for the given context in which it is being assessed, particularly in populations with atypical sensorimotor function such as upper-limb prosthesis users. This includes considering how the specific constituent components shaping the sense of embodiment are measured, how these measures relate to one another, and how they may differ from the wealth of literature describing data derived from normative, able-bodied populations. By employing an upper-limb prosthesis simulator, our study offers a pathway toward a more comprehensive understanding of embodiment in the context of advanced mechatronic upper-limb prosthesis use. Through systematic manipulation of motor control and sensory feedback, we demonstrated that specific components of embodiment, including SoO, SoA, and PPS, can be selectively elicited or suppressed, either independently or in combination. Furthermore, the observed relationships between sensorimotor conditions and embodiment measures, as well as the interrelationships among these measures, did not consistently align with findings reported in the able-bodied cohorts, highlighting the need for tailored approaches in prosthetic embodiment research.

Our results revealed that explicit SoO was present when the robotic hand was actively controlled in both the BUZ and NB conditions, with the strongest effects observed in the BUZ condition, where congruent tactile vibration feedback was present at the participants' fingertips. These results highlight the tight link between internal sensorimotor representations and externally delivered feedback in shaping greater ownership experiences and are consistent with previous studies [**75**], including studies involving able-bodied individuals [**9**], [**76**], [**77**]. Yet, our data showed ownership questionnaire scores remained within the moderate positive range (a positive score between 0 and 1), not surpassing the established cut-off score for "strong" ownership (> 1) [**73**], [**74**]. One possible explanation is that our participants had intact limbs, and the presence of biological kinesthetic and proprioceptive feedback may have had minor incongruence with the visual and tactile feedback from the prosthetic hand. Nonetheless, the observed strengthening of explicit SoO with tactile vibration feedback suggests that even limited artificial feedback can partially overcome the absence of natural sensation, supporting greater incorporation of a prosthetic limb into the user's body representation. While the tactile vibration feedback used in our experiment, similar to that employed in many prosthetic systems, inherently lacks the richness and subtlety of natural tactile input, it nonetheless provided sufficient information to modulate ownership experiences. This finding aligns with previous studies [**27**], [**78**], [**79**] and reinforces the notion that some form of tactile feedback, even if simplified, is better than none at all when promoting explicit ownership effects.

We found a greater SoA developed during active control of the robotic hand reinforcing that motor control is a critical contributor to explicit SoA [**80**], [**81**]. Additionally, spatial alignment consistently influenced explicit SoA, but only when both active control and tactile vibration feedback were present. This pattern may be explained by the contribution of SoO: when tactile vibration feedback is available, spatial congruency enhances the perception that the prosthesis is part of the body, which in turn strengthens the sense of agency. For example, the BUZ condition (associated with the strongest explicit SoO) also elicited the strongest explicit SoA, suggesting that agency is most robust when directed toward movements of body parts most strongly perceived as one's own. Our findings support the idea that the explicit SoO and SoA are interrelated, and that achieving both in prosthetic systems may have compounding effects that promote a stronger sense of embodiment of the device. This aligns with existing evidence suggesting that the sense of agency is closely tied to actual bodily movement and is informed by activity from peripheral somatosensory receptors [**13**], [**36**]. Thus, when users volitionally actuate a prosthesis, this contributes to forming a sense of authorship over the resulting movement (SoA), which is related to, and may strengthen, the SoO. Conversely, when a prosthetic limb is already associated with a strong sense of ownership, engaging it in movement may further reinforce the SoA. Furthermore, the effect of tactile vibration feedback on the explicit SoA was limited to situations in which the robotic prosthesis was spatially aligned with the actual hand (close position). In contrast, tactile vibration feedback did not significantly influence agency when the hand was positioned at medium or far positions. These findings suggest that voluntary control, when combined with spatially congruent visual and tactile feedback, is critical for maximizing the sense of agency, whereas tactile vibration feedback alone may be insufficient to override the influence of proprioceptive mismatch, as the intact somatosensory system continues to signal the location of the biological limb. Although voluntary motor intention is a key driver of agency, the integration of tactile feedback to enhance the SoA appears to require alignment with internal proprioceptive maps.

We examined two implicit measures that contribute to the greater sense of embodiment: intentional binding, a temporal marker conventionally described as relating to implicit SoA, and peripersonal space, often interpreted as an implicit measure of SoO although some argue it is a distinct perceptual phenomenon [**9**], [**13**], [**18**], [**36**], [**37**], [**39**], [**74**], [**82**]. Our findings showed that intentional binding was significantly greater in the BUZ condition, indicating enhanced temporal binding when artificial tactile feedback matched the outcomes of volitional control (the prosthesis contacting the light box). This finding appeared to be independent of spatial alignment. In contrast, no significant difference in intentional binding was found between the NB (voluntary control without tactile vibration feedback) and WAT (passive control) conditions, suggesting that motor intention alone is insufficient to produce temporal compression effects [**15**], [**83**], [**84**], [**85**], [**86**].

Interpreted within the framework of a comparator model underlying volitional motor control - which states that the brain monitors and adjusts goal-directed movements by comparing predicted sensory outcomes of motor commands with actual sensory feedback - our results suggest that when volitional movement and sensory outcomes align, intentional binding occurs regardless of the spatial congruency of the robotic hand. This highlights the importance of appropriate sensory feedback tightly linked to prosthetic motor actions and suggests that intentional binding depends on the convergence of motor output, predicted sensory consequences, and actual sensory feedback generated during the action [**80**], [**87**].

We also found PPS expanded toward the robotic prosthesis only when voluntary control was paired with tactile vibration feedback (BUZ condition), supporting the role of sensory input in integrating the prosthesis into the body's spatial representation. Specifically, the BUZ condition elicited greater PPS expansion compared to the NB and WAT conditions, which lacked this effect. These results align with previous findings demonstrating that artificial tactile vibration, despite its limitations in replicating natural touch, can facilitate prosthetic limb integration into body representation [**88**], [**89**].

While proprioceptive drift has traditionally been used as an implicit measure of the sense of ownership (SoO) and reflects the dynamic nature of peripersonal space [**9**], [**13**], [**74**], [**82**], our findings revealed no significant correlation between explicit SoO and the magnitude of proprioceptive drift. In line with previous work in able-bodied individuals, this suggests that explicit self-reports and implicit indicators of ownership, such as proprioceptive drift, may reflect distinct aspects of embodiment rather than two converging measures of SoO [**18**], [**36**], [**37**], [**39**]. The lack of correlation in our results supports this dissociation, suggesting that proprioceptive drift and SoO questionnaire sets may capture separate underlying processes of embodiment. This dissociation is further emphasized by the differential influence of sensorimotor factors on each measure. For example, while voluntary control without tactile feedback (NB condition) elicited a sense of ownership as reflected in the questionnaire responses, it did not lead to an expansion of peripersonal space, as indicated by the lack of significant proprioceptive drift relative to the passive observation condition (WAT condition, Fig. 2.5). These results imply that the presence of tactile feedback appears to serve as a key sensory cue for extending the body's spatial boundary, yet this induced proprioceptive drift may be a separate, perceptually distinct phenomenon from explicit SoO.

Furthermore, both SoA questionnaires and intentional binding are conventionally assumed to reflect the underlying sense of agency. Consistent with this view, our findings showed that participants who explicitly reported a greater sense of agency over robotic movements also exhibited stronger intentional binding effects (Fig. 2.7). However, we also found that intentional binding was not modulated by the robotic hand position but was modulated by tactile vibration feedback (Fig. 2.4). However, when examining SoA questionnaire scores, tactile vibration feedback only had an effect in the close hand position (BUZ vs. NB conditions), and position did in fact have a significant effect (Fig. 2.2). The fact that SoA questionnaire scores and intentional binding results were correlated yet held different relationships with haptic feedback and hand position may support the view that SoA is a multidimensional construct. In line with this suggestion, others have proposed SoA comprises of a 'feeling of agency' that is pre-reflective and at the fringe level of consciousness, and a 'judgment of agency' is a higher order and belief-like process [**90**]. From this perspective, intentional binding may capture more subtle, pre-reflective aspects of agency that are less influenced by spatial configuration. Together our findings show that explicit SoA and intentional binding are distinct yet complementary measures of agency. Their distinct behaviors under varying sensorimotor conditions provide further insight into the interconnected layers underlying agency perception [**35**], [**45**], [**46**], [**47**], [**48**], [**49**].

Together, our findings showed a positive correlation between explicit SoO and both explicit SoA as well as intentional binding (Fig. 2.7). Interestingly, explicit SoO and SoA exhibited the strongest correlation among all measures examined. This suggests that these components may reflect closely related aspects of embodiment, and explicit top-down judgments of SoO and SoA may draw on similar cognitive-perceptual processes rather than representing entirely independent constructs. A positive correlation was found between explicit SoA and intentional binding results, which are conventionally used as explicit and implicit SoA measures, respectively. Interestingly, PPS, which is often considered an implicit measure of SoO, showed weak-negative to no correlation with the other measures, including SoO questionnaire responses. This suggests that PPS may reflect a perceptually distinct aspect of embodiment, rather than directly aligning with other ownership-related measures.

2.6 Conclusion

Our study demonstrates how individual components of embodiment can be independently modulated in the context of embodying prosthetic limb systems by manipulating motor control and sensory feedback. We provide detailed empirical evidence showing that while SoO, SoA, and PPS are often interrelated, they are mediated by distinct yet sometimes overlapping sensorimotor mechanisms. Although these components co-occurred under conditions of congruent sensorimotor feedback, their dissociation under other conditions suggests that embodiment is not a binary phenomenon in which a prosthesis is either embodied or not. Rather, it is a fluid and emergent experience shaped by interdependent processes, each influenced by specific sensory and motor conditions. Our findings revealed patterns of both correlation and dissociation among embodiment measures and the sensorimotor conditions that elicited them, often diverging from findings reported in studies involving biologically intact limbs. For example, PPS, which is often considered an implicit measure of SoO, showed virtually no correlation with explicit SoO questionnaire responses. Additionally, while explicit and implicit measures of agency (e.g., questionnaire responses and intentional binding) were strongly correlated, their relationship with ownership varied depending on sensory feedback.

However, it is critical to note that these differences may be application-specific, as prosthetic systems can present sensorimotor conditions that diverge from those of biological limbs, including control delays, predefined movement patterns, and feedback that relies on sensory substitution. In our system, for example, we observed a control delay of 142.6 ± 21.0 ms [**91**]. Furthermore, bench-top testing found that the delay between prosthetic hand contact and the onset of tactile vibration feedback reached up to 90 ms. Although these values fall below commonly accepted thresholds at which users describe perceiving the delays as diminished control (> 300 ms, [**92**]) or tactile asynchrony ($> 111 \pm 62.0$) ms, [**93**]), such delays, whether consciously perceived or not, may still affect the sensorimotor integration processes that underpin SoA and SoO, respectively. As such, understandings of the constituent components of embodiment derived from able-bodied participants may not fully generalize to prosthesis users. Our findings underscore the importance of validating embodiment measures in these distinct contexts to better understand the unique experiences of prosthesis users.

References

[1] J. Zbinden, E. Lendaro, and M. Ortiz-Catalan, "Prosthetic embodiment: systematic review on definitions, measures, and experimental paradigms," *Journal of NeuroEngineering and Rehabilitation*, vol. 19, p. 37, Dec. 2022.

[2] H. H. Huang, L. J. Hargrove, M. Ortiz-Catalan, and J. W. Sensinger, "Integrating Upper-Limb Prostheses with the Human Body: Technology Advances, Readiness, and Roles in Human–Prosthesis Interaction," *Annual Review of Biomedical Engineering*, vol. 26, pp. 503–528, July 2024.

[3] J. Zbinden, E. Lendaro, and M. Ortiz-Catalan, "A multi-dimensional framework for prosthetic embodiment: a perspective for translational research," *Journal of NeuroEngineering and Rehabilitation*, vol. 19, p. 122, Nov. 2022.

[4] M. Pazzaglia and M. Molinari, "The embodiment of assistive devices—from wheelchair to exoskeleton," *Physics of Life Reviews*, vol. 16, pp. 163–175, Mar. 2016.

[5] J. Klein, Y. Moon, and R. W. Picard, "This computer responds to user frustration," in *CHI '99 extended abstracts on Human factors in computing systems - CHI '99*, (Pittsburgh, Pennsylvania), p. 242, ACM Press, 1999.

[6] J. S. Schofield, M. A. Battraw, A. S. R. Parker, P. M. Pilarski, J. W. Sensinger, and P. D. Marasco, "Embodied Cooperation to Promote Forgiving Interactions With Autonomous Machines," *Frontiers in Neurorobotics*, vol. 15, p. 661603, Apr. 2021.

[7] J. L. Segil, L. M. Roldan, and E. L. Graczyk, "Measuring embodiment: A review of methods for prosthetic devices," *Frontiers in Neurorobotics*, vol. 16, p. 902162, Dec. 2022.

[8] M. R. Longo, F. Schüür, M. P. Kammers, M. Tsakiris, and P. Haggard, "What is embodiment? A psychometric approach," *Cognition*, vol. 107, pp. 978–998, June 2008.

[9] M. Botvinick and J. Cohen, "Rubber hands 'feel' touch that eyes see," *Nature*, vol. 391, pp. 756–756, Feb. 1998.

[10] A. Schettler, V. Raja, and M. L. Anderson, “The Embodiment of Objects: Review, Analysis, and Future Directions,” *Frontiers in Neuroscience*, vol. 13, p. 1332, Dec. 2019.

[11] N. Braun, S. Debener, N. Spychala, E. Bongartz, P. Sörös, H. H. O. Müller, and A. Philipsen, “The Senses of Agency and Ownership: A Review,” *Frontiers in Psychology*, vol. 9, p. 535, Apr. 2018.

[12] K. Kilteni, A. Maselli, K. P. Kording, and M. Slater, “Over my fake body: body ownership illusions for studying the multisensory basis of own-body perception,” *Frontiers in Human Neuroscience*, vol. 9, Mar. 2015.

[13] A. Kalckert and H. H. Ehrsson, “Moving a Rubber Hand that Feels Like Your Own: A Dissociation of Ownership and Agency,” *Frontiers in Human Neuroscience*, vol. 6, 2012.

[14] S. Gallagher, “Philosophical conceptions of the self: implications for cognitive science,” *Trends in Cognitive Sciences*, vol. 4, pp. 14–21, Jan. 2000.

[15] J. W. Moore and S. S. Obhi, “Intentional binding and the sense of agency: A review,” *Consciousness and Cognition*, vol. 21, pp. 546–561, Mar. 2012.

[16] P. Haggard, “Sense of agency in the human brain,” *Nature Reviews Neuroscience*, vol. 18, no. 4, pp. 196–207, 2017.

[17] D. M. Page, J. A. George, D. T. Kluger, C. Duncan, S. Wendelken, T. Davis, D. T. Hutchinson, and G. A. Clark, “Motor Control and Sensory Feedback Enhance Prosthesis Embodiment and Reduce Phantom Pain After Long-Term Hand Amputation,” *Frontiers in Human Neuroscience*, vol. 12, p. 352, Sept. 2018.

[18] O. Blanke, “Multisensory brain mechanisms of bodily self-consciousness,” *Nature Reviews Neuroscience*, vol. 13, pp. 556–571, Aug. 2012.

[19] N. P. Holmes, H. J. Snijders, and C. Spence, “Reaching with alien limbs: Visual exposure to prosthetic hands in a mirror biases proprioception without accompanying illusions of ownership,” *Perception & Psychophysics*, vol. 68, pp. 685–701, May 2006.

[20] M. Tsakiris and P. Haggard, “The Rubber Hand Illusion Revisited: Visuotactile Integration and Self-Attribution.,” *Journal of Experimental Psychology: Human Perception and Performance*, vol. 31, no. 1, pp. 80–91, 2005.

[21] A. Kalckert and H. H. Ehrsson, “The moving rubber hand illusion revisited: Comparing movements and visuotactile stimulation to induce illusory ownership,” *Consciousness and Cognition*, vol. 26, pp. 117–132, May 2014.

[22] J. W. Moore, “What Is the Sense of Agency and Why Does it Matter?,” *Frontiers in Psychology*, vol. 7, Aug. 2016.

[23] N. P. Holmes, C. Spence, P. C. Hansen, C. E. Mackay, and G. A. Calvert, “The Multisensory Attentional Consequences of Tool Use: A Functional Magnetic Resonance Imaging Study,” *PLoS ONE*, vol. 3, p. e3502, Oct. 2008.

[24] K. Ma and B. Hommel, “Body-ownership for actively operated non-corporeal objects,” *Consciousness and Cognition*, vol. 36, pp. 75–86, Nov. 2015.

[25] L. Cardinali, S. Jacobs, C. Brozzoli, F. Frassinetti, A. C. Roy, and A. Farnè, “Grab an object with a tool and change your body: tool-use-dependent changes of body representation for action,” *Experimental Brain Research*, vol. 218, pp. 259–271, Apr. 2012.

[26] H. R. Khan and J. Turri, “Phenomenological Origins of Psychological Ownership,” *Review of General Psychology*, vol. 26, pp. 446–463, Dec. 2022.

[27] P. D. Marasco, J. S. Hebert, J. W. Sensinger, C. E. Shell, J. S. Schofield, Z. C. Thumser, R. Nataraj, D. T. Beckler, M. R. Dawson, D. H. Blustein, S. Gill, B. D. Mensh, R. Granja-Vazquez, M. D. Newcomb, J. P. Carey, and B. M. Orzell, “Illusory movement perception improves motor control for prosthetic hands,” *Science Translational Medicine*, vol. 10, p. eaao6990, Mar. 2018.

[28] P. D. Marasco, J. S. Hebert, J. W. Sensinger, D. T. Beckler, Z. C. Thumser, A. W. Shehata, H. E. Williams, and K. R. Wilson, “Neurorobotic fusion of prosthetic touch,

kinesthesia, and movement in bionic upper limbs promotes intrinsic brain behaviors," *Science Robotics*, vol. 6, p. eabf3368, Sept. 2021.

[29] R. Bekrater-Bodmann, J. Foell, and H. Flor, "Chronic Pain and Body Experience: Neuroscientific Basis and Implications For Treatment," in *Clinical Systems Neuroscience* (K. Kansaku, L. G. Cohen, and N. Birbaumer, eds.), pp. 249–268, Tokyo: Springer Japan, 2015.

[30] C. Spence, "The Cognitive Neuroscience of Incorporation: Body Image Adjustment and Neuroprosthetics," in *Clinical Systems Neuroscience* (K. Kansaku, L. G. Cohen, and N. Birbaumer, eds.), pp. 151–168, Tokyo: Springer Japan, 2015.

[31] C. Murray, "An interpretative phenomenological analysis of the embodiment of artificial limbs," *Disability and Rehabilitation*, vol. 26, pp. 963–973, Aug. 2004.

[32] C. D. Murray, "Embodiment and Prosthetics," in *Psychoprosthetics* (P. Gallagher, D. Desmond, and M. MacLachlan, eds.), pp. 119–129, London: Springer London, 2008.

[33] T. R. Makin, F. De Vignemont, and A. A. Faisal, "Neurocognitive barriers to the embodiment of technology," *Nature Biomedical Engineering*, vol. 1, p. 0014, Jan. 2017.

[34] M. Niedernhuber, D. G. Barone, and B. Lenggenhager, "Prostheses as extensions of the body: Progress and challenges," *Neuroscience & Biobehavioral Reviews*, vol. 92, pp. 1–6, Sept. 2018.

[35] P. Haggard, S. Clark, and J. Kalogeras, "Voluntary action and conscious awareness," *Nature Neuroscience*, vol. 5, pp. 382–385, Apr. 2002.

[36] N. Braun, J. D. Thorne, H. Hildebrandt, and S. Debener, "Interplay of Agency and Ownership: The Intentional Binding and Rubber Hand Illusion Paradigm Combined," *PLoS ONE*, vol. 9, p. e111967, Nov. 2014.

[37] A. Maselli and M. Slater, "Sliding perspectives: dissociating ownership from self-location during full body illusions in virtual reality," *Frontiers in Human Neuroscience*, vol. 8, Sept. 2014.

[38] M. Rohde, M. Di Luca, and M. O. Ernst, "The Rubber Hand Illusion: Feeling of Ownership and Proprioceptive Drift Do Not Go Hand in Hand," *PLoS ONE*, vol. 6, p. e21659, June 2011.

[39] M. Gallagher, C. Colzi, and A. Sedda, "Dissociation of proprioceptive drift and feelings of ownership in the somatic rubber hand illusion," *Acta Psychologica*, vol. 212, p. 103192, Jan. 2021.

[40] G. Tosi, B. Mentesana, and D. Romano, "The correlation between proprioceptive drift and subjective embodiment during the rubber hand illusion: A meta-analytic approach," *Quarterly Journal of Experimental Psychology*, vol. 76, pp. 2197–2207, Oct. 2023.

[41] E. Satta, S. Ferrari-Toniolo, F. Visco-Comandini, R. Caminiti, and A. Battaglia-Mayer, "Development of motor coordination during joint action in mid-childhood," *Neuropsychologia*, vol. 105, pp. 111–122, Oct. 2017.

[42] M. Synofzik, G. Vosgerau, and A. Newen, "I move, therefore I am: A new theoretical framework to investigate agency and ownership," *Consciousness and Cognition*, vol. 17, pp. 411–424, June 2008.

[43] G. Tosi and D. Romano, "The network of the subjective experience in embodiment phenomena," *Psychological Research*, vol. 87, pp. 1043–1056, June 2023.

[44] K. Matsumiya, "Awareness of voluntary action, rather than body ownership, improves motor control," *Scientific Reports*, vol. 11, p. 418, Jan. 2021.

[45] J. A. Dewey and G. Knoblich, "Do Implicit and Explicit Measures of the Sense of Agency Measure the Same Thing?," *PLoS ONE*, vol. 9, p. e110118, Oct. 2014.

[46] J. W. Moore and P. Haggard, "Intentional binding and higher order agency experience," *Consciousness and Cognition*, vol. 19, pp. 490–491, Mar. 2010.

[47] K. Engbert, A. Wohlschläger, and P. Haggard, "Who is causing what? The sense of agency is relational and efferent-triggered," *Cognition*, vol. 107, pp. 693–704, May 2008.

[48] J. W. Moore, D. M. Wegner, and P. Haggard, "Modulating the sense of agency with external cues," *Consciousness and Cognition*, vol. 18, pp. 1056–1064, Dec. 2009.

[49] J. P. Ebert and D. M. Wegner, "Time warp: Authorship shapes the perceived timing of actions and events," *Consciousness and Cognition*, vol. 19, pp. 481–489, Mar. 2010.

[50] P. D. Marasco, K. Kim, J. E. Colgate, M. A. Peshkin, and T. A. Kuiken, "Robotic touch shifts perception of embodiment to a prosthesis in targeted reinnervation amputees," *Brain*, vol. 134, pp. 747–758, Mar. 2011.

[51] N. Jiang, S. Dosen, K.-R. Muller, and D. Farina, "Myoelectric control of artificial limbs—is there a need to change focus? [in the spotlight]," *IEEE Signal Processing Magazine*, vol. 29, no. 5, pp. 152–150, 2012.

[52] E. Scheme and K. Englehart, "Electromyogram pattern recognition for control of powered upper-limb prostheses: State of the art and challenges for clinical use," *The Journal of Rehabilitation Research and Development*, vol. 48, no. 6, p. 643, 2011.

[53] A. Chadwell, L. Kenney, S. Thies, A. Galpin, and J. Head, "The Reality of Myoelectric Prostheses: Understanding What Makes These Devices Difficult for Some Users to Control," *Frontiers in Neurorobotics*, vol. 10, Aug. 2016.

[54] J. S. Schofield, K. R. Evans, J. P. Carey, and J. S. Hebert, "Applications of sensory feedback in motorized upper extremity prosthesis: a review," *Expert Review of Medical Devices*, vol. 11, pp. 499–511, Sept. 2014.

[55] G. Valle, "Peripheral neurostimulation for encoding artificial somatosensations," *European Journal of Neuroscience*, vol. 56, pp. 5888–5901, Nov. 2022.

[56] K.-H. Hong, P. H. D. Trieu, and J. S. Schofield, "Characterizing the Sense of Embodiment: the Development of a Sensorimotor Robotic Platform," in *2023 32nd IEEE International Conference on Robot and Human Interactive Communication (RO-MAN)*, (Busan, Korea, Republic of), pp. 191–196, IEEE, Aug. 2023.

[57] R. Oldfield, "The assessment and analysis of handedness: The Edinburgh inventory," *Neuropsychologia*, vol. 9, pp. 97–113, Mar. 1971.

[58] R. T. Azevedo, V. Ainley, and M. Tsakiris, “Cardio-visual integration modulates the subjective perception of affectively neutral stimuli,” *International Journal of Psychophysiology*, vol. 99, pp. 10–17, Jan. 2016.

[59] E. A. Caspar, A. Cleeremans, and P. Haggard, “The relationship between human agency and embodiment,” *Consciousness and Cognition*, vol. 33, pp. 226–236, May 2015.

[60] K. Engbert, A. Wohlschläger, R. Thomas, and P. Haggard, “Agency, subjective time, and other minds.,” *Journal of Experimental Psychology: Human Perception and Performance*, vol. 33, no. 6, pp. 1261–1268, 2007.

[61] R. Fereday and M. J. Buehner, “Temporal binding and internal clocks: No evidence for general pacemaker slowing.,” *Journal of Experimental Psychology: Human Perception and Performance*, vol. 43, no. 5, pp. 971–985, 2017.

[62] G. R. Humphreys and M. J. Buehner, “Magnitude estimation reveals temporal binding at super-second intervals.,” *Journal of Experimental Psychology: Human Perception and Performance*, vol. 35, no. 5, pp. 1542–1549, 2009.

[63] A. W. Shehata, M. Rehani, Z. E. Jassat, and J. S. Hebert, “Mechanotactile Sensory Feedback Improves Embodiment of a Prosthetic Hand During Active Use,” *Frontiers in Neuroscience*, vol. 14, p. 263, Mar. 2020.

[64] J. S. Schofield, C. E. Shell, Z. C. Thumser, D. T. Beckler, R. Nataraj, and P. D. Marasco, “Characterization of the Sense of Agency over the Actions of Neural-machine Interface-operated Prostheses,” *Journal of Visualized Experiments*, p. 58702, Jan. 2019.

[65] M. Tsakiris, P. Haggard, N. Franck, N. Mainy, and A. Sirigu, “A specific role for efferent information in self-recognition,” *Cognition*, vol. 96, pp. 215–231, July 2005.

[66] D. Bates, M. Mächler, B. Bolker, and S. Walker, “Fitting Linear Mixed-Effects Models Using **lme4**,” *Journal of Statistical Software*, vol. 67, no. 1, 2015.

[67] H. Akaike, “A new look at the statistical model identification,” *IEEE Transactions on Automatic Control*, vol. 19, pp. 716–723, Dec. 1974.

[68] M. E. Brooks, K. Kristensen, K. J. van Benthem, A. Magnusson, C. W. Berg, A. Nielsen, H. J. Skaug, M. Mächler, and B. M. Bolker, "glmmTMB Balances Speed and Flexibility Among Packages for Zero-inflated Generalized Linear Mixed Modeling," *The R Journal*, vol. 9, no. 2, p. 378, 2017.

[69] A. Kuznetsova, P. B. Brockhoff, and R. H. B. Christensen, "**lmerTest** Package: Tests in Linear Mixed Effects Models," *Journal of Statistical Software*, vol. 82, no. 13, 2017.

[70] F. Hartig, "DHARMa: Residual Diagnostics for Hierarchical (Multi-Level / Mixed) Regression Models," Aug. 2016. Institution: Comprehensive R Archive Network Pages: 0.4.7.

[71] J. C. Pinheiro and D. M. Bates, *Mixed-effects models in S and S-PLUS*. Springer, 2000.

[72] R. V. Lenth, "emmeans: Estimated Marginal Means, aka Least-Squares Means," Oct. 2017. Institution: Comprehensive R Archive Network Pages: 1.11.2.

[73] V. I. Petkova and H. H. Ehrsson, "When Right Feels Left: Referral of Touch and Ownership between the Hands," *PLoS ONE*, vol. 4, p. e6933, Sept. 2009.

[74] H. H. Ehrsson, C. Spence, and R. E. Passingham, "That's My Hand! Activity in Premotor Cortex Reflects Feeling of Ownership of a Limb," *Science*, vol. 305, pp. 875–877, Aug. 2004.

[75] U. Wijk, I. K. Carlsson, C. Antfolk, A. Björkman, and B. Rosén, "Sensory Feedback in Hand Prostheses: A Prospective Study of Everyday Use," *Frontiers in Neuroscience*, vol. 14, p. 663, July 2020.

[76] M. Markovic, M. A. Schweisfurth, L. F. Engels, D. Farina, and S. Dosen, "Myocontrol is closed-loop control: incidental feedback is sufficient for scaling the prosthesis force in routine grasping," *Journal of NeuroEngineering and Rehabilitation*, vol. 15, p. 81, Dec. 2018.

[77] P. Beckerle, R. Kõiva, E. A. Kirchner, R. Bekrater-Bodmann, S. Dosen, O. Christ, D. A. Abbink, C. Castellini, and B. Lenggenhager, "Feel-Good Robotics: Requirements on

Touch for Embodiment in Assistive Robotics," *Frontiers in Neurorobotics*, vol. 12, p. 84, Dec. 2018.

[78] D. Blustein, A. Wilson, and J. Sensinger, "Assessing the quality of supplementary sensory feedback using the crossmodal congruency task," *Scientific Reports*, vol. 8, p. 6203, Apr. 2018.

[79] I. Cuberovic, A. Gill, L. J. Resnik, D. J. Tyler, and E. L. Graczyk, "Learning of Artificial Sensation Through Long-Term Home Use of a Sensory-Enabled Prosthesis," *Frontiers in Neuroscience*, vol. 13, p. 853, Aug. 2019.

[80] S.-J. Blakemore, D. M. Wolpert, and C. D. Frith, "Abnormalities in the awareness of action," *Trends in Cognitive Sciences*, vol. 6, pp. 237–242, June 2002.

[81] P. Haggard, "Conscious intention and motor cognition," *Trends in Cognitive Sciences*, vol. 9, pp. 290–295, June 2005.

[82] M. V. Sanchez-Vives, B. Spanlang, A. Frisoli, M. Bergamasco, and M. Slater, "Virtual Hand Illusion Induced by Visuomotor Correlations," *PLoS ONE*, vol. 5, p. e10381, Apr. 2010.

[83] W. Kirsch, W. Kunde, and O. Herbort, "Intentional binding is unrelated to action intention.," *Journal of Experimental Psychology: Human Perception and Performance*, vol. 45, pp. 378–385, Mar. 2019.

[84] G. Kong, C. Aberkane, C. Desoche, A. Farnè, and M. Vernet, "No evidence in favor of the existence of "intentional" binding.," *Journal of Experimental Psychology: Human Perception and Performance*, vol. 50, pp. 626–635, June 2024.

[85] M. J. Buehner and G. R. Humphreys, "Causal Binding of Actions to Their Effects," *Psychological Science*, vol. 20, pp. 1221–1228, Oct. 2009.

[86] A. M. Cravo, P. M. E. Claessens, and M. V. C. Baldo, "Voluntary action and causality in temporal binding," *Experimental Brain Research*, vol. 199, pp. 95–99, Oct. 2009.

[87] T. Kawabe, W. Roseboom, and S. Nishida, "The sense of agency is action–effect causality perception based on cross-modal grouping," *Proceedings of the Royal Society B: Biological Sciences*, vol. 280, p. 20130991, July 2013.

[88] M. D'Alonzo, F. Clemente, and C. Cipriani, "Vibrotactile Stimulation Promotes Embodiment of an Alien Hand in Amputees With Phantom Sensations," *IEEE Transactions on Neural Systems and Rehabilitation Engineering*, vol. 23, pp. 450–457, May 2015.

[89] M. D'Alonzo and C. Cipriani, "Vibrotactile Sensory Substitution Elicits Feeling of Ownership of an Alien Hand," *PLoS ONE*, vol. 7, p. e50756, Nov. 2012.

[90] M. Synofzik, G. Vosgerau, and A. Newen, "Beyond the comparator model: A multifactorial two-step account of agency," *Consciousness and Cognition*, vol. 17, pp. 219–239, Mar. 2008.

[91] M. Dawson, H. Williams, G. Murgatroyd, J. Hebert, and P. Pilarski, "brachIOplexus: Myoelectric Training Software for Clinical and Research Applications," *Myoelectric Controls Symposium*, July 2020. Artwork Size: 33MB Publisher: Myoelectric Controls Symposium.

[92] K. Englehart and B. Hudgins, "A robust, real-time control scheme for multifunction myoelectric control," *IEEE Transactions on Biomedical Engineering*, vol. 50, pp. 848–854, July 2003.

[93] B. P. Christie, E. L. Graczyk, H. Charkhkar, D. J. Tyler, and R. J. Triolo, "Visuotactile synchrony of stimulation-induced sensation and natural somatosensation," *Journal of Neural Engineering*, vol. 16, p. 036025, June 2019.

Chapter 3 Tactile and visual information to support spatial navigation

The majority of this chapter is in preparation for submission as:

Hong, K., I. Soltani Bozchalooi, & Schofield, J. S. (In preparation 2026, April). Tactile sensory substitution for path guidance and spatial localization across visual experience. Scientific Reports.

3.1 Chapter preface

This chapter examines tactile sensory substitution for path guidance and spatial localization across individuals with varying visual acuity. Specifically, it asks whether structured tactile cues can support navigation-relevant behavior when vision is impaired, and whether these cues are used differently by individuals with visual impairment compared with sighted individuals navigating without visual information. A central objective of this chapter is to determine how visual experience shapes the interpretation and use of tactile cues. The results can inform the design of tactile guidance systems that deliver interpretable spatial information and support mobility in environments where visual feedback is limited. Finally, this chapter discusses future directions toward developing assistive devices that use tactile sensory substitution to improve mobility for individuals with vision loss.

3.2 Introduction

Humans integrate multiple sensory cues from the external environment to navigate independently in familiar or unfamiliar environments [**1**]. Through multisensory integration, individuals establish their location relative to nearby landmarks, select appropriate routes, and continuously monitor progress to confirm arrival at a destination [**2**]. In most everyday contexts, vision typically dominates this process by providing a primary spatial reference for landmark recognition, heading estimation, and route monitoring, with other modalities serving complementary or compensatory roles when visual information is limited [**3**].

When vision is reduced or unavailable, whether temporarily in sighted people or chronically in people with visual impairments, the nervous system can recruit alternative sensory channels through sensory substitution, in which task-relevant information is delivered through a different modality than the one that is impaired [**4**]. A well-known example is Braille reading, where tactile patterns convey text that is ordinarily acquired visually. For mobility and wayfinding, people with visual impairments, ranging from those with moderate vision problems to those facing complete blindness, often rely on tactile and auditory cues to gather and encode spatial information for navigation [**5**], [**6**], [**5**]. Common mobility aids include white canes and guide dogs, which assist with obstacle detection and safe travel, and people with visual impairments often also use auditory cues to infer aspects of spatial representations. Despite these compensatory strategies, navigating environments remains challenging because reduced visual access can limit distance estimation and the ability to infer spatial relationships from the surrounding layout [**7**], [**8**]. These constraints may reduce autonomy and confidence, increase anxiety before and during navigation, contribute to disorientation, and ultimately restrict participation in societal roles [**9**], [**10**].

Cognitive spatial maps are internal mental representations of an environment that support wayfinding beyond immediate sensory cue following. They enable individuals to localize themselves relative to landmarks, plan and replan routes, estimate distances, infer spatial relationships such as connectivity and direction, and exploit shortcuts when available [**11**], [**12**], [**13**], [**14**]. In particular, cognitive maps may help individuals keep track of where they are and which way they are facing as they move, by updating orientation and movement direction in complementary reference frames, namely egocentric and allocentric spatial representations. In an egocentric reference frame, direction and location are encoded relative to the individual's body and current direction of travel, supporting actions such as maintaining a heading and executing turns based on one's own perspective. In an allocentric reference frame, direction and location are encoded relative to the external environment, for example with respect to stable landmarks or a global layout, supporting alignment and planning based on relationships among locations in the space.

For people with visual impairments, tactile information can convey layout structure and support the formation of cognitive map like representations [**15**], [**16**], [**17**], [**18**], [**19**], [**20**], [**21**]. To use such information for navigation, however, people with visual impairments may use spatial scaling, which is the ability to translate distances and directions represented on the tactile cue into actions in the full-sized environment. However, it is often found to be difficult for those as vision often conveys more informative spatial cues compared to other sensory modalities [**22**]. For this reason, even though people with visual impairments can form cognitive maps through tactile sensation, their cognitive maps may be less accurate or detailed [**23**], [**24**].

Although many studies indicate the potential of tactile maps to support people with visual impairments in navigation [**25**], [**26**], tactile map based navigation is often studied using displays that provide static layout information, rather than providing adaptive cues that can be accessed continuously while walking. Moreover, because tactile perception has limited spatial bandwidth, tactile maps often require strong generalization and careful filtering of features; otherwise, they become cluttered and difficult to parse, with large spaces often requiring multiple maps [**27**]. This creates practical tradeoffs: larger-scale maps can reduce portability and complicate deployment in real settings, while small-format tactile maps may omit details needed for effective use [**28**]. Finally, because different studies use different tasks and measures, it remains unclear when tactile map information primarily supports route-level (egocentric) behavior versus survey-level (allocentric) representations, and how this tradeoff varies across visual experience [**29**], [**30**].

Together, these limitations motivate an important open question; that is when tactile information is sparse and only provides a scaled representation of the environment, how accurately can people with visual impairments translate that scale into navigation, maintain and update orientation, and localize goals, compared with sighted people? Addressing this gap requires evaluating navigation under tactile cues that do not explicitly encode full spatial structure, but instead require the user to infer distances and directions through scaling and reference frame updating.

Accordingly, we tested whether structured tactile cues could support navigation-relevant behavior when vision is unavailable, and how performance differs across visual experience. In this study, we provided tactile displays that presented only a scaled representation of the outer boundary of the experimental space. This boundary cue was intended to calibrate participants' sense of the environment's global extent and shape and to support spatial scaling by linking distance on the tactile cue to distance experienced while walking. Our tasks therefore examined how access to this minimal global-extent cue influenced navigation behaviors during (i) trajectory following under tactile guidance and (ii) target localization without trajectory guidance, and how these effects differ across visual experience.

We quantified navigation performance at three complementary levels. First, we evaluated how accurately participants followed prescribed routes through tactile trajectory cues, comparing individuals with visual impairment with sighted participants navigating without vision. Second, we assessed heading control during movement by decomposing errors present in egocentric and allocentric reference frames, which helped distinguish body-centered orientation updating from environment-centered alignment. Third, we measured the ability to localize two target areas without tactile trajectory cues. Because the first target began from a standardized starting position, its error primarily reflected interpretation of tactile scale and target location; the second target, by contrast, reflected how spatial error accumulated after movement and reorientation. Together, these measures tested whether tactile cues supported both immediate guidance and map-based spatial reasoning, and whether these abilities depended on visual experience.

3.3 Methods

3.3.1 Participants

We recruited a cohort of sighted participants (N= 16) aged 18-30 years (mean age: 21.3 years; 53% male) and people with visual impairments (VIP, N=6). Most of the VIPs lost their vision later in life, except for one individual who lost vision at approximately three months of age. All participants provided written informed consent prior to participation, and protocols were approved by the UC Davis Institutional Review Board.

3.3.2 Experimental setup

Custom-designed tactile displays (50 mm $\times$ 50 mm) were scaled to dimensionally represent the 3.7 m $\times$ 3.7 m experimental space. Using raised dots, each tile conveyed navigational instructions for two tasks.

For the path following task, each tactile display encoded the prescribed route as a sequence of raised dots that participants traced to infer the intended direction of travel. Turns were indicated by changes in the direction of consecutive dots. The first turning point was positioned at a fixed distance from the starting point along the initial path and corresponded to reaching 1/4, 2/4, or 3/4 of the experimental-space's length depending on the prescribed path. In the one-turn paths, participants followed the initial straight dot sequence to the first turning point, executed a 90 degree left or right turn, and then continued along the final straight segment until reaching the boundary. In the two-turn paths, participants executed the first turn at as above, and then executed a second 90 degree turn at the midpoint of the remaining distance along the subsequent segment, as illustrated in Fig. 3.1A.

For the target localization task, two target areas were selected on each trial from four candidate target areas, where each candidate was represented as a dot-defined square region. The candidate target centers were positioned at fixed locations relative to the starting point, which was located at the midpoint of the bottom boundary. Specifically, the two lower

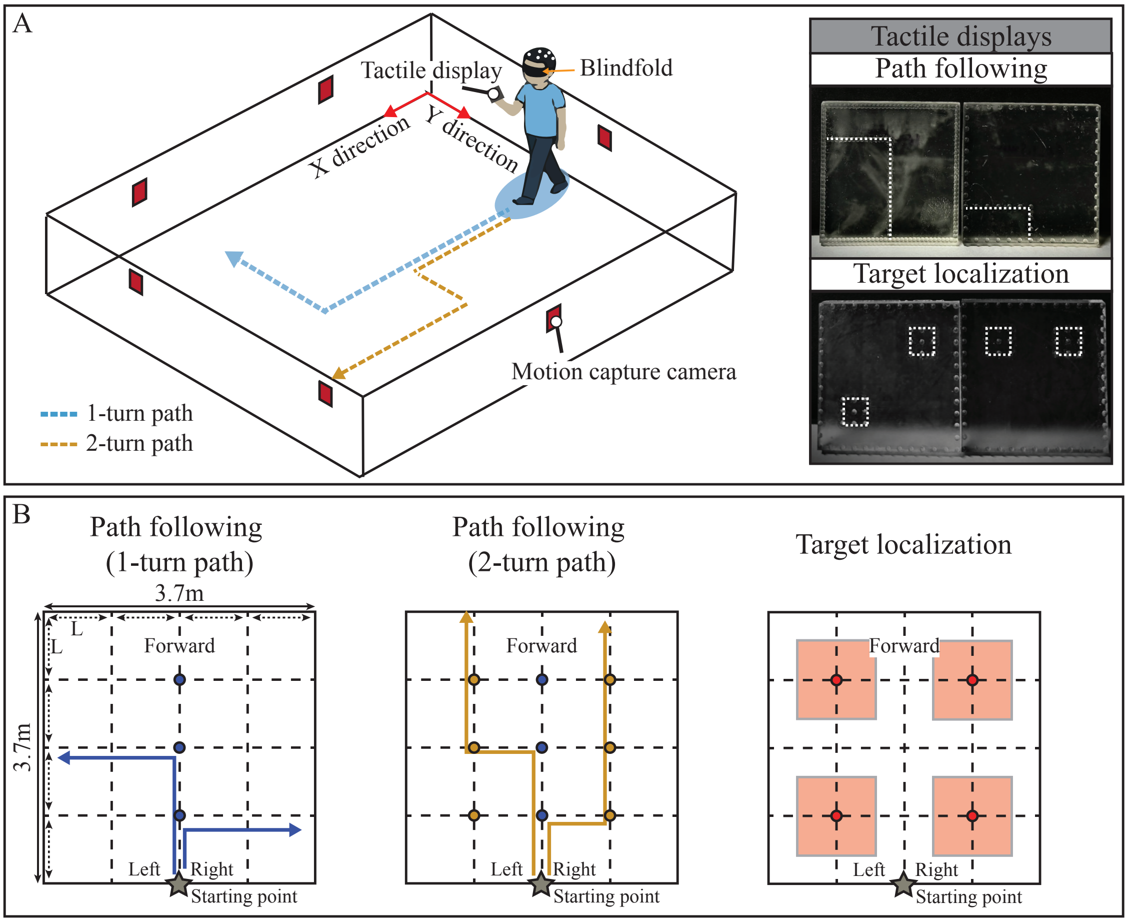

FIGURE 3.1. Experimental setup and task schematics. (A) Overview of the setup, including the motion capture camera system, example tactile displays used for the path following and target localization tasks, and a participant wearing a blindfold and a marker cap for tracking position during each trial. (B) Participants completed both tasks within a 3.7 m * 3.7 m experimental-space, where L represents 1/4 of the experimental-space length. The experimental-space was divided into four equal segments along each dimension, where L indicates one quarter of the side length. In the path following task, participants began at the fixed starting position (gray star). In the left-panel (1-turn path), blue circles indicate possible first turning points at L, 2L, or 3L from the starting point along the initial forward segment. In the middle panel (2-turn path), blue circles again indicate possible first turning points along the initial forward path. After the first turn, orange circles indicate possible second turning points positioned along the horizontal line extending left or right from the first turning point. All turning points were located at predefined grid intersections at L intervals. In the target localization task, shaded square regions indicate candidate target areas.

candidate centers were located 1/4 of the experimental-space's length above the bottom boundary and 1/4 of the length to the left or right of the starting point, and the two upper candidates were located 3/4 of the length above the bottom boundary and 1/4 of the length to the left or right of the starting point. Each target area was rendered as a square cluster of raised dots centered on the candidate center, with a square side length equal to 1/4 of the experimental-space's length, as illustrated in Fig. 3.1B.

Participants wore a hat instrumented with reflective markers (12.7 mm (1/2) M3 Markers) for motion capture to capture their precise position in the experimental space throughout the task. Participants completed two task in a fixed order: (1) path following task and (2)target localization task. In the **path following task**, participants followed the path guidance presented on the tactile displays. Before each trial, participants were positioned at the fixed starting point located at the midpoint of the bottom boundary of the experimental-space and oriented along the forward direction, corresponding to the initial walking direction (Fig. 3.1B). Participants were then randomly assigned one of 12 path-following tactile displays, comprising six two-turn cases and six one-turn cases. Each participant completed a subset of eight randomly assigned path following trials in total, including four one-turn path trials and four two-turn path trials. In the **target localization task**, the tactile displays presented two target areas selected from the four predefined target areas, as described in Fig. 3.1. Before each trial, participants started from the bottom center of the workspace (starting point) and were aligned to face the forward direction to ensure a consistent initial orientation. Participants completed 12 ordered target pair cases, corresponding to all ordered combinations of two targets chosen from the four predefined target locations (Fig. 3.1B). In each trial, participants were instructed to localize two sequential target areas, and the 12 cases were presented in a randomized order.

Across both tasks, participants completed 20 trials in total (path-following: 8; target localization: 12). Sighted participants completed the full 20-trial protocol twice, with sessions separated by one week: once without a blindfold and once while blindfolded to minimize learning effects. The order of these visual conditions was counterbalanced across participants.

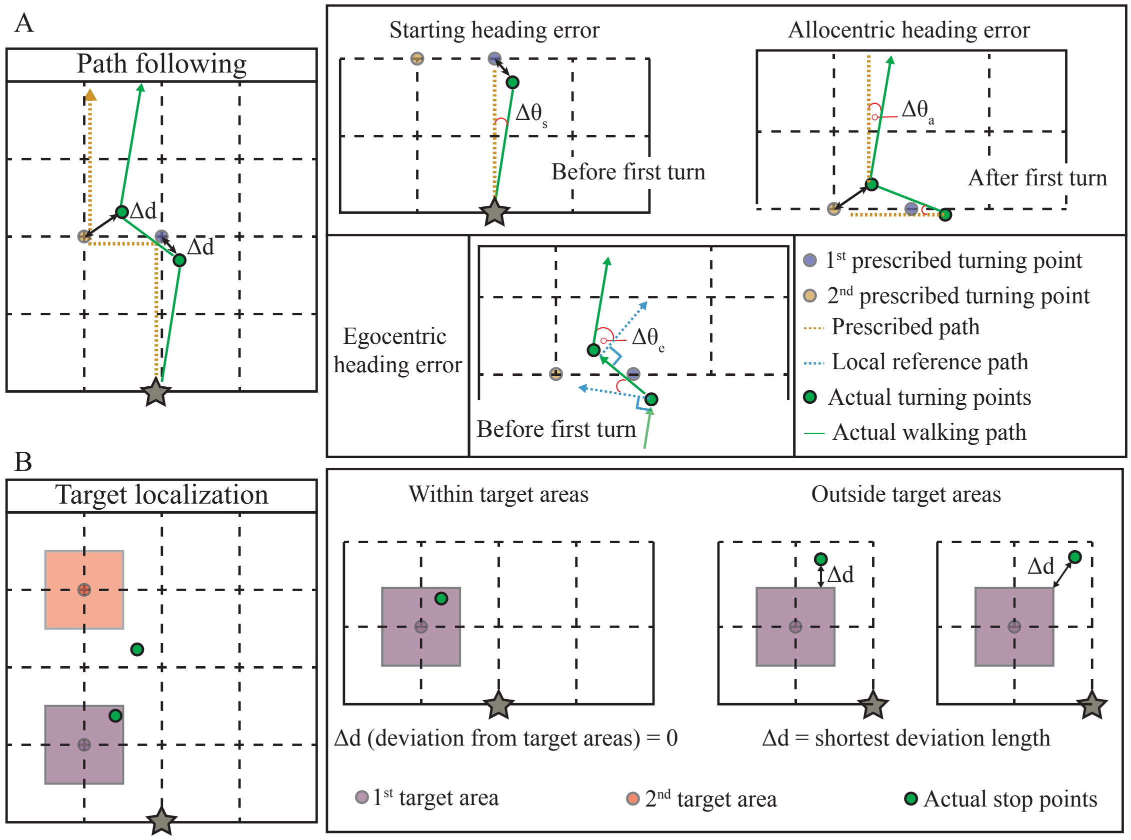

FIGURE 3.2. Description of tactile navigation outcome metrics. Schematic overview of how outcome measures were computed for each task. (A) Path following task: path deviation from the prescribed turning points (Δd), starting heading error ($\Delta\theta_s$), defined as the heading difference between the prescribed initial straight path segment and the participant's actual initial path, allocentric heading error ($\Delta\theta_a$), quantified as the heading difference between the prescribed path segment and the participant's actual path segment, and egocentric heading error ($\Delta\theta_e$), defined as the heading difference between the local reference path segment(90 degree to the preceding actual path segment) and the participant's subsequent actual path segment (B) Target localization task: deviation from target areas (Δd), computed as the minimum distance between the candidate target area and the participant's actual stop points.

3.3.3 Outcome measures

Participants' two dimensional position data were recorded using six motion capture systems (Flex3, OptiTrack Inc.). Reflective markers mounted on a hat were tracked throughout each trial to obtain planar x and y trajectories in the experimental space. The raw marker trajectories were exported and processed offline to generate a continuous 2D position time series for each trial. Missing samples caused by temporary marker occlusion were gap-filled through the Kalman filter option provided in the OptiTrack motion capture software, and the resulting trajectories were smoothed using a low-pass Butterworth filter to reduce measurement noise. The filtered 2D position data were then used for computation of the performance outcome measures described below (Fig. 3.2).

(1) Path deviation: To quantify the accuracy with which participants inferred and executed direction changes at each prescribed turning points, path deviation at prescribed turning points was analyzed in the path following task. To quantify how accurately they estimate turning points using the tactile cues, the **path deviation from the prescribed path** is quantified as the distance between the prescribed turning points and the participant's actual turning point. A control trajectory for each path condition was computed from the data collected from the sighted participants without the blindfold (S group) using the medoid trajectory. The medoid trajectory was defined as the trajectory that minimized the sum of Procrustes distances to all other sighted trajectories. This medoid trajectory was used as the control path for comparison to normative sighted performance. Then, the **path deviation from the control path** is quantified as the distance between turning points from the control path and the participant's actual turning point.

(2) Heading error: To quantify directional accuracy during tactile navigation, heading error was computed as the angular difference between participants' observed walking direction and either the direction of the prescribed path segment or the expected 90 degree change in heading at turning points. In path following task, participants interpreted the tactile cues to orient themselves at each turning point (left or right) with the intent of maintaining straight walking following each prescribed path segment. Before computing heading errors (descriptions below), each prescribed path segment was defined as the straight line connecting consecutive prescribed waypoints (start to turning point 1, turning point 1 to turning point 2 for two-turn cases, and the final turning point to the endpoint). Participants' observed headings along the

corresponding path segments were then compared against prescribed path headings to compute three complementary heading metrics.

Starting heading error was defined as the angular deviation between the participant's initial observed heading and the direction of the first prescribed straight path segment (start to turning point 1). This metric reflects how accurately they maintained straight walking.

Allocentric heading error was defined as the angular deviation between the participant's observed heading along each post-turn path segment and the direction of the corresponding prescribed path segment in the global coordinate frame (turning point 1 to turning point 2, or the final turning point to the endpoint). It allows to capture how accurately participants aligned their walking direction with the externally defined path.

Egocentric heading error was defined as the angular deviation between the participant's observed heading along each post-turn path segment and the expected post-turn heading, which was defined as a 90 degree relative to the participant's preceding walking direction. This metric captures how accurately participants executed the required turn in a body-centered reference frame.

(3) Target deviation: To capture how accurately participants localized the target areas without trajectory guidance in the target localization task, target deviation was quantified as the minimum Euclidean distance between the target area and the participant's final stopping point. If the participant stopped within the target area, the target deviation was set to zero. It reflects how accurately they inferred the scaled tactile layout into a cognitive map of target locations in the experimental space.

3.4 Results

Participants were grouped as sighted without a blindfold (S), sighted with the blindfold (S-BF), and participants with visual impairments (VIP). All subsequent analyses are reported using these group labels.

3.4.1 Path deviation in the path following task

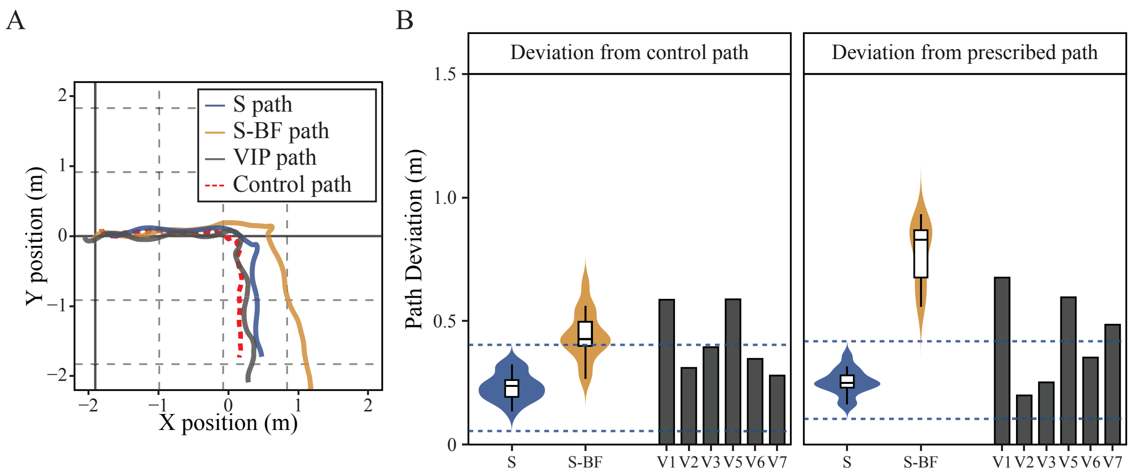

FIGURE 3.3. Path deviation in the path-following task across groups. (A) Examples of trajectories for each group (S: sighted individuals without a blindfold, S-BF: sighted individuals with the blindfold, and VIP: participants with visual impairments), with the sighted control path shown as a red dashed line. (B) Path deviation from the prescribed turning point and from the sighted control path. For sighted participants (S and S-BF), distributions are shown with the median and interquartile range (IQR); for participants with visual impairments (VIP), individual medians are shown (V1 - V7). The blue dashed line denotes the range observed in the sighted group without a blindfold (S).

Path deviation in the path following task was quantified as the Euclidean distance between the prescribed turning point and the participant's actual turning point. To enable comparison across groups, we also computed a medoid trajectory by averaging the trajectories of sighted participants to obtain a control "sighted" path, which served as a baseline for evaluating deviations in other participant groups/conditions.

Sighted participants who wore a blindfold and relied on the tactile display (S-BF) exhibited significantly greater path deviation than sighted participants without a blindfold (S) (Wilcoxon rank-sum test; $p < 0.001$ for deviation from both the prescribed turning point and the sighted control path), as shown in Fig. 3.3B. For participants with visual impairments (V1 - V7), path deviation was summarized at the individual level as the median [IQR] across trials for deviation from the prescribed turning point and from the sighted control path. V1 and V5 exhibited the greater deviations among VIPs (V1: $\Delta d = 0.68$ [0.43, 1.27] from the prescribed path, $\Delta d = 0.59$ [0.52, 1.29] from the control path, V5: $\Delta d = 0.60$ [0.56, 0.93] from the prescribed path, $\Delta d = 0.59$ [0.40, 0.93] from the control path). Notably, the deviations for V1 and V5 exceeded the range observed in the sighted group without a blindfold (S) for both metrics, whereas the remaining VIPs exhibited deviations that overlapped with the S distribution.

3.4.2 Heading error in the path following task

Heading error in the path following task was quantified as the difference in actual participant's heading from the prescribed path (allocentric heading error) and from the local reference path (egocentric heading error). Additionally, starting heading quantified participants' ability to initiate the trial by walking straight along the prescribed initial segment, computed as the angular difference between the direction of the initial straight portion of the participant's trajectory and the prescribed initial path direction.

Sighted participants showed no differences in any of the three heading error measures when comparing trials performed with versus without a blindfold (Wilcoxon rank-sum test; $p > 0.05$). In contrast, the distribution of heading errors in sighted participants with the blindfold (S-BF) was shifted relative to the sighted, no-blindfold condition (S).

For the starting heading error, V1 and V5 exhibited larger heading error among VIPs and fell outside the sighted without blindfold data (S) distribution (V1: $\Delta\theta_s = -14.0$ [-17.33, -10.67]; V5: $\Delta\theta_s = -14.85$ [-18.45, -11.25]), whereas the remaining VIPs exhibited starting heading error values that overlapped with the S distributions. After completing the initial straight segment, VIPs oriented to the subsequent 90° turn in a manner comparable to sighted participants, with egocentric heading errors largely within

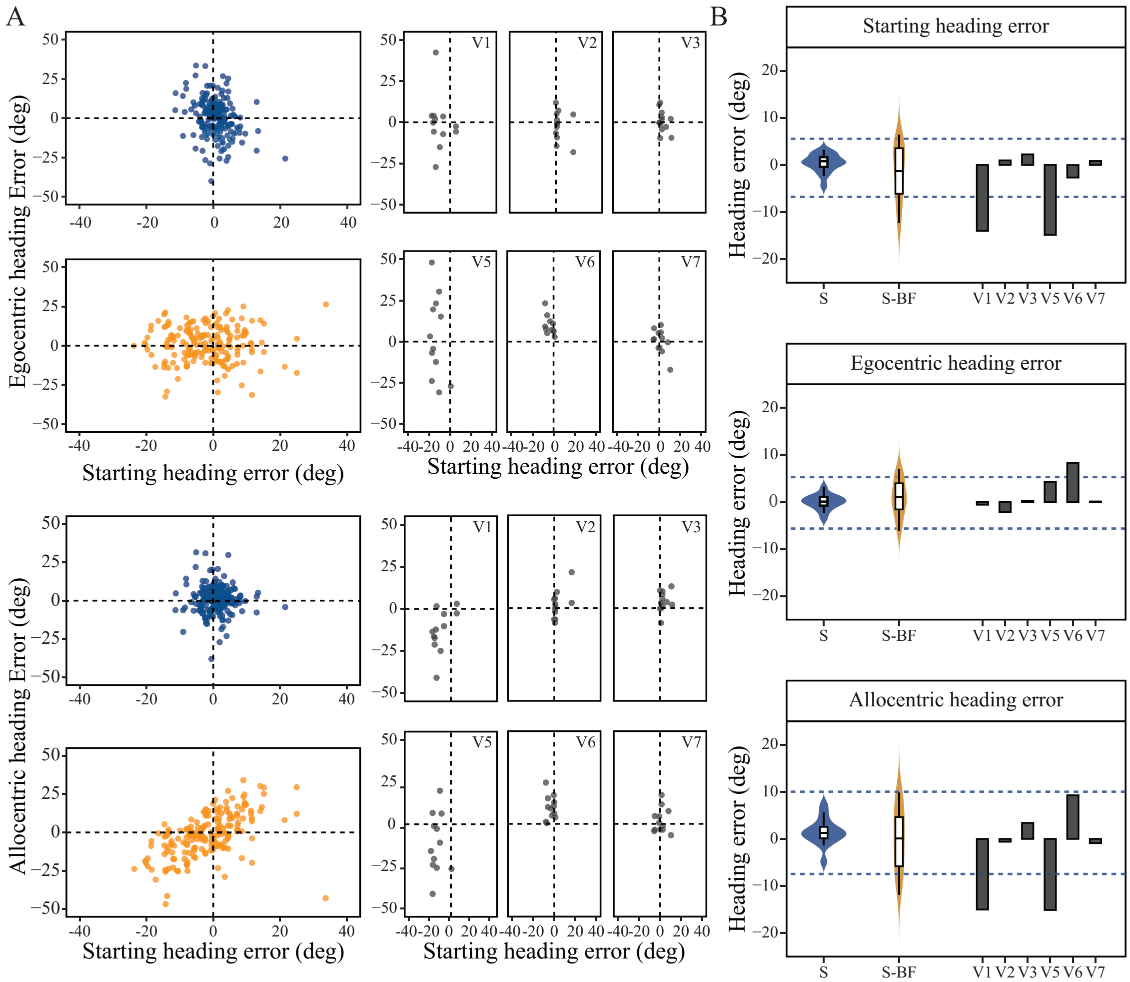

FIGURE 3.4. Heading error in the path-following task across groups. (A) Scatter plots show the relationship between starting heading error and egocentric heading error or allocentric heading error for sighted participants without a blindfold (S, blue), sighted participants with a blindfold (S-BF, orange), and each participants with visual impairments (V1 - V7, gray). (B) Summary plots show the group distributions for S and S-BF with median and interquartile range (IQR), and individual median values for V1 - V7. Blue dashed horizontal lines denote the range observed in the sighted group without a blindfold (S).

the S distribution; V6 was the only exception and deviated from the S distribution (V6: $\Delta\theta_e = 8.25$ [6.17, 10.34]).

For the allocentric heading error, which reflects how accurately participants followed the prescribed path segments, V1 and V5 again showed larger hearing error among VIPs and fell out of S distributions (V1: $\Delta\theta_a = -15.0$ [-19.26 $-$ 10.75]]; V5: $\Delta\theta_a = -15.11$ [-21.12, -9.09]).

3.4.3 Target deviation in the target localization task

Target deviation was defined as the minimum Euclidean distance from the boundary of the target area to the participant's final stopping point, computed separately for each target order.

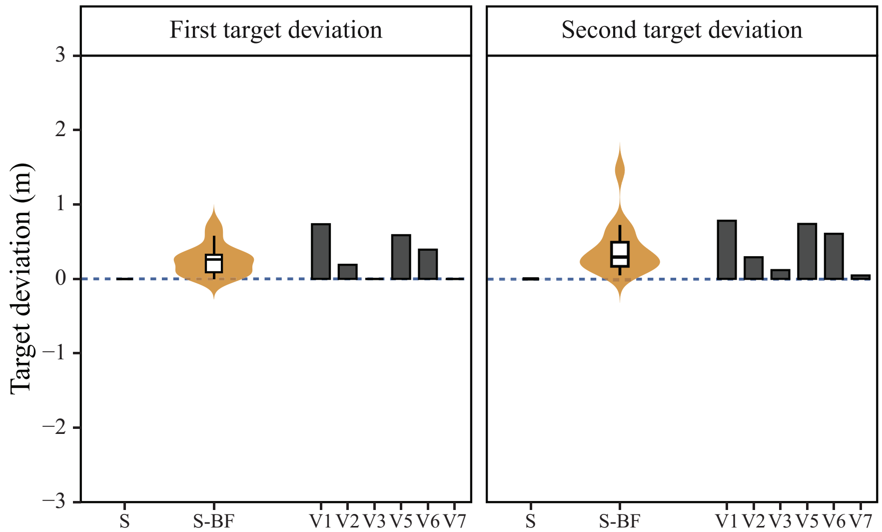

FIGURE 3.5. Target deviation for the target localization task across visual experience groups. Violin plots show the distribution for sighted participants without a blindfold (S) and sighted participants with a blindfold (S-BF), with median and interquartile range (IQR) overlaid. The blue dashed line indicates zero deviation (i.e., stopping within the target region). Sighted participants clustered near zero deviation, which compresses the distributions and makes the violins less visually prominent. (A) First target deviation. (B) Second target deviation. S distributions

Compared to sighted people without a blindfold (S), S-BF (sighted people with the blindfold) showed significantly greater deviation from both target areas (Wilcoxon rank-sum test; $p < 0.001$). In contrast, for the first target deviation, V3 and V7 reached the target area, with first target deviations of 0 [−0.005, 0.005] and 0 [−0.05, 0.05], respectively, whereas the remaining VIPs deviated from the target area. Notably, although V2 did not reach the first target area, V2's first target deviation (0.19 [0.05, 0.33]) was smaller than the S-BF's first target deviation (0.26 [0.09, 0.32]). For the second target deviation, VIPs showed more deviations from the second target area than for the first target area. However, V3 and V7 exhibited smaller target deviations than the S-BF group (S-BF: 0.30 [0.17, 0.50], V3: 0.12 [−0.07, 0.30], and V7: 0.05 [−0.03, 0.12]).

3.5 Discussion

Our results quantify the degree to which tactile cues can convey a scaled representation of space, together with trajectory guidance or goal location information, to support navigation relevant behavior when vision is limited, and how performance differs across visual experience. Across three complementary outcome measures, our results suggest a clear pattern; that is, removing vision in sighted participants increased navigation-relevant errors, whereas several participants with visual impairments (VIPs) performed within the range of the sighted individuals without a blindfold on multiple measures. Importantly, many tactile map studies evaluate performance through static tactile exploration tasks rather than the navigation [**29**], [**18**]. While at least one prior study has investigated navigation with tactile support in VIP populations [**31**], it did not systematically decompose navigation performance as in the present work. Together, these findings support that effective use of tactile cues depends not only on access to tactile information itself, but also on the user's ability to translate scale, stabilize heading, and update orientation during movement.

In the path-following task, path deviation indicates that removing vision reduced sighted participants' ability to estimate when to initiate a turn from the scaled tactile cue, producing significantly larger deviations than the sighted no-blindfold control. In contrast, most VIPs exhibited deviations that overlapped the sighted no blindfold control range, whereas V1 and V5 exceeded that range. Because deviation was computed at the prescribed turning points, these effects are consistent with differences in spatial scaling, that is, how participants translated distance on the tactile display into walked distance in the full-sized experimental-space. Spatial scaling strategies may therefore vary with visual experience, leading some participants to under- or over-estimate the distance to the turning point even when the same tactile information is available.

Prior work suggests that blindfolded adults can rely on a mental transformation strategy when scaling tactile maps, and that scaling uncertainty increases as the mismatch between map and workspace grows [**32**]. Consistent with this account, the larger turning point deviations in blindfolded sighted participants may reflect greater uncertainty in scaling when distance to the turn must be inferred from a small tactile representation rather than continuously monitored visually. For VIPs, overlap with the sighted individuals without a blindfold range indicates that a sparse tactile boundary cue can be sufficient to support accurate distance calibration for route execution in some individuals. However, the larger deviations observed for V1 and V5 suggest that mapping the tactile scale to action can vary across VIPs, potentially reflecting differences in calibration or strategy selection. Together, these findings indicate that tactile boundary cues can support accurate path execution, but that some users may benefit from additional information or training to achieve stable distance scaling. This may be explained by the fact that the lack of visual experience impairs the calibration of non-visual modalities [**33**].

Decomposing heading error into egocentric and allocentric components helps distinguish body centered turn execution from environment centered alignment. A notable pattern in the visually impaired group is that egocentric heading error generally overlapped the sighted no blindfold range, with V6 as the exception. This suggests that most participants with visual impairments could execute the required self-orientation in a body centered reference comparably to sighted participants, even when vision was unavailable. This result is aligned with previous studies which demonstrated that people with visual impairments mostly employ egocentric representation [**22**], [**6**]. In contrast, allocentric heading error showed larger deviations for V1 and V5. As allocentric heading compares the participant's post turn walking direction to the prescribed path direction, elevated allocentric error can reflect drift in global alignment after the turn. One possible explanation is that while VIPs can form an allocentric spatial representation, they seem to face more difficulties constructing it [**34**], [**35**], [**30**]. Our starting heading error results provide a plausible contributor to this pattern. Starting heading error can be interpreted as a baseline measure of participants' ability to begin the trial with a straight trajectory aligned to the prescribed initial segment. Because it is computed before any turning occurs, it primarily reflects initial heading calibration and straight line maintenance rather than post turn updating. When vision is unavailable, maintaining a straight heading depends more heavily on vestibular and proprioceptive signals, and individual differences in the reliability or weighting of these signals can increase variability in straight line walking [**36**].

Without trajectory guidance, target deviation reflects how accurately participants can localize the target areas using tactile information alone. Because participants were placed at a standardized starting position and oriented to a fixed forward direction at the start of each trial, the first target deviation primarily reflects how effectively they interpret the scaled tactile cue and use an allocentric representation to plan the initial movement to the goal. In contrast, the second target deviation reflects accumulated error after the first movement, because participants must update their internal estimate of position and orientation after reaching the first target before navigating to the second.

Within the visually impaired group, V3 and V7 reached the first target area and also showed smaller second target deviations than the sighted blindfold group. This pattern suggests that at least some participants with visual impairments can use the sparse tactile cue to form a sufficiently accurate internal representation of goal locations and maintain, or recover, orientation during movement. Across participants with visual impairments, second target deviation was generally larger than first target deviation. This is expected because the second target begins from a state that is no longer externally calibrated. After the first target, participants must rely more heavily on internal updating of position and heading based on self motion cues, which is susceptible to drift and compounding uncertainty. Any small error in distance estimation, stopping position, or reorientation at the first target propagates into the starting state for the second movement, and heading biases can further amplify spatial error over the subsequent walking distance. Thus, the increase from first to second target supports the idea that, under sparse tactile cues, the primary limitation is not only initial interpretation of the tactile scale, but also the stability of orientation updating and the accumulation of integration noise across sequential movements.

By providing only a scaled boundary cue, our results clarify what aspects of navigation can be supported by tactile scale information and where failures are likely to occur when vision is unavailable. The data suggest that many participants with visual impairments can use tactile scale information to construct a workable internal representation of the space, map their own position onto that representation, and update orientation across segments, whereas others show larger errors that appear to arise from initial heading calibration and environment centered alignment. This pattern indicates that navigation performance depends on vision history and individual strategy selection, but also that tactile scaling and updating may be supported through interface design and training. We note that this study included a small VIP cohort and summarized performance at the individual level, which highlights variability but limits statistical generalization. VIP participants also differed in vision history, and most lost vision later in life. Future work with larger cohorts and stratification by vision history will be needed to determine how visual experience moderates reliance on tactile scaling and reference frame updating, and to identify which interface features best support users who show larger initial heading and allocentric alignment errors.

Overall, the results show that a tactile scale cue can support meaningful navigation relevant behavior without vision, but performance depends strongly on the user's ability to translate scale and maintain stable orientation across movement. The heading decomposition suggests that body centered turn execution can remain relatively intact even when environment centered alignment is degraded, and the increase in error for the second target emphasizes the role of accumulated orientation updating. Furthermore, our data further indicate that using sighted individuals with occluded vision as a proxy for people with visual impairments may not accurately capture between-group performance differences. Accordingly, future studies of navigation ability, as well as the development and evaluation of assistive devices for individuals with visual impairments, should carefully consider participant cohort selection and interpret findings within the context of the specific population from which the data were derived. These findings help clarify when tactile cues may support route execution versus map based reasoning, and they motivate tactile aid designs that prioritize scale calibration and orientation stabilization while maintaining portability.

References

[1] K. Lynch, ““the image of the environment” and “the city image and its elements”: From the image of the city (1960),” in *The urban design reader*, pp. 125–138, Routledge, 2013.

[2] R. M. Downs and D. Stea, “Cognitive maps and spatial behaviour: Process and products,” in *The Map Reader* (M. Dodge, R. Kitchin, and C. Perkins, eds.), pp. 312–317, Wiley, 1 ed., 2011.

[3] M. E. Struiksma, M. L. Noordzij, and A. Postma, “What is the link between language and spatial images? behavioral and neural findings in blind and sighted individuals,” *Acta Psychologica*, vol. 132, no. 2, pp. 145–156, 2009.

[4] P. Bach-Y-Rita, C. C. Collins, F. A. Saunders, B. White, and L. Scadden, “Vision substitution by tactile image projection,” *Nature*, vol. 221, no. 5184, pp. 963–964, 1969.

[5] R. Passini and G. Proulx, “Wayfinding without vision: An experiment with congenitally totally blind people,” *Environment and Behavior*, vol. 20, no. 2, pp. 227–252, 1988.

[6] A. Pasqualotto and M. J. Proulx, “The role of visual experience for the neural basis of spatial cognition,” *Neuroscience & Biobehavioral Reviews*, vol. 36, no. 4, pp. 1179–1187, 2012.

[7] F. Gaunet and C. Thinus-Blanc, “Early-blind subjects’ spatial abilities in the locomotor space: Exploratory strategies and reaction-to-change performance,” *Perception*, vol. 25, no. 8, pp. 967–981, 1996.

[8] J. F. Herman, S. P. Chatman, and S. F. Roth, “Cognitive mapping in blind people: Acquisition of spatial relationships in a large-scale environment,” *Journal of Visual Impairment & Blindness*, vol. 77, no. 4, pp. 161–166, 1983.

[9] W. Jeamwatthanachai, M. Wald, and G. Wills, “Indoor navigation by blind people: Behaviors and challenges in unfamiliar spaces and buildings,” *British Journal of Visual Impairment*, vol. 37, no. 2, pp. 140–153, 2019.

[10] R. Velázquez, “Mobility of visually impaired people: fundamentals and ict assistive technologies,” *OPENAIRE*, 2017.

[11] L. K. Morgan, S. P. MacEvoy, G. K. Aguirre, and R. A. Epstein, “Distances between real-world locations are represented in the human hippocampus,” *Journal of Neuroscience*, vol. 31, no. 4, pp. 1238–1245, 2011.

[12] L. Deuker, J. L. Bellmund, T. Navarro Schröder, and C. F. Doeller, “An event map of memory space in the hippocampus,” *elife*, vol. 5, p. e16534, 2016.

[13] W. R. Wiener, *Foundations of Orientation and Mobility: History and Theory - Volume I*. American Printing House for the Blind, fourth edition ed., 2010.

[14] R. G. Golledge, *Wayfinding behavior: Cognitive mapping and other spatial processes*. JHU press, 1999.

[15] P. Caddeo, F. Fornara, A. M. Nenci, and A. Piroddi, “Wayfinding tasks in visually impaired people: the role of tactile maps,” *Cognitive Processing*, vol. 7, pp. 168–169, 2006.

[16] M. Espinosa and E. Ochaíta, “Using tactile maps to improve the practical spatial knowledge of adults who are blind,” *Journal of Visual Impairment & Blindness*, vol. 92, no. 5, pp. 338–345, 1998.

[17] M. Espinosa, S. Ungar, E. Ochaíta, M. Blades, and C. Spencer, “Comparing methods for introducing blind and visually impaired people to unfamiliar urban environments,” *Journal of Environmental Psychology*, vol. 18, no. 3, pp. 277–287, 1998.

[18] M. Bleau, C. Van Acker, N. Martiniello, J. P. Nemargut, and M. Ptito, “Cognitive map formation in the blind is enhanced by three-dimensional tactile information,” *Scientific Reports*, vol. 13, no. 1, p. 9736, 2023.

[19] S. Ungar, M. Blades, and C. Spencer, “The role of tactile maps in mobility training,” *British Journal of Visual Impairment*, vol. 11, no. 2, pp. 59–61, 1993.

[20] S. Ungar, M. Blades, C. Spencer, and K. Morsley, “Can visually impaired children use tactile maps to estimate directions?,” *Journal of Visual Impairment & Blindness*, vol. 88, no. 3, pp. 221–233, 1994.

[21] N. A. Giudice, B. A. Guenther, N. A. Jensen, and K. N. Haase, "Cognitive mapping without vision: Comparing wayfinding performance after learning from digital touchscreen-based multimodal maps vs. embossed tactile overlays," *Frontiers in Human Neuroscience*, vol. 14, p. 87, 2020.

[22] C. Thinus-Blanc and F. Gaunet, "Representation of space in blind persons: Vision as a spatial sense?," *Psychological Bulletin*, vol. 121, no. 1, pp. 20–42, 1997.

[23] S. Chiesa, S. Schmidt, C. Tinti, and C. Cornoldi, "Allocentric and contra-aligned spatial representations of a town environment in blind people," *Acta Psychologica*, vol. 180, pp. 8–15, 2017.

[24] A. Afonso, A. Blum, B. F. G. Katz, P. Tarroux, G. Borst, and M. Denis, "Structural properties of spatial representations in blind people: Scanning images constructed from haptic exploration or from locomotion in a 3-d audio virtual environment," *Memory & Cognition*, vol. 38, no. 5, pp. 591–604, 2010.

[25] M. Simonnet, A. M. Brock, A. Serpa, B. Oriola, and C. Jouffrais, "Comparing interaction techniques to help blind people explore maps on small tactile devices," *Multimodal Technologies and Interaction*, vol. 3, no. 2, p. 27, 2019.

[26] M. d. X.M.Almeida, L. B. Martins, and F. J. Lima, "Analysis of wayfinding strategies of blind people using tactile maps," *Procedia Manufacturing*, vol. 3, pp. 6020–6027, 2015.

[27] A. Brock and C. Jouffrais, "Interactive audio-tactile maps for visually impaired people," *ACM SIGACCESS Accessibility and Computing*, no. 113, pp. 3–12, 2015.

[28] J. Wabiński, A. Mościcka, and G. Touya, "Guidelines for standardizing the design of tactile maps: A review of research and best practice," *The Cartographic Journal*, vol. 59, no. 3, pp. 239–258, 2022.

[29] L. Ottink, B. Van Raalte, C. F. Doeller, T. M. Van Der Geest, and R. J. A. Van Wezel, "Cognitive map formation through tactile map navigation in visually impaired and sighted persons," *Scientific Reports*, vol. 12, no. 1, p. 11567, 2022.

[30] G. Ruggiero, F. Ruotolo, and T. Iachini, “Egocentric/allocentric and coordinate/categorical haptic encoding in blind people,” *Cognitive Processing*, vol. 13, pp. 313–317, 2012.

[31] D.-R. Chebat, S. Maidenbaum, and A. Amedi, “Navigation using sensory substitution in real and virtual mazes,” *PloS one*, vol. 10, no. 6, p. e0126307, 2015.

[32] M. Szubielska and W. Möhring, “Blindfolded adults use mental transformation strategies for spatial scaling of tactile maps,” *Scientific Reports*, vol. 12, no. 1, p. 6275, 2022.

[33] K. Hötting, F. Rösler, and B. Röder, “Altered auditory-tactile interactions in congenitally blind humans: an event-related potential study,” *Experimental Brain Research*, vol. 159, no. 3, pp. 370–381, 2004.

[34] Z. Cattaneo, T. Vecchi, C. Cornoldi, I. Mammarella, D. Bonino, E. Ricciardi, and P. Pietrini, “Imagery and spatial processes in blindness and visual impairment,” *Neuroscience & Biobehavioral Reviews*, vol. 32, no. 8, pp. 1346–1360, 2008.

[35] L. L. Corazzini, C. Tinti, S. Schmidt, C. Mirandola, and C. Cornoldi, “Developing spatial knowledge in the absence of vision: Allocentric and egocentric representations generated by blind people when supported by auditory cues,” *Psychologica Belgica*, vol. 50, no. 3, p. 327, 2010.

[36] B. M. Seemungal, S. Glasauer, M. A. Gresty, and A. M. Bronstein, “Vestibular perception and navigation in the congenitally blind,” *Journal of Neurophysiology*, vol. 97, no. 6, pp. 4341–4356, 2007.

Chapter 4 Sensory substitution and augmentation to coordinate multiple limbs

The majority of this chapter has been published and submitted as:

1. ***Hong, K.***, Kanapskyte, A., Gowda, H. T., Joiner, W. M., Miller, L. M., Robinson, S. K., ... & Schofield, J. S. (2024, July). The Influence of Haptic Feedback and Visual Information on Multi-Limb Coordination. In 2024 16th International Conference on Human System Interaction (HSI) (pp. 1-6). IEEE.

2. ***Hong, K.***, Kanapskyte, A., Gowda, H. T., Joiner, W. M., Miller, L. M., Robinson, S. K., ... & Schofield, J. S. (Accepted 2026, February). From Sight to Touch: Haptic Sensory Integration Can Facilitate Multi-Limb Coordination. In IEEE Transactions on Haptics (ToH).

4.1 Chapter preface

This chapter presents my work on multisensory integration during multi-limb coordination, motivated by a central challenge in human–machine interaction: as control dimensions increase, the sensorimotor system must learn new mappings between bodily actions and task outcomes while simultaneously integrating sensory information to maintain accuracy, efficiency, and confidence. In many real-world contexts—teleoperation, wearable robotics, assistive interfaces, and augmented/virtual reality—users are required to coordinate multiple effectors and interpret feedback that is partially novel, delayed, or redistributed across sensory modalities. Understanding how people adapt to these conditions is essential for designing interfaces that remain intuitive as task demands scale.

In this project, I developed and evaluated a multi-limb coordination framework in which two hands and an additional limb jointly control a three-degree-of-freedom task through systematically varied control mappings. The core experimental manipulation was the availability of sensory feedback, allowing performance under visually dominant, haptically dominant, and mixed feedback regimes to be compared within a unified task structure. By examining how performance changes across sessions and across mapping changes, this chapter isolates how users form task-level control strategies that generalize beyond a single fixed limb–axis pairing, and how sensory information availability shapes that learning process.

This chapter contributes (i) an experimental paradigm that enables controlled study of multi-limb coordination under changing limb–DoF assignments, and (ii) quantitative evaluation of task performance and movement organization using metrics such as success, completion time, coordination, and path efficiency. Collectively, these results support the broader dissertation theme that effective human–robot and human–machine systems should be designed around how the nervous system integrates multisensory cues to update internal mappings, rather than treating feedback as a simple add-on. The chapter closes by translating these findings into practical implications for wearable haptic feedback systems and scalable control interfaces, establishing a foundation for subsequent chapters that extend multisensory principles to more complex interaction settings.

4.2 Introduction

The coordinated use of multiple limbs is essential to effectively perform many everyday and skilled activities, ranging from driving a car or playing the drums to complex operations such as teleoperated robotic surgery and interactions with augmentative devices (e.g., prosthetics, exoskeletons, and supernumerary limbs). In all these cases, users must extend control beyond the coordination of two hands, sometimes incorporating additional limbs, and other times relying on alternative control modalities such as muscle contractions or movements from other body parts to offload tasks from the hands and achieve effective control of actions [**1**], [**2**], [**3**], [**4**], [**5**], [**6**].

As an additional limb or control channel, the human body provides multiple candidate human machine interaction (HMI) modalities, including head input, tongue control, gaze, and muscles activity [**7**], [**8**], [**9**], [**10**]. Yet, many of these channels provide limited effective resolution for continuous command signals. In particular, muscle-based interfaces can be sensitive to inter-participant variability and disturbances in signal quality (e.g., electrode placement, skin impedance, and motion artifacts) [**11**], [**12**]. Sustained use may also induce muscle fatigue, which can degrade control sensitivity and reduce the users' capacity to benefit from supplementary feedback that could otherwise guide movements during complex tasks [**13**]. Foot-based control is a long-standing and intuitive alternative that serves as an auxiliary control limb, providing a continuous and independent input stream (via pedal or wearable foot interfaces). While foot input has been proposed as a natural and ergonomic added control modality across applications [**4**], [**5**], [**14**], [**15**], successful adoption of novel foot-based control schemes alongside bimanual coordination requires a clear understanding of human motor behavior to support expressive, high-fidelity interactions [**16**], [**17**].

Incorporating the foot as an auxiliary controller effectively introduces an additional control channel that must be learned and coordinated with hands. When an additional limb or control channel is introduced, unique demands are placed on the sensorimotor system, often necessitating the acquisition of new motor skills. This learning process requires the central nervous system (CNS) to form new internal mappings that link motor commands to resulting task outcomes, enabling predictive feedforward control for coordinated movement [**18**], [**19**], [**20**], [**21**].As a result, effective use of an additional control modality in concert with two hands depends on the CNS's capacity to integrate multisensory information with motor commands (or using multisensory feedback to update motor output), allowing users to monitor ongoing task performance, detect discrepancies, and make real-time corrections that minimize execution errors [**22**], [**23**], [**24**], [**25**], [**26**].

As internal models rely on sensory feedback to reduce uncertainty about the body and task state, the CNS must appropriately weight and integrate available sensory cues based on their reliability. Visual feedback often provides spatial orientation and movement trajectory information, whereas haptic feedback offers immediate, localized information about object interactions and limb movements, including kinesthetic and proprioceptive signals [**27**], [**28**]. Together, these sensory modalities support accurate state estimation and continuous motor updating, enabling robust multi-limb coordination even when one modality is degraded or limited through complementing information from the other.

Building on this multisensory integration process, externally provided feedback can be designed to operate either as sensory substitution or sensory augmentation. In ***sensory augmentation***, existing sensory input is reinforced by adding complementary cues via an additional modality. Prior studies have shown that augmenting haptic feedback to visual information can support action planning during movement [**29**], for example, by assisting gait and postural control [**30**]. Moreover, combining haptic and visual information can mitigate the relatively higher latency and processing demands of visual information, which may otherwise impair reaction time and coordination [**31**], [**32**]. Such delays can be detrimental in tasks requiring rapid or precise motor responses, such as robotic surgery [**33**] or piloting drones and other remote vehicles [**34**]. Across a range of domains - including movement rehabilitation, musical performance, prosthetic or supernumerary limb control, and teleoperated surgery - haptic feedback has been shown to reduce reliance on vision and enhance multi-limb coordination [**17**], [**35**], [**36**], [**37**], [**38**], [**39**], [**40**], [**41**]. However, although bimodal feedback can outperform vision alone, especially for training temporal aspects of movement, its effectiveness may be limited by sensory overload [**17**] when excessive information is presented.

In contrast, ***sensory substitution*** refers to the delivery of information ordinarily available to one sensory modality through another modality [**42**]. The integration of substituted sensory information is thought to rely on cognitive mechanisms that prioritize contextually salient cues during task execution [**43**]. Thus, the brain inherently develops flexible interconnections among available sensory channels to support motor behavior [**25**], [**26**]. Extensive research has demonstrated that haptic perception contributes to precise motor control by providing information about self-movement and limb position [**44**], [**45**] and that it can substitute for visual input in the perception of object shape and texture [**25**], [**46**]. As a substitute cue, haptic feedback has been shown to facilitate motor learning in physical activities [**47**] and improve interaction in surgical teleoperation, virtual environments, and stylus-based interfaces [**48**], [**49**], [**50**]. Importantly, effective use of substituted haptic feedback depends not only on the signal conveyed but also on the learning process and actions employed by individuals adapt their perceptual-motor strategies [**51**], [**52**]. Collectively, while externally provided haptic feedback has known to be effective complementary sensory modality when combined with vision, its successful integration requires experience-dependent learning to incorporate haptic cues into existing sensorimotor frameworks.

Together, these findings highlight that both the motor control demands associated with distributing task control across multiple limbs and the learning process of integrating haptic cues with visual information are important for understanding multi-limb coordination under multisensory conditions. However, it remains unclear to what extent haptic feedback can compensate for reduced visual information, and how such multisensory integration evolves over time under the multi-limb coordination task. Specifically, how combinations of visual and haptic feedback shape the acquisition and execution of multi-limb coordination required for complex, higher dimensional control tasks has yet to be systematically examined.

To address these gaps, this thesis contributes in two ways: (1) by presenting the design and feasibility evaluation of an experimental platform developed to systematically manipulate haptic and visual feedback during a multi-limb coordinated task [**53**], and (2) by examining how varying combinations of visual and haptic feedback affect multi-limb coordination and task performance, as well as how integration between these modalities evolves across experiment sessions. While this initial framework established the feasibility of high-dimensional multi-limb control, it also revealed key limitations - particularly regarding the interpretability of haptic feedback when most of visual information was replaced and the added complexity introduced by EMG-based control. These factors, including susceptibility to muscle fatigue, introduced confounds that limited the isolation of multisensory integration effects. Building on these insights, the second study adopts a refined experimental design featuring a more structured and interpretable haptic feedback scheme and a control interface better suited for examining multisensory integration during multi-limb coordination. Accordingly, the remainder of this thesis adopts the methodology developed in the second study as the primary platform for investigation, enabling a systematic examination of how visual and haptic feedback are integrated over time and how such integration influences performance in complex, higher-dimensional multi-limb control tasks.

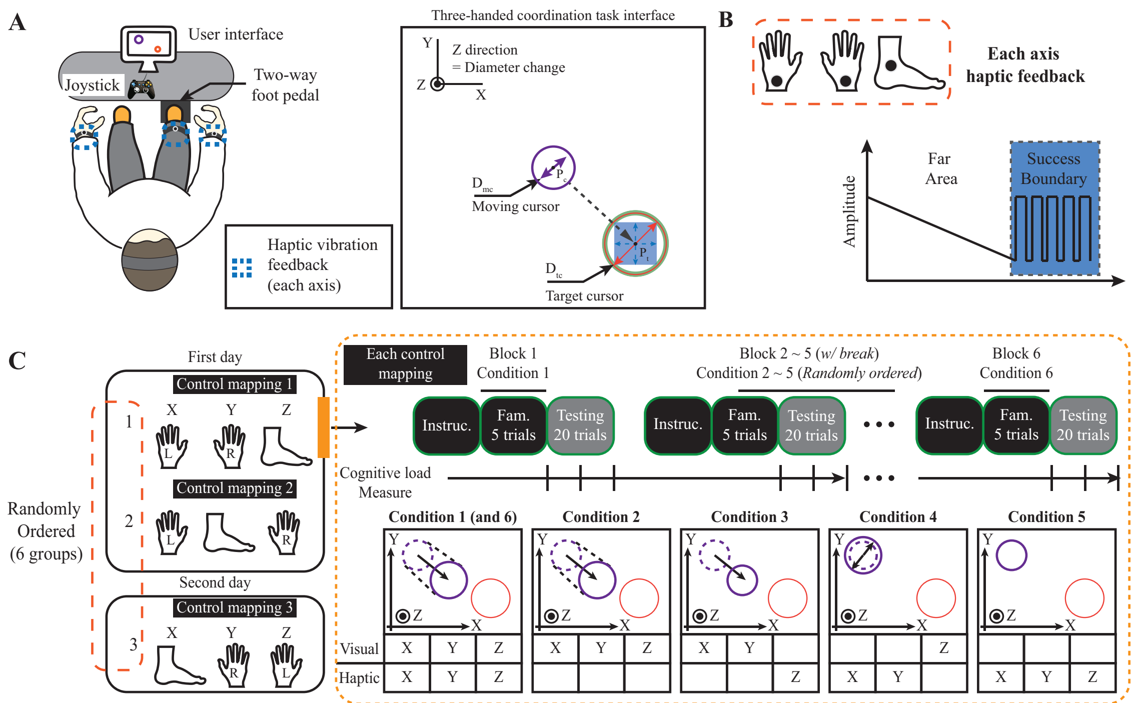

FIGURE 4.1. Experimental setup and experimental procedure. (A) Schematic description of the experimental setup, which includes a game controller and a two-way foot pedal interface for the hands and foot, respectively, and a cursor-to-target task interface displayed on a screen. The task interface allows participants to move a cursor in 3-degrees-of-freedom to reach a target position. (B) Vibrotactile haptic feedback patterns are presented to the corresponding limb for each axis of movement. As the cursor approaches the target position, vibration intensity decreases until it reaches the success region, which is defined depending on the target cursor size and its position. Within this region, vibration is presented in an alternating ON/OFF pattern to ensure it is discernible. (C) Schematic description of the experimental procedure, consisting of three sessions with different control mappings assigned in a randomized order. Each session is divided into six blocks, with each block containing 3 instruction trials, 5 familiarization trials, and 20 testing trials. Sensory feedback conditions (conditions 1 – 6) were randomly assigned to each block, except for the first and last blocks, which always presented conditions 1 and 6, respectively.

4.3 Methods

4.3.1 Participants

A total of N = 25 able-bodied individuals with no known neurological or neuromuscular impairments participated in this study. Participants included 18 female, 6 male, and 1 non-binary individual, with a mean of 22.64 ± 3.97 years. Of the 25 participants, 23 participants self-reported as right-handed, 1 as left-handed, and 1 as ambidextrous. Furthermore, 22 participants self-reported right-foot dominance, 2 as left-foot dominance, and 1 as ambidextrous foot dominance. The study was approved by the University of California Institutional Review Board, and all participants provided written informed consent prior to participating.

4.3.2 Experimental Description

Each participant completed three experimental sessions. Sessions 1 and 2 were conducted consecutively on the same day, with a break of up to 10 minutes provided between sessions to minimize fatigue-related performance declines. Session 3 took place within one week of the first two sessions. The experimental setup and procedures were identical across all sessions, with different control mappings were randomly assigned for each session (see details below).

1) Task Setup:

During the experiment, each participant sat in a chair facing a monitor and was instructed to hold a joystick controller with both hands and place their dominant foot on a foot pedal (see Fig. 4.1A).Three custom straps embedded with eccentric rotating mass vibration actuators (BestTong Model 1030) were placed on distal parts of the limbs—around each wrist and near the ankle—to maximize sensitivity to vibrotactile feedback. The wrist actuators were positioned on the palmar side of each wrist, and the lower-limb actuator was placed near the ankle. Motors were driven at a fixed vibration frequency of approximately 150–180 Hz to avoid inducing proprioceptive movement illusions [**54**]. Vibration amplitude of each actuator was modulated to encode the cursor-target distance by adjusting the actuator input voltage using pulse-width modulation, with an input range of 0 - 3 V, as specified in (4.1). Haptic feedback provided three-dimensional guidance for each corresponding limb along the x, y, and z axes using the same overall structure (graded amplitude in the far region when the cursor was outside the success boundary and an alternating 'ON/OFF' cue within the success boundary, as described in Fig. 4.1B. For the lateral axes (x and y), we defined the signed cursor-center and target-center positions as P_i and T_i ($i \in \{x, y\}$) respectively and computed the axis-specific distance as $d_i = |P_i - T_i|$. A PWM duty-cycle command $u_i \in [0, 1]$ was converted to voltage as $V_i = 3\,u_i$ V. When the cursor was outside the success boundary ($d_i > 0.8R_t$, where R_t is the target radius), the duty-cycle command increased linearly with distance,

$$\begin{cases} q_i(d_i) = \frac{d_i - 0.8R_t}{d_{i,init} - 0.8R_t}, \\ u_i(d_i, t) = \min\{1, \max\{0, q_i(d_i)\}\}, \quad d_i > 0.8R_t, \\ u_i(d_i, t) = b(t), \quad 0 \le d_i \le 0.8R_t. \end{cases} \tag{4.1}$$

where $d_{i,init}$ denotes the initial distance at the start of the trial, and $q_i(d_i) \in \{0, 1\}$ represents a normalized distance that linearly rescales the lateral cursor-target distance d_i into [0,1] outside the success boundary. When the cursor entered the success boundary ($0 \le d_i \le 0.8R_t$), we provided the alternating 'ON/OFF' cue $b(t) \in \{0, 1\}$ that toggled with a fixed temporal interval of 100 ms, so that $u_i(t) = b(t)$ in this region. For the z axis, feedback used the same duty-cycle command structure as the lateral axes, but defined the distance as the radial difference ($d_z = |R_m - R_t|$, where R_m is the cursor radius), with axis-specific thresholds. Specifically, in the far region ($d_z > 3$), the duty-cycle command decreased linearly from 1 to 0 as d_z decreased from its initial value (the radial difference at the start of the trial) to 3. When the cursor entered the success boundary ($d_z \le 3$), we provided the same alternating 'ON/OFF' cue as in the lateral axes. Once all actuators were attached, participants faced a screen displaying a cursor-to-target task adapted from a previous study [**53**]. Participants were instructed to move the cursor with three degrees of freedom (DoFs) by manipulating the thumb sticks on the controller and providing directional input via a two-way foot interface, with each input device controlling movement along its assigned axis. The x-axis corresponded to left–right cursor motion, the y-axis to up–down motion, and the z-axis to changes in cursor diameter (a proxy for in–out motion relative to the screen). For axes assigned to a thumb stick, pushing the stick right/left moved the cursor right/left (x-axis), up/down moved the cursor up/down (y-axis), and for the z-axis, pushing up increased the cursor diameter while pushing down decreased it. For axes assigned to the foot interface, toe presses generated the same command direction as right (x), up (y), or increasing diameter (z), whereas heel presses generated the opposite commands (left, down, or decreasing diameter). Cursor motion was rendered at a constant velocity along each controlled axis.

During movement, vibrotactile feedback was delivered to the corresponding limb(s) depending on which movement axis was actively controlled (Fig. 4.1B). Feedback conveyed cursor–target distance by decreasing vibration intensity as the cursor approached the target, consistent with pilot results indicating that participants reliably interpreted decreasing intensity as signaling proximity to the target. Once the cursor entered the defined success region (Fig. 4.1B), the vibration intensity fluctuated to make the feedback state more readily discernible.

2) Task Procedure:

The experiment consisted of three sessions, each using a different control mapping assigned in a randomized order, where a control mapping specifies which limb controlled each movement axis (see Fig. 4.1C). Three distinct control mapping methods were used, and each participant experienced all three across the three sessions. Mapping order was counterbalanced across participants using the six possible mapping sequences, with each participant randomly assigned to one sequence. This design reduced sequence-related confounds, enabling us to isolate the effects of sensory feedback.

Before each session, participants were instructed on two task objectives. The primary objective was to control the cursor in 3 DoFs and reach the target within 30 s. The secondary objective was to use the upper and lower limbs simultaneously when possible; this behavior was quantified as a coordination percentage that was computed at the end of each trial and displayed on the screen together with trial success or failure.

Each session consisted of six blocks. Each block included three instruction trials, five familiarization trials, and twenty testing trials. The first and last blocks provided full visual and haptic feedback for all 3 DoFs (condition 1 in the first block and condition 6 in the last block). In the four intermediate blocks (conditions 2–5), the availability of visual and haptic cues varied in numbers ranging from 0 to 3 cues to inform the cursor movement in each axis. The order of the intermediate feedback conditions (conditions 2–5) was randomized for each participant and each session to minimize ordering effects. All trials within a block shared the same feedback configuration: condition 2 provided three visual cues and no haptic feedback, condition 5 provided no visual cues and three haptic cues, and conditions 3–4 provided mixed visual and haptic cues (condition 3: two visual and one haptic; condition 4: one visual and two haptic). This approach builds on our prior work [**53**] demonstrating the feasibility of systematically modulating directional information via sensory augmentation or substitution, and enabled us to evaluate how different combinations of visual and haptic feedback influence performance in a multi-limb coordination task.

During each block, the instruction trials showed a mock trial on the screen, giving participants time to understand how visual information could be substituted with haptic feedback and how vibrotactile cues would be presented. The familiarization trials then allowed participants to experience the haptic feedback while actively performing the cursor-to-target task. During the testing trials, targets with varying sizes and locations were presented in a pseudo-randomized order to minimize possible learning effects. Within each block, participants completed the Modified Bedford Workload questionnaire (see Appendix C, Supplementary Fig. 1) three times – after the familiarization trials, halfway through the testing trials, and at the end of the block - to assess perceived cognitive load throughout the task [**55**]. Throughout the experiment, the positions of both the target and the moving cursor were continuously recorded, along with timestamps and trial outcomes (success or failure). The visibility of cursor movement on the screen varied depending on the sensory feedback condition.

3) Outcome Metrics:

The outcome measurements are categorized into three categories: task performance (success rate, trial completion time), movement (coordination score, movement efficiency), and cognitive load (Fig. 4.2).

(1) Success rate: A trial was considered successful if the cursor met both the position and size criteria relative to the target. Specifically, the final cursor center position ($P_{x,y}$) had to lie within the defined positional bound around the target center ($T_{x,y}$), and the final cursor size (R_m) had to lie within the defined size bounds relative to the target size (R_t), as specified in (4.2). The cursor then had to remain within this success region for 1 second. Each trial lasted up to 30 seconds, and the success criterion had to be met within this time window.

$$(4.2)\quad \begin{cases} \text{a.}\quad \text{X and Y position:}\quad |P_{x,y} - T_{x,y}| \le 0.8R_t \\ \\ \text{b.}\quad \text{Size of the cursor:}\quad |R_m - R_t| \le 3 \end{cases}$$

Success rate was measured by calculating the ratio of the number of successful trials to the total number of trials conducted during the testing session.

(2) Trial completion time (T_{total}): When participants controlled the cursor using the game controller and foot pedal, the position of the cursor was updated synchronously with the corresponding timestamps. The last synchronized timestamp refers to the last recorded time when the cursor passed through the success region before stopping.

(3) Coordination percentage (S_{coord}): Coordination percentage was calculated as the ratio of the time spent moving at least two limbs simultaneously (n_{move}) to the trial completion time (T_{total}). This ratio was adjusted by considering the proportion of limbs moving together relative to the required number (N_{limbs}) of limbs, which was defined by the target cursor's position. An indicator term ($I_{coord}(t)$) was defined at each timestamp, with a value of 0 when each limb moved independently and 1 when two or more limbs moved together. This assessment captures how well participants coordinated their limb movements simultaneously in relation to the task's demands.

$$(4.3) \quad \begin{cases} \text{a.} \quad S_{\text{coord}} = \dfrac{1}{T_{\text{total}}} \displaystyle\sum_{t=0}^{T_{\text{total}}} \left(\dfrac{n_{\text{move}}(t)}{N_{\text{limbs}}} \right) I_{\text{coord}}(t) \\ \\ \text{b.} \quad I_{\text{coord}}(t) = \begin{cases} 1 & \text{if } n_{\text{move}}(t) \geq 2 \\ 0 & \text{otherwise} \end{cases} \end{cases}$$

(4) Movement Path Efficiency: Actual path length was calculated as the Euclidean distance traveled by the cursor across the axes (in pixel units) until the last recorded position when the cursor passed through the success region. The optimal path length was compared to the actual path length from the starting position to the target position, and their ratio is reported as movement path efficiency, with a value of 1 denoting most efficient movement.

(5) Cognitive load: Participants reported their perceived cognitive workload using the Modified Bedford Workload Scale, which ranges from 1 ("piece of cake") to 10 ("adequate performance was impossible") (Appendix C, Supplementary Fig. 1). Participants reported their Bedford Workload score three times per each experiment block: after familiarization trials, midway through testing trials, and at the end of testing trials. This was done to assess how workload changed over the course of each sensory feedback condition. Because no significant differences were observed

between the middle and last workload score within each condition (Appendix D, Supplementary Fig. 1), only the last reported Bedford workload score from each block was used for analysis.

4.3.3 Statistical Analysis

Participants' performance, movement, and cognitive load measures were collected using repeated measures across multiple independent variables, with observations nested within participants. Given this hierarchical structure introduced within-subject correlations, all response models assessing the possible effects of different sensory feedback conditions and haptic feedback learning (experimental sessions), were constructed with generalized

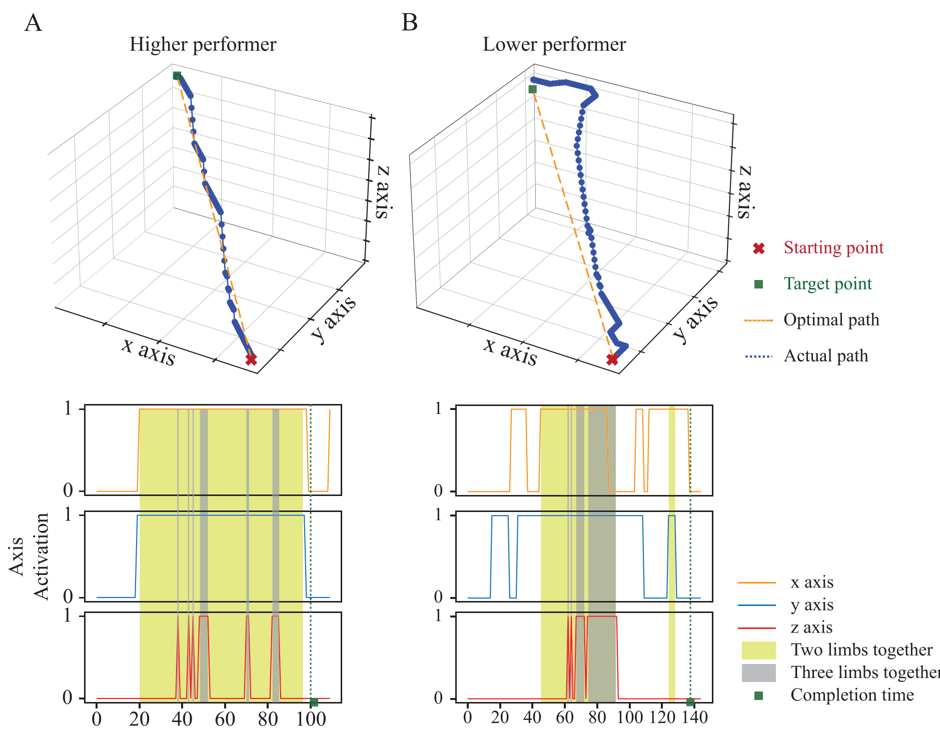

FIGURE 4.2. Sample trial displaying each outcome measurement. A sample cursor to the target path is displayed for a high and a low performer, with their corresponding activation of limbs. (a) For the high performer, the cursor follows a near-optimal path to the target position across x, y, and z axes. The corresponding activation of each limb is displayed over time, with gray segments indicating moments when all limbs are moving simultaneously and green segments indicating when two limbs are moving simultaneously. A green box marks the trial completion time. (b) In contrast, the low performer's cursor path deviates from the optimal trajectory, with reduced simultaneous activation of two or more limbs and a longer trial completion time.

mixed effects models (GLMMs). Three-factor GLMMs were fitted using maximum likelihood estimation with adaptive Gauss-Hermite quadrature [**56**] to assess the effects of sensory feedback conditions, experimental sessions, and control mappings (all fixed effects) on performance and movement measures. In addition, subjects were included as a random intercept to account for individual variability in all GLMM.

Success rate was a binary outcome (success/failure), justifying the use of a binomial distribution family with a logit link function. The expected value of the dependent variable, μ, is related to the linear predictor, η, by $\text{logit}(\mu) = \eta$.

Trial completion time, computed from synchronized timestamps, was treated as a count-based dependent variable exhibiting overdispersion. Accordingly, a negative binomial distribution (nbinom2) with a log link function was employed, where the expected value of the response was modeled as $\log(\mu) = \eta$. This formulation captured the nonlinear relationship between predictors and trial completion time on the original scale, while accounting for overdispersion.

Coordination score was a continuous proportion bounded between 0 and 1; raw values were expressed as percentages and rescaled to [0,1] prior to modeling, A beta distribution wit a logit link (i.e., the relationship between expected variable of the response and the predictor as $\text{logit}(\mu) = \eta$) was used and because the data contained excess zeros, a a zero-inflated beta model was specified (ziformula = 1) to separately estimate the probability of structural zeros alongside the beta-distributed portion.

Movement path efficiency data showed non-normality and right skewness, with values clustering near 1 especially under visual dominant sensory feedback conditions. To address heteroscedasticity, an inverse transformation was applied to the response variable. Then a model was fitted using a Gaussian distribution family and identity link function (i.e., a linear relationship between the expected value of response and predictor, $\mu = \eta$).

Model comparisons were then conducted for each response variable using likelihood ratio tests via the Anova function in R, based on Akaike Information Criterion (AIC) [**57**] and

Chi-square statistics. A model with the lowest AIC was initially selected as the best-fitting model, provided it showed a statistically significant improvement compared to other models ($p < 0.05$) with Chi-square value. Given the best fit model, final model selection was further guided by residual diagnostics; after the model was evaluated visually using diagnostic plots to confirm normality and homoscedasticity. Detailed model specifications for each response variable are provided in the Appendix E, Supplementary Tables 1–5.

Cognitive workload (Modified Bedford Workload) scores were aggregated across participants and control mappings, and the third score reported within each condition was retained. The median value for each condition was calculated and a Friedman test was performed to test for significance, followed by post-hoc pairwise Wilcoxon tests comparing Bedford scores across conditions and across trials (first, middle, and last) with a Bonferroni correction to account for multiple comparisons.

All statistical analyses were conducted in R version 4.3.3 via RStudio, and plots were generated using the ggplot2 package. GLMMs were fit with the glmmTMB function from the glmmTMB package, with DHARMa package for diagnostic assessment [**58**], [**59**]. Adjusted means and pairwise contrasts were calculated using the emmeans package, with a significance level of $\alpha = 0.05$ (two-sided) and Tukey's Honest Significant Difference (HSD) correction for multiple comparisons [**60**].

4.4 Results

4.4.1 Success Rates

To investigate how the relative availability of visual information and haptic feedback influenced task performance, Fig. 4.3 summarizes the average percentage of successful trials (defined as trials in which the cursor maintained its position within the success region for 1 second during the 30-second trial duration), its standard error (SE), and the model-estimated marginal means (with 95% confidence interval) for each sensory feedback condition across experiment sessions. There were significant main effects of sensory feedback condition and session on success rate ($\chi^2 = 691.34$, $df = 5$, $p < 0.001$; and $\chi^2 = 332.50$, $df = 2$, $p < 0.001$, respectively).

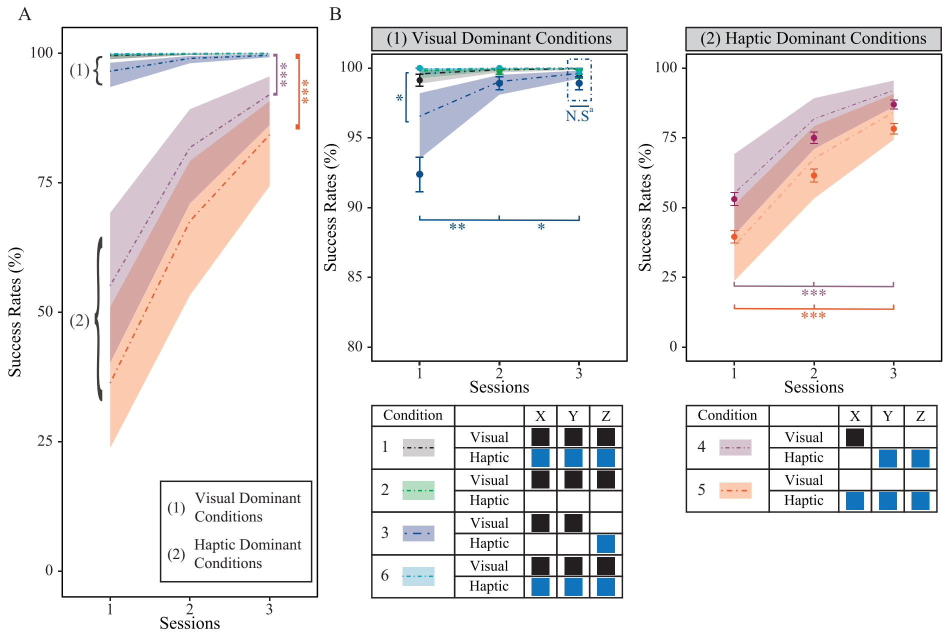

FIGURE 4.3. Success rates depending on sensory feedback conditions and experiment sessions. Raw average success rate values (mean ± SE) are indicated by filled circles and dashed lines represent estimated marginal means with shaded 95 % confidence intervals. (a) Success rates for all conditions across experiment sessions, with statistical significance in the last session between all visual dominant conditions and haptic dominant conditions 4 and 5. (b) Success rates for visual dominant and haptic dominant conditions. In the left panel, N.S[a] indicates no significant differences between condition 3 and conditions 1, 2 and 6 in the final session. Asterisks indicate statistical significance, where $p < 0.05$ (*), $p < 0.01$ (**), $p < 0.001$ (***).

Across sessions, participants maintained near-ceiling performance (> 99%) under full visual information (i.e., conditions 1, 2, and 6). However, when one axis of visual information was replaced with the corresponding haptic feedback, success rate was initially reduced compared to the other visual dominant conditions, with significant differences ($p < 0.04$), as shown in Fig. 4.3B. Over time, in condition 3 (haptic feedback was substituted for visual information in 1 DoF), participants showed significant improvements (95% CI [-0.04, -0.03], $p < 0.01$ between the first and second sessions and 95% CI [-0.01, -0.01], $p < 0.05$ between the second and final sessions).

Under haptic dominant feedback (conditions 4 and 5, where haptic feedback substituted for 2 or more DoFs of visual information), participants achieved final session success rates of 89.6 $\pm$ 1.57% and 78.3 $\pm$ 1.92%, respectively. Both conditions exhibited significant learning effects from the first to the final session (95% CI [-0.48, -0.26], $p < 0.001$ for condition 4, 95% CI [-0.55, -0.41], $p < 0.001$ for condition 5), as depicted in Fig. 4.3B. Nevertheless, despite these improvements in these conditions, their performance remained significantly lower than all visual dominant conditions by the final session ($p < 0.01$, as shown in Fig. 4.3A.

4.4.2 Trial Completion Time

The time required to position the cursor at the final target position was computed for successful trials. Fig. 4.4 presents the mean completion time, SE, and GLMM-estimated marginal means (with 95% confidence intervals) for each sensory feedback condition across experiment sessions. Trial completion time was significantly affected by both sensory feedback condition and session ($\chi^2 = 3535.20$, $df = 5$, $p < 0.001$; and $\chi^2 = 445.92$, $df = 2$, $p < 0.001$, respectively).

Participants generally completed the task faster in later sessions, showing significant improvement relative to the first session (conditions 1-5 $p < 0.001$, condition 6 $p < 0.01$), even under varying sensory feedback conditions, as shown in Fig. 4.4B. Notably, in the haptic dominant conditions (conditions 4 and 5), participants showed significant reductions in completion time from the first and the final session (95% CI [68.09, 102.19], $p < 0.001$ for condition 4, 95% CI [64.32, 107.98], $p < 0.001$ for condition 5), corresponding to reductions of 21.2% and 18.7%, respectively. Despite these improvements, trial completion time in both conditions remained significantly higher than in condition 6 (95% CI [73.71, 94.80], $p < 0.001$ for condition 4, 95% CI [116.53, 145.08], $p < 0.001$ for condition 5), as illustrated in Fig. 4.4A.

In the final session, trial completion time in condition 3 (one DoF of visual feedback replaced by the corresponding haptic feedback) did not differ significantly from condition 2 (visual

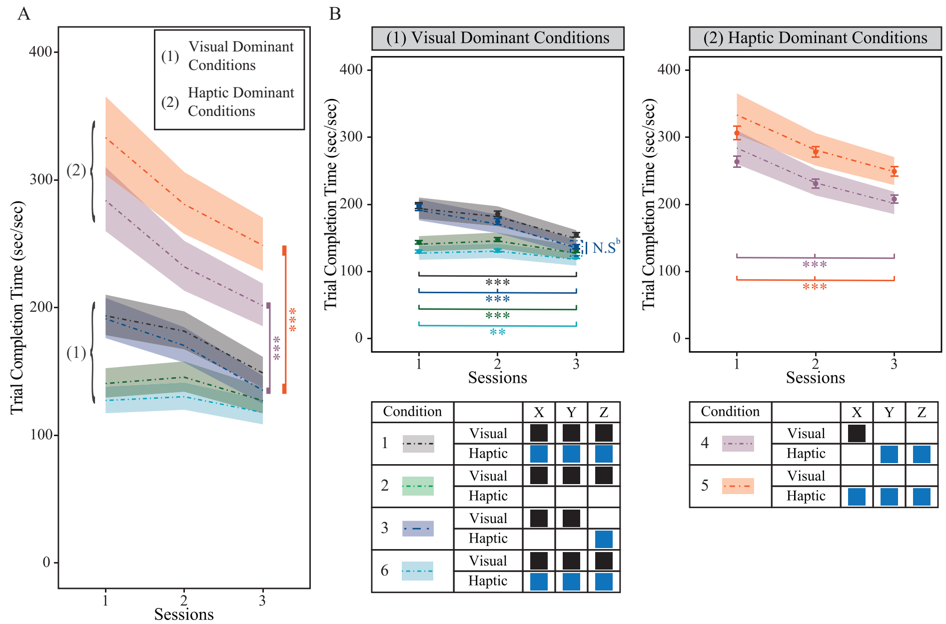

FIGURE 4.4. Trial completion time depending on sensory feedback conditions and experimental sessions. Raw average trial completion time values (mean ± SE) are indicated by filled circles and dashed lines represent estimated marginal means with shaded 95 % confidence intervals. (a) Trial completion time for all conditions across experiment sessions, with statistical significance in the last session between all visual dominant conditions and haptic dominant conditions 4 and 5. (b) Trial completion time for the visual dominant and haptic dominant conditions. In the left panel, N.S[b] indicates that, in session 3, conditions 2 and 3 are not significantly different. By contrast, all other pairwise comparisons against condition 6 in session 3 are significant ($p < 0.001$). Asterisks indicate statistical significance, where $p < 0.01$ (**), and $p < 0.001$ (***).

only; 95% CI [-14.16, -1.24], $p = 0.18$). However, condition 3 remained significantly slower than condition 6 (full visual and haptic feedback in the last block of the same session; 95% CI [10.66, 23.36], $p < 0.001$), as shown in Fig. 4.4B.

4.4.3 Coordination Percentage

Coordination percentage was calculated as the ratio of the time spent moving at least two limbs simultaneously (any two of the three limbs: left/right hands and one foot) to the trial completion time. Fig. 4.5 reports the mean coordination percentage, SE, and GLMM-estimated marginal means of coordination percentage with 95% confidence intervals, reflecting the extent to which participants could move multiple limbs concurrently without interference. The model indicated significant effects of both sensory feedback conditions and sessions ($\chi^2 = 1803.20$, $df = 5$, $p < 0.001$; and $\chi^2 = 182.78$, $df = 2$, $p < 0.001$, respectively).

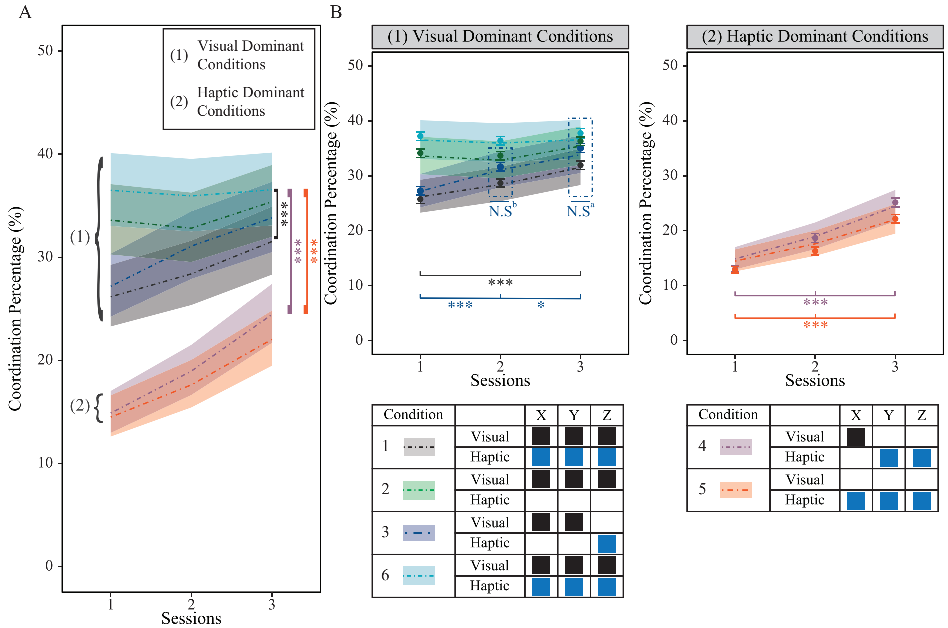

FIGURE 4.5. Coordination percentage depending on sensory feedback conditions and experimental sessions. Raw average coordination percentage values (mean ± SE) are indicated by filled circles and dashed lines represent estimated marginal means with shaded 95% confidence intervals. (a) Coordination percentage for all conditions across experiment sessions, with statistical significance in the last session between all visual dominant conditions and haptic dominant conditions 4 and 5. (b) Coordination percentage for the visual dominant and haptic dominant conditions. In the left panel, N.S^{a} indicates that, in session 3, condition 3 does not differ from other conditions. N.S^{b} indicates that in session 2, condition 3 is not significantly different from conditions 1 and 2 but differs significantly from condition 6 ($p < 0.001$). Asterisks indicate statistical significance, where $p < 0.05$ (*), $p < 0.001$ (***).

Although participants used different control mapping methods across sessions, when presented with full visual and haptic feedback during the initial block of the experiment session (condition 1), participants attempted multi-limb coordination, with simultaneous movement of at least two limbs increasing from 25.7 ± 0.74% in the first session to 31.9 ± 0.74% by the last session (Fig. 4.5B). This increase was statistically significant (95% CI [-0.07, -0.03], $p < 0.001$) . However, coordination percentages in condition 1 remained lower than in both condition 2 (full visual feedback without haptic feedback) and condition 6 (full visual feedback with haptic feedback) across sessions, with significant differences observed in the final session ($p < 0.001$), as shown in Fig. 4.5A.

Interestingly, when one axis of visual information was replaced by haptic feedback (condition 3), participants achieved coordination levels similar to those under condition 2 by the second session (95% CI [0, 0.04], $p = 0.50$), although it remained lower than condition 6,(95% CI [-0.07, -0.03], $p < 0.001$). In haptic dominant conditions, coordination percentages remained low below 15% in the initial session, indicating limited simultaneous movement across multiple DoFs, as is shown in Fig. 4.5B. However, participants significantly improved in synchronizing their limb movements by the final session in both condition 4 (95% CI [-0.11, -0.07], $p < 0.001$ and condition 5 (95% CI [-0.09, -0.06], $p < 0.001$), reaching above 20% coordination in the last session (Fig. 4.5B).

4.4.4 Movement Path Efficiency

Movement path efficiency was quantified by comparing the optimal path (Euclidean distance from the starting point to the target) with the actual distance traveled by the cursor during successful trials. An efficiency value of 1 indicates a trial where the cursor followed the optimal path (see Fig. 4.6). As shown in Fig. 4.6, path efficiency values appeared a wider distribution under the haptic dominant conditions (conditions 4 and 5), whereas values under visual dominant conditions were more tightly clustered near 1 (For more summary statistics, see Appendix F, Supplementary Table 1).

The estimated model data for movement path efficiency, alongside the mean and SE of raw data, are shown in Fig. 4.7. The model indicated significant effects of sensory feedback condition ($\chi^2 = 1351.50$, $df = 5$, $p < 0.001$) and experiment session ($\chi^2 = 154.25$, $df = 2$, $p < 0.001$) on movement path efficiency. Movement path efficiency showed a trend of improvement across experiment sessions, with all conditions showing significant improvement between experiment sessions 2 and 3 ($p < 0.001$), as shown in Fig. 4.7A and B. Furthermore, conditions 2 (only visual feedback) and 3 (one Dof of visual feedback replaced by haptic

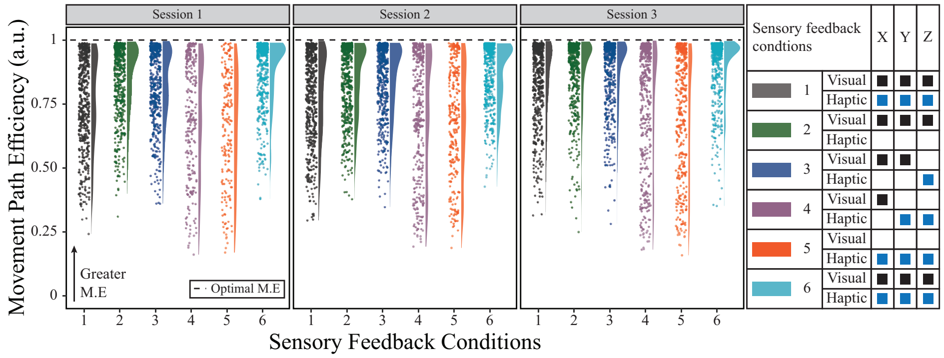

FIGURE 4.6. Movement path efficiency for each sensory feedback condition across experiment sessions is shown. Each point represents one trial for the respective condition/session, and the histograms are determined over all subjects. Movement efficiency (ME) was evaluated by comparing the optimal cursor travel length to the actual travel length from the starting point to the final target position for successful trials. A value close to 1 indicates the cursor followed the optimal path closely.

feedback) did not differ significantly across sessions($p = 0.698$), as shown in Fig. 4.7B. However, both conditions also remained significantly lower than condition 6 (full visual-haptic information in the last block) across all sessions ($p < 0.001$).

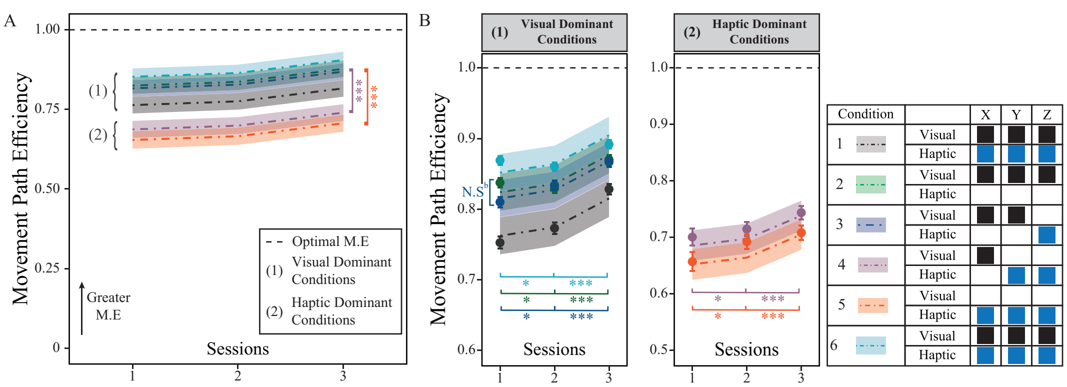

FIGURE 4.7. Movement path efficiency depending on sensory feedback conditions and experiment sessions. Raw average movement path efficiency values (mean ± SE) are indicated by filled circles and dashed lines represent estimated marginal means with shaded 95% confidence intervals. (a) Movement path efficiency for all conditions across experiment sessions, with statistical significance in the last session between all visual dominant conditions and haptic dominant conditions 4 and 5. (b) Movement path efficiency for the visual dominant and haptic dominant conditions. In the left panel, N.S^{b} indicates no significant difference between conditions 2 and 3 across all sessions. All other pairwise comparisons against condition 6 across all sessions are significant ($p < 0.001$). Asterisks denote statistical significance, where $p < 0.05$ (*), and $p < 0.001$ (***).

4.4.5 Task Cognitive Load

Participants reported perceived cognitive workload using the Modified Bedford Workload scale [**55**] three times within each experiment block. To evaluate subjective cognitive load across sensory feedback conditions, the final Bedford score from each block (condition) was used (Fig. 4.8). Median Bedford scores varied significantly by condition (Friedman $\chi^2 = 95.94$, $df = 5$, $p < 0.001$).

Condition 5 (all haptic feedback) exhibited a greater skew towards higher scores compared to the other sensory feedback conditions and was significantly different from condition 1 ($p = 0.003$), condition 2 ($p < 0.001$), condition 3 ($p < 0.001$) and condition 6 ($p < 0.001$). In contrast, condition 3 (with one axis of visual feedback replaced by haptic feedback) was perceived with similarly to conditions 1 and 2 (where all axes of visual feedback were present), with no significant difference($p = 0.147$ and $p = 0.054$, respectively). By the end of the session (condition 6), their perceived cognitive workload shifted to lower values, with significant differences from condition 1 ($p = 0.001$), condition 3 ($p = 0.003$), and conditions 4 and 5 ($p < 0.001$).

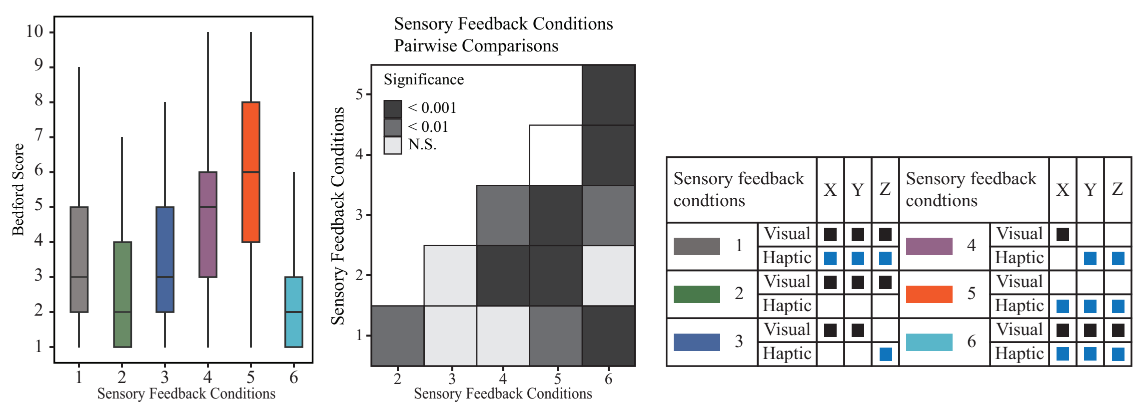

FIGURE 4.8. Bedford scores across sensory feedback conditions. The median Bedford score across participants is shown for each sensory feedback condition. The whisker extends from the 25th percentile to the 75th percentile of the Bedford score, indicating variability in subjective workload ratings across individuals. Higher scores indicate greater perceived cognitive load. The pairwise comparisons heatmap denotes significance between combinations of sensory feedback conditions

4.5 Discussions

Our results highlight how participants coordinate multiple limbs and adjust to novel control mappings in the presence of varying visual and haptic feedback. We found that during our 3D cursor-to-target computer task, visual information served as the primary sensory modality that participants relied on for successful task execution. However, haptic feedback was able to substitute for one dimension of visual input, providing meaningful information to guide performance. Additionally, we observed clear learning effects, as evidenced by marked improvements in task performance, movement metrics, and perceived cognitive load across experimental sessions.

4.5.1 Task Performance

Our task performance metrics, including success rate and trial completion time, indicated two key findings. First, we found that participants primarily relied on visual feedback when performing our multi-limb cursor-to-target task. Second, although we introduced participants to a different control mapping input during each experiment session, participants maintained and even improved their performance. Given our task's similarity to visually dominant digital environments that people interact with daily, such as computer interfaces and video games, we expected participants to quickly adapt to the task's visual feedback conditions. Our results confirmed this, showing that under full visual feedback conditions (conditions 1, 2, and 6), success rate did not show significant improvement across sessions. This likely reflects a ceiling effect, wherein task performance was already at a high level from the initial session, thereby constraining subsequent sessions for further improvements.

Previous studies have demonstrated that the absence of visual information during early stages of learning can lead to difficulties in performing later experimental tasks (e.g., recognizing objects) [**46**]. Consistent with this, in our work, when some visual cues were replaced by haptic feedback, an initial decline in task performance was observed, as supported by our findings showing a significant decrease in performance metrics during the first experiment session and when at least one visual cue was missing (conditions 3, 4, and 5). This initial decline could in part be explained by the guidance hypothesis, which suggests that dominant sensory modalities can suppress engagement with other sensory inputs early in learning [**61**], [**62**]. As the sessions progressed, significant improvements in both movement and task performance metrics were observed, even when haptic feedback was the sole source of guidance. By the final condition in each experimental session, when full haptic feedback was congruent with full visual cues (condition 6), participants showed a significant improvement in trial completion time compared to when they relied only on full visual cues alone (i.e., estimated marginal mean difference between the two conditions: 95% CI [3.25 15.37], $p = 0.03$, Fig. 4.4). However, it is important to note that both feedback conditions were performed within the same experimental sessions. Therefore, improvements observed between these conditions could partly reflect the general motor control learning effects occurring within the session, rather than being solely attributed to sensory integration processes.

Notably, our findings showed that when visual feedback was replaced with haptic feedback in two or more DoFs, performance remained significantly lower compared to the other visual dominant conditions. However, by the final experimental session, participants in condition 3 (where haptics replaced visual feedback for only one DoF) were able to achieve comparable performance measures to the full-visual conditions (i.e., estimated marginal mean difference between conditions 3 and 6 in success rate: 95% CI [-0.01 0.00], $p = 0.06 > 0.05$, Fig. 4.4).This indicates that haptic feedback can substitute for corresponding missing visual cues, which may be explained by the learning of multisensory associations and the development of a sensory integration strategy, allowing reliance on vision to be reduced in visually demanding tasks. This explanation aligns with previous studies which demonstrate that a proprioceptive sense can be established through training with mechanotactile or vibrotactile stimulation to allow precise motor control of arm movements [**63**], [**64**], [**65**], and that visual information can be replaced through rapid cross-modal training to develop perceptual strategies across sensory modalities for recognizing objects [**25**], [**46**]. Together, these results highlight the brain's capacity to adaptively integrate multisensory inputs to support flexible and efficient motor behavior.

In contrast, despite the introduction of a new control mapping each session (this changed which limb controlled which DoF, thus minimizing potential learning effects), trial completion time progressively decreased when participants performed the task under the full visual and haptic feedback condition (condition 1). Specifically, within each session, we observed a clear learning effect across control mappings between conditions 1 and 6, with a significant decrease in trial completion time. This effect also persisted across other movement metrics. However, we must note that different control mappings produced significant differences across task and movement metrics. Control mapping 3 (x: foot, y: right hand, z: left hand) underperformed relative to control mappings 1 (x: left hand, y: right hand, z: foot) and 2 (x: left hand, y: foot, z: right hand). This finding implicates that performance may depend on which task dimension was assigned to the foot, consistent with prior works showing that foot-operated input is effective when the controlled variable's representation is compatible with the natural pedal-like motion of the foot [**66**], [**67**]. Despite this difference, the consistent improvement effect over sessions and control mappings may be explained by the long-established finding that skills can transfer between limbs, where learning a skill with one hand can improve performance in the other untrained hand [**68**], [**69**], [**70**], [**71**], [**72**]. In our case, it's possible that learning transfers across three limbs (both upper and lower) as a new control mapping is learned each experiment session, despite different sensorimotor mappings to the experimental task. Other studies [**71**], [**73**], [**74**], [**75**], [**76**], [**77**] indicate that multisensory integration appears to facilitate a skill improvement in an untrained limb after training the opposite limb on a skill, supporting the idea that sensorimotor representations can be utilized across the upper limbs. In our task, it may be the case that limb-independent sensorimotor representations benefit performance across upper and lower limbs. Throughout the task, participants may have learned integration strategies that compensated for the temporal mismatch between the sensory modalities, particularly the higher latency and cognitive demands associated with the visual information compared to the more immediate nature of haptic feedback [**78**], [**79**].

4.5.2 Movement Metrics

Beyond the perspective of task performance metrics, it is important to understand how sensory substitution influences multi-limb coordination, as temporal and spatial demand across limbs can interfere with efficient movement. Even simple movements, when performed simultaneously, can disrupt coordination [**80**], [**81**], [**82**]. These constraints highlight the importance to quantify how well individuals coordinate multiple limbs and how efficiently they execute goal-directed movements. To this end, we also assessed movement path efficiency, measuring how directly participants controlled cursor movements to reach the target position without redundant movement. Given that attempting to move multiple limbs together was not the primary task goal, our findings indicate that participants prioritized task completion over this secondary task, thus resulting in coordination percentages remaining below 50% across all experimental conditions and sessions (Fig. 4.5). This task prioritization is not surprising; for example, another coordination study where participants had to control an extra robotic limb in combination with their biological limbs also found that task completion was prioritized over other performance measures [**83**]. Furthermore, task instructions and context have been shown to influence experimental outcomes in other motor learning and sensory integration studies [**84**], [**85**]. The low coordination percentages may be explained by the fact that coordinating non-homologous limb pairs, such as combining movement of an arm and a leg, is inherently more challenging and less stable, which may further contribute to reduced coordination performance [**86**], [**87**].

More importantly, we also observed an overall upward trend in coordination percentages across experiment sessions (Fig. 4.5), accompanied by improvements in movement path efficiency within the same condition (Fig. 4.7). This suggests that throughout the experiment, participants may have progressively improved their ability to interpret and integrate multisensory feedback. Notably, when comparing the first condition (condition 1) and last condition (condition 6) of each experiment session, where all visual and haptic cues were present, the last condition yielded the greatest coordination and we saw a significant learning effect across most experiment sessions. In addition, participants were able to align their cursor trajectory with the optimal path, indicating enhanced sensorimotor performance. In the first experiment condition when the task is first learned with a new control mapping method, participants may have relied heavily on visual cues to build their sensorimotor mapping. In intermediate conditions where visual cues were gradually replaced with haptic feedback, participants had to interpret the haptic feedback and, in turn, rebuild their sensorimotor mappings to rely less on visual cues. This likely facilitated a more balanced integration of sensory inputs so that when both visual and haptic feedback were reintroduced in the final experiment condition, participants could leverage their refined multisensory integration to achieve greater coordination and movement path efficiency. Other studies support this finding, showing that concurrent sensory feedback can improve performance in complex tasks and decrease task error rates [**72**], [**88**], [**89**], [**90**], [**91**], [**92**].

The unfamiliarity with a new control mapping method and reliance on visual feedback in the initial experiment condition may also explain the lower movement performance metrics observed in haptic dominant conditions later in the session. Specifically, in conditions 4 and 5 (where two to three visual DOFs were removed and replaced with haptic feedback), coordination percentage and movement path efficiencies were significantly lower compared to other visual-dominant conditions (Fig. 4.5B and Fig. 4.7B). These declines in movement performance align with the guidance hypothesis, which proposes that continuous, highly informative feedback (such as visual information) during skill acquisition can lead to over-reliance on that feedback, potentially hindering performance when it is mostly removed or reduced [**61**], [**62**]. However, we also observed that coordination and movement efficiency in these conditions improved over sessions, suggesting that participants were learning and sensory reweighing may have occurred.

Furthermore, similar to our findings for success rates, when one visual DoF was replaced by haptic feedback, coordination percentages achieved comparable levels to the full visual and haptic feedback condition by the last experiment session. Interestingly, movement path efficiency in this condition was comparable to that of the visual feedback only condition throughout all experiment sessions. This suggests that even when visual information was partially removed, the addition of haptic feedback along one movement axis was sufficient to maintain participants' ability to execute trajectories close to the optimal path, even as the task conditions change. This is important to note, as multiple studies have brought to light the influence that task contexts can have on the incorporation and effectiveness of sensory feedback [**84**].

Overall, the previously mentioned findings suggest that haptic and visual feedback can be successfully integrated and that sensory substitution, to an extent, can be achieved without detrimental effects on task performance and even movement coordination.

4.5.3 Cognitive Load

Performance and movement metrics provide an objective assessment of task performance. However, qualitative measures are also important in gaining insight into the operator's perception of the task. In our study, we utilized the Modified Bedford Workload Scale which assesses cognitive workload after a task is performed [**55**]. Many similar measures have been developed by NASA, where understanding human performance in challenging environments is critical. In our study, we saw that cognitive perception of the task was correlated to the actual performance of the task (see Appendix G, Supplementary Fig 1).

If we consider the first experiment condition within a session as the "baseline," we see that participants, when first introduced to the task and the combination of full visual and haptic feedback, rated their cognitive load near the center of the scale. Replacing one visual cue with haptic feedback maintained "baseline" levels of workload however as more visual cues were substituted by haptic feedback, the perceived workload went up to a point where some reported the task as “impossible.” Interestingly, as we discussed in the prior sections, participants were still able to improve their task performance and movement metrics in these conditions throughout the experiment sessions. This discrepancy suggests that the sensory reweighing taking place challenged participants cognitively, but the performance and movement measures also indicated that the haptic feedback was actively incorporated. Other studies support this finding, demonstrating that as visual feedback is removed, the brain shifts reliance to other available feedback modalities [**93**], [**94**]. In the last experiment condition where all visual and haptic feedback were reintroduced, we observed that workload shifted from “baseline” to lower values, where a score of one indicates the task to be “a piece of cake.” It is likely that participants judged the full visual and haptic feedback condition as less difficult than prior task conditions, as well as perceived a lesser workload due to repeated task exposure. The haptic feedback corresponding to visual cues could have lessened the cognitive workload, and in fact other studies have shown that multi-sensory feedback can improve task performance compared to a single sensory modality [**95**], [**96**]. Altogether, these observations support our understanding that haptic and visual feedback can be integrated for successful task completion, and that a proportion of visual feedback can be substituted by haptic feedback without detriment to task performance.

4.6 Conclusions

In this study, we investigated how individuals coordinate three limbs under varying exposure to visual and haptic feedback, and how they learn to integrate these cues over time. We found evidence that multisensory integration is a dynamic process that adapts to varying sensorimotor constraints, enabling effective sensory integration by allowing haptic feedback to partially compensate for the absence of visual input during a multi-limb coordination task. Our results showed that participants adapted to varying sensory feedback conditions, leading to preserved or improved performance across multiple domains, including task performance metrics, movement metrics, and mental effort.

Crucially, these results were observed over three experimental sessions. Despite exposure to new control mapping methods each session, participants maintained or improved their performance across sessions, indicating learning processes in which participants became more effective at integrating haptic and visual cues over time. In addition, within each session, the consistent difference across multiple performance measures between initial and terminal conditions (conditions 1 and 6) further demonstrates learning, suggesting that participants were not simply adapting within isolated conditions, but were developing more generalizable strategies for coordinating multiple limbs across multiple sensory feedback modalities. Taken together, these patterns suggest that learning was not limited to isolated conditions within a single session, and that some components of performance improvement may carry over across sessions despite changes in limb-axis allocation.

These findings should also be interpreted in the context of the task design. In the current paradigm, the target remained visually available across all conditions, regardless of the sensory feedback conditions, in order to maintain a balanced comparison between sensory modalities. Accordingly, the task was designed to compare the processing of a single visual state change with a single haptic state change. Nevertheless, it is possible that participants may have continued to rely on visual information for aspects of task execution even when only haptic information was presented to complete the task. As a result, the superior performance we observed across task metrics in visual dominant conditions may be a factor of the task's visual nature rather than a failure of haptic information to act as an effective sensory substitute. Importantly, despite this visual availability, participants demonstrated robust learning and maintained performance when an axis of visual feedback was replaced by a haptic cue, indicating that haptic information can be effectively integrated to support multi-limb coordination under mixed sensory feedback. Thus, these results more appropriately support the conclusion that humans can adapt their sensorimotor strategies to maintain coordinated control under mixed visual–haptic feedback, rather than a direct comparison of visual versus haptic dominance. Future studies may further isolate the contribution of haptic substitution by systematically reducing the reliability of visual information or evaluating coordination tasks in which task goals are not explicitly defined by visual targets.

Another consideration is that the visual and haptic cues differed in temporal dynamics and saliency. Haptic feedback varied as a function of cursor-target distance and included an abrupt transition upon entering the success region, whereas visual feedback was conveyed primarily via a size/position change. Because the latency of rapid visuomotor corrections depends on the defining visual features (e.g., color, size, and luminance), feature choice and cue dynamics may influence correction timing and perceived responsiveness [**97**]. Future work should therefore factorially manipulate visual features to quantify how visual feature latency and feature redundancy affect performance and modality comparisons. Additionally, although control mapping order was fully counterbalanced across participants, individuals assigned to the same experimental session could operate under different limb–axis mappings. Consequently, our analyses focused on identifying effects of session and sensory feedback conditions that generalized across control mappings, rather than isolating mapping-specific learning trajectories within individual sessions. While this approach allowed us to characterize robust learning and multisensory integration effects, it does not fully disentangle how control mapping may interact with session-level learning or sensory feedback over time. Future work may benefit from designs that hold control mapping constant within sessions, or explicitly treat mapping as a primary factor, to more directly assess its interaction with learning and sensory feedback.

In addition to the validation and findings of our present study, several opportunities remain for future work. Future studies should include follow-up sessions over even greater, extended time intervals (e.g. weeks) to better understand the robustness and consolidation of multisensory integration learning. Such studies would help determine how long the benefits of haptic-based sensory information persist and the extent to which performance gains are sustained or decay over time. Additionally, since participants were told to coordinate their limbs as much as possible as a secondary task goal, the observed coordination levels likely reflect voluntary engagement, with participants prioritizing the primary task of reaching the target in time. While visual information is effective for guiding simple tasks, it's important to consider other modes of sensory feedback in complex tasks since visual feedback alone may not be sufficient. It remains an open question whether different patterns of sensory integration would emerge under task constraints that explicitly require coordinated, multi-limb movements. Future studies should examine how task constraints on coordination (i.e. requiring coordination to successfully complete the task) influence multisensory integration strategies and whether similar compensatory behaviors emerge when coordinated movement is required rather than optional.

Overall, this study is a step towards understanding how humans learn to integrate multisensory feedback while coordinating multiple limbs. Our findings highlight the adaptability to multiple modes of sensory feedback and indicate potential for haptic input to supplement visual information in meaningful ways. These findings provide relevant insights that can enhance usability, adaptability, and user experiences in human-computer interaction environments, with potential applications in rehabilitation, assistive technologies, supernumerary robotics and training for high-stakes environments where visual feedback may be limited.

References

[1] Y. Huang, W. Lai, L. Cao, E. Burdet, and S. J. Phee, "Design and Evaluation of a Foot-Controlled Robotic System for Endoscopic Surgery," *IEEE Robotics and Automation Letters*, vol. 6, pp. 2469–2476, Apr. 2021.

[2] Y. Huang, E. Burdet, L. Cao, P. T. Phan, A. M. H. Tiong, and S. J. Phee, "A Subject-Specific Four-Degree-of-Freedom Foot Interface to Control a Surgical Robot," *IEEE/ASME Transactions on Mechatronics*, vol. 25, pp. 951–963, Apr. 2020.

[3] S.-w. Leigh and P. Maes, "Body Integrated Programmable Joints Interface," in *Proceedings of the 2016 CHI Conference on Human Factors in Computing Systems*, (San Jose California USA), pp. 6053–6057, ACM, May 2016.

[4] Y. Huang, W. Lai, L. Cao, J. Liu, X. Li, E. Burdet, and S. J. Phee, "A Three-Limb Teleoperated Robotic System with Foot Control for Flexible Endoscopic Surgery," *Annals of Biomedical Engineering*, vol. 49, pp. 2282–2296, Sept. 2021.

[5] F. Zhong, P. Li, J. Shi, Z. Wang, J. Wu, J. Y. K. Chan, N. Leung, I. Leung, M. C. F. Tong, and Y.-H. Liu, "Foot-Controlled Robot-Enabled EnDOscope Manipulator (FREEDOM) for Sinus Surgery: Design, Control, and Evaluation," *IEEE Transactions on Biomedical Engineering*, vol. 67, pp. 1530–1541, June 2020.

[6] A. Noccaro, J. Eden, G. Di Pino, D. Formica, and E. Burdet, "Human performance in three-hands tasks," *Scientific Reports*, vol. 11, p. 9511, May 2021.

[7] D. Johansen, C. Cipriani, D. B. Popović, and L. N. Struijk, "Control of a robotic hand using a tongue control system—a prosthesis application," *IEEE Transactions on Biomedical Engineering*, vol. 63, no. 7, pp. 1368–1376, 2016.

[8] S. S. Kommu, P. Rimington, C. Anderson, and A. Rané, "Initial experience with the endoassist camera-holding robot in laparoscopic urological surgery," *Journal of robotic surgery*, vol. 1, no. 2, pp. 133–137, 2007.

[9] K. Fujii, G. Gras, A. Salerno, and G.-Z. Yang, "Gaze gesture based human robot interaction for laparoscopic surgery," *Medical image analysis*, vol. 44, pp. 196–214, 2018.

[10] Y. Sasaki and T. Kondo, "A proposal of emg-based teleoperation interface for distance mobility," in *2011 IEEE International Conference on Systems, Man, and Cybernetics*, pp. 2904–2909, IEEE, 2011.

[11] D. A. Engemann and A. Gramfort, "Automated model selection in covariance estimation and spatial whitening of meg and eeg signals," *NeuroImage*, vol. 108, pp. 328–342, 2015.

[12] S. O'Meara, S. Robinson, and S. Joshi, "Pilot study for myoelectric control of a supernumerary robot during a coordination task," in *International Conference on Human-Computer Interaction*, pp. 518–536, Springer, 2022.

[13] J. Han, S. Park, S. Jung, Y. Choi, and H. Song, "Comparisons of changes in the two-point discrimination test following muscle fatigue in healthy adults," *Journal of Physical Therapy Science*, vol. 27, no. 3, pp. 551–554, 2015.

[14] J. J. LaViola, D. A. Feliz, D. F. Keefe, and R. C. Zeleznik, "Hands-free multi-scale navigation in virtual environments," in *Proceedings of the 2001 symposium on Interactive 3D graphics*, pp. 9–15, ACM, Mar. 2001.

[15] S. F. Paulo, F. Relvas, H. Nicolau, Y. Rekik, V. Machado, J. Botelho, J. J. Mendes, L. Grisoni, J. Jorge, and D. S. Lopes, "Touchless interaction with medical images based on 3D hand cursors supported by single-foot input: A case study in dentistry," *Journal of Biomedical Informatics*, vol. 100, p. 103316, Dec. 2019.

[16] M. M. Hayhoe, "Vision and Action," *Annual Review of Vision Science*, vol. 3, pp. 389–413, Sept. 2017.

[17] R. Sigrist, G. Rauter, R. Riener, and P. Wolf, "Augmented visual, auditory, haptic, and multimodal feedback in motor learning: A review," *Psychonomic Bulletin & Review*, vol. 20, pp. 21–53, Feb. 2013.

[18] J. W. Krakauer, A. M. Hadjiosif, J. Xu, A. L. Wong, and A. M. Haith, "Motor Learning," *Comprehensive Physiology*, vol. 9, pp. 613–663, Apr. 2019.

[19] D. Sternad, "It's not (only) the mean that matters: variability, noise and exploration in skill learning," *Current Opinion in Behavioral Sciences*, vol. 20, pp. 183–195, Apr. 2018.

[20] C. S. Yang, N. J. Cowan, and A. M. Haith, "De novo learning versus adaptation of continuous control in a manual tracking task," *eLife*, vol. 10, p. e62578, June 2021.

[21] A. M. Haith, C. S. Yang, J. Pakpoor, and K. Kita, "De novo motor learning of a bimanual control task over multiple days of practice," *Journal of Neurophysiology*, vol. 128, pp. 982–993, Oct. 2022.

[22] K. E. Cullen, "The vestibular system: multimodal integration and encoding of self-motion for motor control," *Trends in Neurosciences*, vol. 35, pp. 185–196, Mar. 2012.

[23] N. H. Bhanpuri, A. M. Okamura, and A. J. Bastian, "Predictive Modeling by the Cerebellum Improves Proprioception," *The Journal of Neuroscience*, vol. 33, pp. 14301–14306, Sept. 2013.

[24] J. X. Brooks and K. E. Cullen, "Predictive Sensing: The Role of Motor Signals in Sensory Processing," *Biological Psychiatry: Cognitive Neuroscience and Neuroimaging*, vol. 4, pp. 842–850, Sept. 2019.

[25] M. O. Ernst and M. S. Banks, "Humans integrate visual and haptic information in a statistically optimal fashion," *Nature*, vol. 415, pp. 429–433, Jan. 2002.

[26] M. O. Ernst, "Multisensory Integration: A Late Bloomer," *Current Biology*, vol. 18, pp. R519–R521, June 2008.

[27] H. Culbertson, S. B. Schorr, and A. M. Okamura, "Haptics: The Present and Future of Artificial Touch Sensation," *Annual Review of Control, Robotics, and Autonomous Systems*, vol. 1, pp. 385–409, May 2018.

[28] S. J. Lederman and R. L. Klatzky, "Haptic perception: A tutorial," *Attention, Perception & Psychophysics*, vol. 71, pp. 1439–1459, Oct. 2009.

[29] E. Basalp, P. Wolf, and L. Marchal-Crespo, "Haptic Training: Which Types Facilitate (re)Learning of Which Motor Task and for Whom? Answers by a Review," *IEEE Transactions on Haptics*, vol. 14, pp. 722–739, Oct. 2021.

[30] Y.-T. Pan, H. U. Yoon, and P. Hur, "A Portable Sensory Augmentation Device for Balance Rehabilitation Using Fingertip Skin Stretch Feedback," *IEEE Transactions on Neural Systems and Rehabilitation Engineering*, vol. 25, pp. 31–39, Jan. 2017.

[31] B. D. Cameron, C. De La Malla, and J. López-Moliner, "The role of differential delays in integrating transient visual and proprioceptive information," *Frontiers in Psychology*, vol. 5, 2014.

[32] R. L. Sainburg, H. Poizner, and C. Ghez, "Loss of proprioception produces deficits in interjoint coordination," *Journal of Neurophysiology*, vol. 70, pp. 2136–2147, Nov. 1993.

[33] A. Okamura, "Methods for haptic feedback in teleoperated robot-assisted surgery," *Industrial Robot: An International Journal*, vol. 31, pp. 499–508, Dec. 2004.

[34] J. R. Cauchard, K. Y. Zhai, M. Spadafora, and J. A. Landay, "Emotion encoding in Human-Drone Interaction," in *2016 11th ACM/IEEE International Conference on Human-Robot Interaction (HRI)*, (Christchurch, New Zealand), pp. 263–270, IEEE, Mar. 2016.

[35] S. Holland, A. J. Bouwer, M. Dalgelish, and T. M. Hurtig, "Feeling the beat where it counts: fostering multi-limb rhythm skills with the haptic drum kit," in *Proceedings of the fourth international conference on Tangible, embedded, and embodied interaction*, (Cambridge Massachusetts USA), pp. 21–28, ACM, Jan. 2010.

[36] J. Eden, M. Bräcklein, J. Ibáñez, D. Y. Barsakcioglu, G. Di Pino, D. Farina, E. Burdet, and C. Mehring, "Principles of human movement augmentation and the challenges in making it a reality," *Nature Communications*, vol. 13, p. 1345, Mar. 2022.

[37] P. G. Sagastegui Alva, S. Muceli, S. Farokh Atashzar, L. William, and D. Farina, "Wearable multichannel haptic device for encoding proprioception in the upper limb," *Journal of Neural Engineering*, vol. 17, p. 056035, Oct. 2020.

[38] A. Noccaro, L. Raiano, M. Pinardi, D. Formica, and G. D. Pino, "A Novel Proprioceptive Feedback System for Supernumerary Robotic Limb," in *2020 8th IEEE RAS/EMBS*

International Conference for Biomedical Robotics and Biomechatronics (BioRob), (New York City, NY, USA), pp. 1024–1029, IEEE, Nov. 2020.

[39] W. Amanhoud, J. Hernandez Sanchez, M. Bouri, and A. Billard, “Contact-initiated shared control strategies for four-arm supernumerary manipulation with foot interfaces,” *The International Journal of Robotics Research*, vol. 40, pp. 986–1014, Aug. 2021.

[40] S. Manoharan and H. Park, “Supernumerary Body Schema Extension to Non-Corporeal Object by Adding Artificial Tactile Feedback using Electrical Stimulation,” in *2019 9th International IEEE/EMBS Conference on Neural Engineering (NER)*, (San Francisco, CA, USA), pp. 989–992, IEEE, Mar. 2019.

[41] J. Bluteau, S. Coquillart, Y. Payan, and E. Gentaz, “Haptic Guidance Improves the Visuo-Manual Tracking of Trajectories,” *PLoS ONE*, vol. 3, p. e1775, Mar. 2008.

[42] Y. Visell, “Tactile sensory substitution: Models for enaction in HCI,” *Interacting with Computers*, vol. 21, pp. 38–53, Jan. 2009.

[43] H. R. Dinse, C. Wilimzig, and T. Kalisch, “Learning effects in haptic perception,” in *Human Haptic Perception: Basics and Applications* (M. Grunwald, ed.), pp. 165–182, Basel: Birkhäuser Basel, 2008.

[44] J. Tanner, G. Orthlieb, D. Shumate, and S. Helms Tillery, “Effect of Tactile Sensory Substitution on the Proprioceptive Error Map of the Arm,” *Frontiers in Neuroscience*, vol. 15, p. 586740, July 2021.

[45] L. Velásquez and J. D. Brown, “Understanding the Utility of State-Based Haptic Feedback in Tendon-Driven Anthropomorphic Prostheses,” *IEEE Transactions on Neural Systems and Rehabilitation Engineering*, vol. 33, pp. 2055–2063, 2025.

[46] Y. Zilbershtain-Kra, S. Graffi, E. Ahissar, and A. Arieli, “Active sensory substitution allows fast learning via effective motor-sensory strategies,” *iScience*, vol. 24, p. 101918, Jan. 2021.

[47] J. Van Der Linden, R. Johnson, J. Bird, Y. Rogers, and E. Schoonderwaldt, “Buzzing to play: lessons learned from an in the wild study of real-time vibrotactile feedback,”

in *Proceedings of the SIGCHI Conference on Human Factors in Computing Systems*, (Vancouver BC Canada), pp. 533–542, ACM, May 2011.

[48] Z. F. Quek, S. B. Schorr, I. Nisky, W. R. Provancher, and A. M. Okamura, "Sensory Substitution and Augmentation Using 3-Degree-of-Freedom Skin Deformation Feedback," *IEEE Transactions on Haptics*, vol. 8, pp. 209–221, Apr. 2015.

[49] L. Meli, C. Pacchierotti, and D. Prattichizzo, "Sensory Subtraction in Robot-Assisted Surgery: Fingertip Skin Deformation Feedback to Ensure Safety and Improve Transparency in Bimanual Haptic Interaction," *IEEE Transactions on Biomedical Engineering*, vol. 61, pp. 1318–1327, Apr. 2014.

[50] N. Cooper, F. Milella, C. Pinto, I. Cant, M. White, and G. Meyer, "The effects of substitute multisensory feedback on task performance and the sense of presence in a virtual reality environment," *PLOS ONE*, vol. 13, p. e0191846, Feb. 2018.

[51] J. Gibson, "The ecological approach to visual perception: classic edition," 2014.

[52] L. H. Favela, M. A. Riley, K. Shockley, and A. Chemero, "Perceptually Equivalent Judgments Made Visually and via Haptic Sensory-Substitution Devices," *Ecological Psychology*, vol. 30, pp. 326–345, Oct. 2018.

[53] K. Hong, A. Kanapskyte, H. T. Gowda, W. M. Joiner, L. M. Miller, S. K. Robinson, S. S. Joshi, and J. S. Schofield, "The Influence of Haptic Feedback and Visual Information on Multi-Limb Coordination," in *2024 16th International Conference on Human System Interaction (HSI)*, (Paris, France), pp. 1–6, IEEE, July 2024.

[54] M. W. Taylor, J. L. Taylor, and T. Seizova-Cajic, "Muscle Vibration-Induced Illusions: Review of Contributing Factors, Taxonomy of Illusions and User's Guide," *Multisensory Research*, vol. 30, no. 1, pp. 25–63, 2017.

[55] S. M. Casner and B. F. Gore, "Measuring and evaluating workload: A primer," Technical Memorandum NASA/TM-2010-216395, NASA Ames Research Center, Moffett Field, CA, USA, 2010.

[56] D. Bates, M. Mächler, B. Bolker, and S. Walker, "Fitting Linear Mixed-Effects Models Using **lme4**," *Journal of Statistical Software*, vol. 67, no. 1, 2015.

[57] H. Akaike, "A new look at the statistical model identification," *IEEE Transactions on Automatic Control*, vol. 19, pp. 716–723, Dec. 1974.

[58] M. E. Brooks, K. Kristensen, K. J. Van Benthem, A. Magnusson, C. W. Berg, A. Nielsen, H. J. Skaug, M. Mächler, and B. M. Bolker, "glmmTMB Balances Speed and Flexibility Among Packages for Zero-inflated Generalized Linear Mixed Modeling," *The R Journal*, vol. 9, no. 2, p. 378, 2017.

[59] F. Hartig, "DHARMa: Residual Diagnostics for Hierarchical (Multi-Level / Mixed) Regression Models," Aug. 2016. Institution: Comprehensive R Archive Network Pages: 0.4.7.

[60] R. V. Lenth, "emmeans: Estimated Marginal Means, aka Least-Squares Means," Oct. 2017. Institution: Comprehensive R Archive Network Pages: 1.11.2.

[61] A. W. Salmoni, R. A. Schmidt, and C. B. Walter, "Knowledge of results and motor learning: A review and critical reappraisal.," *Psychological Bulletin*, vol. 95, no. 3, pp. 355–386, 1984.

[62] R. A. Schmidt, D. E. Young, S. Swinnen, and D. C. Shapiro, "Summary knowledge of results for skill acquisition: Support for the guidance hypothesis.," *Journal of Experimental Psychology: Learning, Memory, and Cognition*, vol. 15, no. 2, pp. 352–359, 1989.

[63] L. K. Amann, V. Casasnovas, J. Hainke, and A. Gail, "Optimality of multisensory integration while compensating for uncertain visual target information with artificial vibrotactile cues during reach planning," *Journal of NeuroEngineering and Rehabilitation*, vol. 21, p. 155, Sept. 2024.

[64] A. J. Suminski, D. C. Tkach, A. H. Fagg, and N. G. Hatsopoulos, "Incorporating Feedback from Multiple Sensory Modalities Enhances Brain–Machine Interface Control," *The Journal of Neuroscience*, vol. 30, pp. 16777–16787, Dec. 2010.

[65] A. Blank, A. M. Okamura, and K. J. Kuchenbecker, “Identifying the role of proprioception in upper-limb prosthesis control: Studies on targeted motion,” *ACM Transactions on Applied Perception*, vol. 7, pp. 1–23, June 2010.

[66] F. P. Garcia and K.-P. L. Vu, “Effectiveness of hand- and foot-operated secondary input devices for word-processing tasks before and after training,” *Computers in Human Behavior*, vol. 27, pp. 285–295, Jan. 2011.

[67] K. W. Chan and A. H. Chan, “Spatial stimulus–response (S-R) compatibility for foot controls with visual displays,” *International Journal of Industrial Ergonomics*, vol. 39, pp. 396–402, Mar. 2009.

[68] N. Birbaumer, “Motor Learning: Passing a Skill from One Hand to the Other,” *Current Biology*, vol. 17, pp. R1024–R1026, Dec. 2007.

[69] E. W. Scripture, T. L. Smith, and E. M. Brown, “On the education of muscular control and power,” *Stud Yale Psychol Lab*, vol. 2, no. 5, 1894.

[70] K. Japikse, S. Negash, J. Howard, and D. Howard, “Intermanual transfer of procedural learning after extended practice of probabilistic sequences,” *Experimental Brain Research*, vol. 148, pp. 38–49, Jan. 2003.

[71] J. De Havas, P. Haggard, H. Gomi, S. Bestmann, Y. Ikegaya, and N. Hagura, “Evidence that endpoint feedback facilitates intermanual transfer of visuomotor force learning by a cognitive strategy,” *Journal of Neurophysiology*, vol. 127, pp. 16–26, Jan. 2022.

[72] S. P. Swinnen, T. D. Lee, S. Verschueren, D. J. Serrien, and H. Bogaerds, “Interlimb coordination: Learning and transfer under different feedback conditions,” *Human Movement Science*, vol. 16, pp. 749–785, Nov. 1997.

[73] B. M. Sexton, Y. Liu, and H. J. Block, “Increase in weighting of vision vs. proprioception associated with force field adaptation,” *Scientific Reports*, vol. 9, p. 10167, July 2019.

[74] Y. Makino, T. Hayashi, and D. Nozaki, “Divisively normalized neuronal processing of uncertain visual feedback for visuomotor learning,” *Communications Biology*, vol. 6, p. 1286, Dec. 2023.

[75] W. M. Joiner, J. B. Brayanov, and M. A. Smith, "The training schedule affects the stability, not the magnitude, of the interlimb transfer of learned dynamics," *Journal of Neurophysiology*, vol. 110, pp. 984–998, Aug. 2013.

[76] N. Malfait and D. J. Ostry, "Is Interlimb Transfer of Force-Field Adaptation a Cognitive Response to the Sudden Introduction of Load?," *The Journal of Neuroscience*, vol. 24, pp. 8084–8089, Sept. 2004.

[77] T. Stöckel, T. J. Carroll, J. J. Summers, and M. R. Hinder, "Motor learning and cross-limb transfer rely upon distinct neural adaptation processes," *Journal of Neurophysiology*, vol. 116, pp. 575–586, Aug. 2016.

[78] F. Crevecoeur, D. P. Munoz, and S. H. Scott, "Dynamic Multisensory Integration: Somatosensory Speed Trumps Visual Accuracy during Feedback Control," *The Journal of Neuroscience*, vol. 36, pp. 8598–8611, Aug. 2016.

[79] S. Kasuga, F. Crevecoeur, K. P. Cross, P. Balalaie, and S. H. Scott, "Integration of proprioceptive and visual feedback during online control of reaching," *Journal of Neurophysiology*, vol. 127, pp. 354–372, Feb. 2022.

[80] S. P. Swinnen, "Intermanual coordination: From behavioural principles to neural-network interactions," *Nature Reviews Neuroscience*, vol. 3, pp. 348–359, May 2002.

[81] J. S. Kelso, D. L. Southard, and D. Goodman, "On the coordination of two-handed movements.," *Journal of Experimental Psychology: Human Perception and Performance*, vol. 5, no. 2, pp. 229–238, 1979.

[82] J. A. S. Kelso, D. L. Southard, and D. Goodman, "On the Nature of Human Interlimb Coordination," *Science*, vol. 203, pp. 1029–1031, Mar. 1979.

[83] G. Dominijanni, D. L. Pinheiro, L. Pollina, B. Orset, M. Gini, E. Anselmino, C. Pierella, J. Olivier, S. Shokur, and S. Micera, "Human motor augmentation with an extra robotic arm without functional interference," *Science Robotics*, vol. 8, p. eadh1438, Dec. 2023.

[84] M. M. Murray, D. J. Lewkowicz, A. Amedi, and M. T. Wallace, "Multisensory Processes: A Balancing Act across the Lifespan," *Trends in Neurosciences*, vol. 39, pp. 567–579, Aug. 2016.

[85] N. M. Kitchen, J. Yuk, A. Przybyla, R. A. Scheidt, and R. L. Sainburg, "Bilateral arm movements are coordinated via task-dependent negotiations between independent and codependent control, but not by a "coupling" control policy," *Journal of Neurophysiology*, vol. 130, pp. 497–515, Sept. 2023.

[86] J. A. Kelso and J. J. Jeka, "Symmetry breaking dynamics of human multilimb coordination.," *Journal of Experimental Psychology: Human Perception and Performance*, vol. 18, no. 3, pp. 645–668, 1992.

[87] S. Swinnen, N. Dounskaia, S. Verschueren, D. Serrien, and A. Daelman, "Relative phase destabilization during interlimb coordination: the disruptive role of kinesthetic afferences induced by passive movement," *Experimental Brain Research*, vol. 105, Feb. 1990.

[88] S. J. Snodgrass, D. A. Rivett, V. J. Robertson, and E. Stojanovski, "Real-time feedback improves accuracy of manually applied forces during cervical spine mobilisation," *Manual Therapy*, vol. 15, pp. 19–25, Feb. 2010.

[89] M. Huet, C. Camachon, L. Fernandez, D. M. Jacobs, and G. Montagne, "Self-controlled concurrent feedback and the education of attention towards perceptual invariants," *Human Movement Science*, vol. 28, pp. 450–467, Aug. 2009.

[90] E. Todorov, R. Shadmehr, and E. Bizzi, "Augmented Feedback Presented in a Virtual Environment Accelerates Learning of a Difficult Motor Task," *Journal of Motor Behavior*, vol. 29, pp. 147–158, June 1997.

[91] I. Oakley, M. R. McGee, S. Brewster, and P. Gray, "Putting the feel in 'look and feel'," in *Proceedings of the SIGCHI conference on Human Factors in Computing Systems*, (The Hague The Netherlands), pp. 415–422, ACM, Apr. 2000.

[92] J. L. Burke, M. S. Prewett, A. A. Gray, L. Yang, F. R. B. Stilson, M. D. Coovert, L. R. Elliot, and E. Redden, "Comparing the effects of visual-auditory and visual-tactile

feedback on user performance: a meta-analysis," in *Proceedings of the 8th international conference on Multimodal interfaces*, (Banff Alberta Canada), pp. 108–117, ACM, Nov. 2006.

[93] S. Levy-Tzedek, M. B. Tov, and A. Karniel, "Rhythmic movements are larger and faster but with the same frequency on removal of visual feedback," *Journal of Neurophysiology*, vol. 106, pp. 2120–2126, Nov. 2011.

[94] R. Ronsse, V. Puttemans, J. P. Coxon, D. J. Goble, J. Wagemans, N. Wenderoth, and S. P. Swinnen, "Motor Learning with Augmented Feedback: Modality-Dependent Behavioral and Neural Consequences," *Cerebral Cortex*, vol. 21, pp. 1283–1294, June 2011.

[95] S. Jeong, J. Kim, and J. Lee, "The Differential Effects of Multisensory Attentional Cues on Task Performance in VR Depending on the Level of Cognitive Load and Cognitive Capacity," *IEEE Transactions on Visualization and Computer Graphics*, vol. 30, pp. 2703–2712, May 2024.

[96] M. K. Ngo and C. Spence, "Auditory, tactile, and multisensory cues facilitate search for dynamic visual stimuli," *Attention, Perception, & Psychophysics*, vol. 72, pp. 1654–1665, Aug. 2010.

[97] M. M. Veerman, E. Brenner, and J. B. J. Smeets, "The latency for correcting a movement depends on the visual attribute that defines the target," *Experimental Brain Research*, vol. 187, pp. 219–228, May 2008.

Chapter 5 Sensory substitution and augmentation for robotic teleoperation

The majority of this chapter has been published and submitted as:

1. **Hong, K.**, Zhang, R., Lee, K. G., Young, P. R., Joiner, W. M., Robinson, S. K., ... & Schofield, J. S. (2024, October). A wearable haptic sleeve interface for spaceflight robotic arm operations. In Companion of the 2024 on ACM International Joint Conference on Pervasive and Ubiquitous Computing (pp. 318-322).

2. ***Hong, K.***, Syeda, Y. Z., Jeshurun, L., Brian, H., Weiwei, Z., Joiner, W. M., Robinson, S. K., ... & Schofield, J. S. (Submitted 2026, March). Effect of haptic feedback on skill learning and visual dependence for a robotic teleoperation. In IEEE International Conference on Robot and Human Interactive Communication (RO-MAN).

5.1 Chapter preface

Robotic teleoperation in complex and safety-critical environments places substantial demands on human operators. During these tasks, operators must continuously monitor spatial relationships, trajectory evolution, and dynamic system states - most often through vision alone. This heavy reliance on visual feedback can overload perceptual and cognitive resources, increasing the likelihood of errors and limiting learning efficiency. Augmenting robotic teleoperation with haptic feedback offers a promising means to redistribute information across sensory modalities and enhance human-robot interaction, particularly in situations where visual information is limited, degraded, or unreliable.

This chapter presents two studies that develop a wearable vibrotactile haptic feedback system and examine its success in supporting robotic control by conveying task-relevant information. **Section 5.2** focuses on the development and feasibility testing of haptic encoding strategies that represent robotic motion information. **Section 5.3** examines how these haptic cues influence human perception, teleoperation performance, and motor learning through the development of a multimodal experimental framework and a biobehavioral assessment battery integrating performance metrics and physiological measures.

Together, these studies examine how wearable haptic interfaces can shift robotic teleoperation from a visually dominated interaction toward a multisensory control paradigm. Finally, future directions are discussed to further investigate the role of haptic feedback in skill acquisition and its influence on eye-related behavioral and cognitive responses during robotic teleoperation.

5.2 Introduction

Human-robot interactions are prevalent in performing tasks that are hazardous, complex, or otherwise inaccessible to direct human involvement, including search and rescue, space exploration, and robot-assisted minimally invasive surgery. These systems that combine synergy between human perception, sensorimotor control, and adaptive decision-making with the precision, strength, and repeatability of robotic systems allow humans to safely extend their capabilities beyond physical and environmental limitations. As robotic systems are increasingly deployed in such high-stakes settings, understanding how users acquire and refine operational skills is critical for ensuring safety, efficiency, and task success.

In tele-robotic systems operated under the control, guidance, or supervision of remote users, situational awareness is often conveyed almost primarily through visual feedback. Operators are typically required to process large volumes of visual information to monitor spatial relationships, trajectory evolution, and dynamic system states, while simultaneously generating appropriate control commands. Practical constraints, such as limited field of view, motion scaling, and communication latency, further complicate this process and increase task difficulty. Together, these factors impose substantial cognitive demands as operators manage complex visuomotor mappings between controller inputs, vision-based observation, and the robot's physical motion within the workspace [**1**], [**2**]. When visual processing demands exceed available attentional resources, operators may experience visual overload, which can degrade situational awareness, impair attention allocation, and reduce task performance, ultimately increasing the likelihood of operational errors [**3**].

Multi-sensory integration in robot teleoperation can address these challenges by distributing perceptual and cognitive demands across multiple sensory channels. By supporting both the use and acquisition of teleoperation skills, multisensory feedback enables operators to perceive remote environments more effectively and respond appropriately, thereby enhancing situational awareness and facilitating the execution of complex tasks. Among additional sensory channels, haptic feedback is another important piece of feedback in robotic teleoperation, which has been widely investigated for its potential to manage cognitive load associated with robotic operations and potentially improve operator's performance by relieving excessive dependency on heavily taxed visual sensory channels [**4**], [**5**], [**6**]. Conveying task-relevant information, haptic feedback can complement visual constraints, enhance task awareness, and support error detection and correction, particularly in visually demanding or constrained environments [**7**], [**8**].

Wearable haptic interfaces have emerged as a practical and flexible approach for delivering haptic feedback in robotic teleoperation. Wearable systems can provide distributed tactile cues directly on the body without constraining operator movement or requiring rigid mechanical coupling to the robot. Vibrotactile wearables, in particular, offer advantages in terms of lightweight design, low power consumption, scalability, and ease of integration with existing teleoperation platforms. These interfaces support sensory augmentation and sensory substitution by conveying a wide range of task-relevant information, including continuous guidance cues that indicate movement direction, magnitude, or deviation from a desired trajectory, as well as discrete notifications such as collisions and contact information.

However, the effectiveness of wearable haptic feedback in robotic teleoperation depends critically on how task-relevant information is encoded and how users learn to interpret and integrate these cues during control [**9**]. Before haptic feedback can meaningfully support teleopeartion, it is necessary to establish that the conveyed tactile information is perceptually interpretable and intuitively mapped to robotic behavior. In particular, although vibrotactile stimulation can represent different types of information through modulation of its physical characteristics (e.g., frequency and amplitude) [**10**], [**11**], [**12**], [**13**], the design of vibrotactile haptic interfaces requires a careful understanding of human tactile perception and the response properties of skin mechanoreceptors. This introduces an inherent trade-off between the richness of information that can be encoded in vibrotactile signals and the limits of perceptual discriminability. Without such validation, haptic cues risk increasing cognitive load or being disregarded by operators, limiting their potential benefit.

Beyond the development of novel vibrotactile haptic interfaces, their effectiveness also depends on how operators incorporate tactile cues into their control strategies and adapt to their use over time. Because cognitive mechanisms underlying sensorimotor control involve tight interactions between available sensory channels and motor actions, learning to utilize haptic feedback requires the learning process and actions to update their perceptual-motor strategies [**14**], [**15**]. Teleoperation is not a static interaction but a sensorimotor skill learning process, in which users progressively refine mappings between control inputs, sensory feedback, and robot behavior. Accordingly, investigating multi-sensory integration in both the usage and learning of robot teleoperation interfaces is essential. Research on natural human motor control research [**16**], [**17**], [**18**] has shown that coordinated action depends on the adaptive integration of sensory feedback and motor commands, suggesting that similar principles may be relevant for understanding and designing teleoperation systems. In this context, examining how operators learn to use haptic feedback is critical for the design of wearable haptic interfaces, understanding whether the interfaces can produce sustained benefits in teleoperation performance and promote a shift away from visually dominated control toward a more balanced multisensory strategy.

Building on these considerations, this chapter investigates wearable vibrotactile haptic feedback from both a system design and a human performance perspective. Specifically, the chapter structured into two complementary sub-chapters that address distinct but interrelated aspects of multisensory teleoperation. **Section 5.2** focuses on the development and feasibility evaluation of a wearable vibrotactile haptic interface, including the design of encoding strategies that convey robotic motion through tactile cues. This study examines whether such information can be reliably perceived and interpreted by users. **Section 5.3** extends this work by introducing an experimental framework to examine how wearable haptic feedback influences teleopeartion performance, visual dependence, and motor learning over time. By integrating behavioral performance metrics with measures related to visual demand and operator state, this sub-chapter builds and validates a biobehavioral assessment battery that captures motor learning and the direct influence of haptic on learning as reflected in performance outcomes and physiological measures (eye-gaze behavior). Together, these sub-chapters provide a cohesive examination of how wearable haptic interfaces can be designed and evaluated to promote a shift from visually dominated teleopeartion toward a more balanced multisensory control strategy.

5.3 Design of a wearable haptic sleeve interface for teleoperations

5.3.1 Background

Wearable vibrotactile haptic feedback has been increasingly investigated as a means of conveying task-relevant information in human-robot interaction and teleoperation contexts [**19**], [**20**], [**21**], [**22**], [**23**], [**24**]. In the context of teleoperation, vibrotactile feedback has been applied to support motion guidance, collision awareness, and situational awareness by augmenting or substituting visual information. As interest in vibrotactile haptic feedback actuators across the body continues to grow across a range of applications [**25**], [**26**], [**27**], [**28**], [**23**], this work presents the design and feasibility testing of a wearable haptic interface in a sleeve form factor tailored for teleoperations.

As vibration has its inherent capacity to convey various information through systematic manipulation of amplitude and frequency, we propose that a promising approach to communicating task-relevant information lies in exploiting **tactile stroke illusions**, a form of moving tactile sensation that use multiple vibration sources applied to the forearm [**29**].

Tactile stroke illusion: refers to the sensation of moving tactile sensation achieved through the sequential activation of vibration patterns [**29**]. This technique strategically manipulates the physical characteristics of vibrations to convey a wealth of information. It has shown wide applicability across a variety of fields including navigational guidance and virtual reality applications [**30**], [**31**]. This phenomenon is grounded in two separate yet related psychophysical models of touch illusions: (1) **apparent tactile motion (ATM)**, and (2) **phantom sensation (PS) illusions**. ATM occurs when the activation timing of two (or more) closely positioned vibrotactors on the skin overlaps, creating the sensation of a single wave of vibration passing between them [**32**], [**33**]. PS describes the experience of a single "virtual" vibration source perceived between two physical vibrotactors, and the location varying depending on their relative vibration amplitudes [**34**], [**35**]. Collectively, these illusions have demonstrated a promising path to generating rich tactile experiences in a compact and efficient manner [**36**], [**37**], [**38**].

While haptic interfaces that leverage these illusions offer strong potential for high-bandwidth information delivery, their effectiveness depends on practical design choices, particularly actuator placement and site-specific perceptual sensitivity. In other words, designers must consider where on the body an interface is mounted and how actuator spacing and stimulation parameters are tuned to ensure that illusory motion remains reliably perceivable at the chosen skin location.

Although fingers and hands contain the highest density of mechanoreceptors and are the most perceptually sensitive area of the skin [**39**], [**40**], placing haptic devices on these areas can obstruct object manipulation and interfere with natural interaction with the physical environment [**41**], [**42**], [**43**]. To counter this issue of interaction, this work focuses on the upper limb as a site for haptic feedback delivery. The upper limb is one of the body parts that can efficiently receive haptic feedback because it provides a balance between tactile sensitivity and functional usability. While tactile acuity varies across the upper limb, these regions collectively exhibits relatively high tactile acuity compared to many other body sites [**44**], and are strongly represented in the primary somatosensory cortex [**45**].

In addition to actuator placement on the body, the perceptual effectiveness of vibrotactile feedback is shaped by key stimulation parameters that directly inform interface design, particularly vibration frequency, amplitude, and spatial arrangement. Numerous studies have explored the role of vibration frequency in the detection and perception of cutaneous vibration stimuli. Most studies have highlighted that vibration frequencies between 30 - 350Hz can be readily detected, and these values align with the excitation frequency range of Meissner and Pacinian corpuscles, the skin-based mechanoreceptors responsible for sensing vibration [**46**], [**47**]. Optimal sensitivity has been reported to occur at vibration frequencies between 150 and 300Hz across various body sites [**48**].

While variations in the amplitude of vibration can also be harnessed for conveying a rich stream of information, research focusing solely on the influence of amplitude remains relatively unexplored. This is primarily due to the common use of eccentric rotating mass vibrotactors in the literature, where the physics of these systems means that vibration frequency and amplitude cannot be separated and controlled independently of one another.

Beyond temporal stimulation parameters, the spatial configuration of vibrotactors is also an important factor to be considered for conveying reliable tactile perception and illusion formation. As an ability to discriminate individually between two vibration sources is dependent on the dermatomal representation of the upper arm, a two-point discrimination distance can drive the selection of spacing between multiple vibrotactors. Prior works indicate that human capacity to discriminate spatial gaps between two vibration actuators applied to the upper limb falls within the range of 3cm to 5cm [**49**], [**50**], [**51**]. Furthermore, maximum spacing threshold for reliably inducing phantom sensations have been reported to be approximately 6–7 cm on the forearm and around 7 cm on the upper arm. Finally, individual variability in upper-limb anthropometric measurements must be considered when designing wearable haptic interfaces to ensure consistent and robust perceptual outcomes across users [**52**].

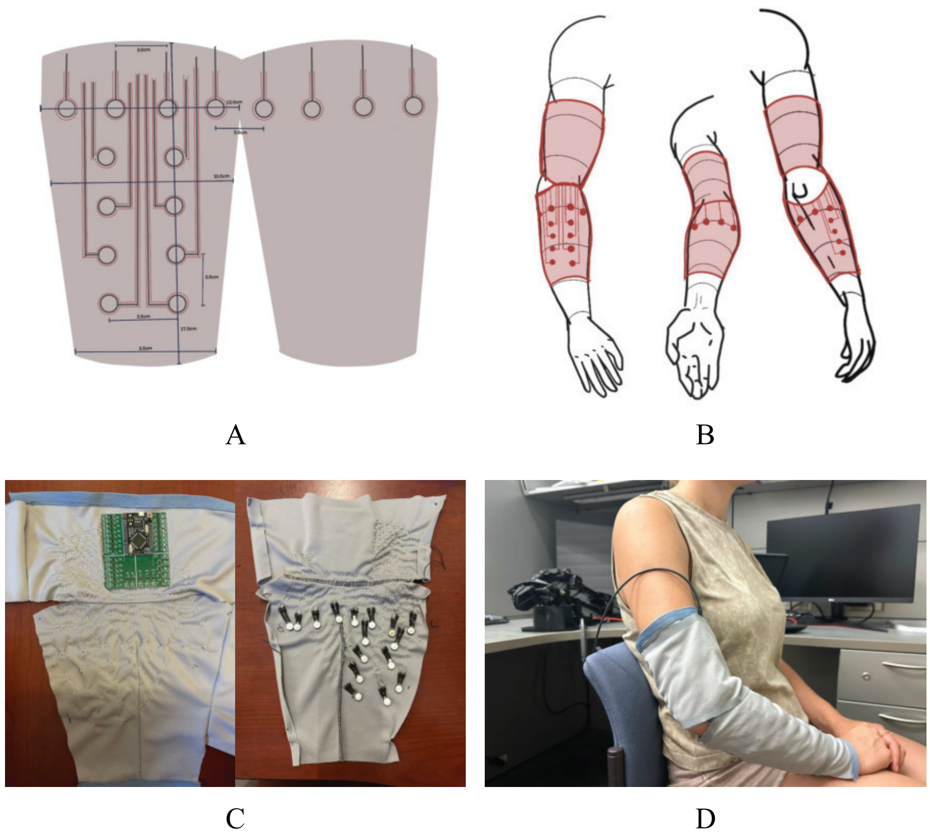

FIGURE 5.1. (A) Schematic orientation of vibrotactors, (B) wearable haptic sleeve, and (C) e-textile signal transmission and vibrotactor connections (D) a haptic sleeve on the forearm

5.3.2 Prototype development

The wearable haptic sleeve prototype incorporated 16 vibrotactors and a control unit, providing precise, task-relevant haptic feedback for robotic arm teleoperation. Vibrotactors were strategically spaced and positioned to cover the entire length of the forearm, while the control unit is housed on the upper arm. Adjacent vibroatctors were spaced approximately 3.0 cm apart longitudinally and circumferentially, consistent with known spatial discrimination thresholds on the upper limb. This spacing ensured reliable perceptual separation of stimuli while maintaining a low profile for factor not to hinder movement (Fig. 5.1A).

This spatial arrangement was designed to support both ATM and PS illusions for encoding three-dimensional robotic movement and velocity information. We developed two rendering algorithms to translate end-effector movements in Euclidean space onto vibrotactor activation patterns on the forearm (Fig. 5.1B). Movements in the positive and negative X-directions were encoded as sequential waves of vibration (ATM), traveling along the medial (positive X direction) or lateral portions (negative X direction) of the forearm. Movements in the Y-direction were represented by waves of vibration traveling proximally or distally along

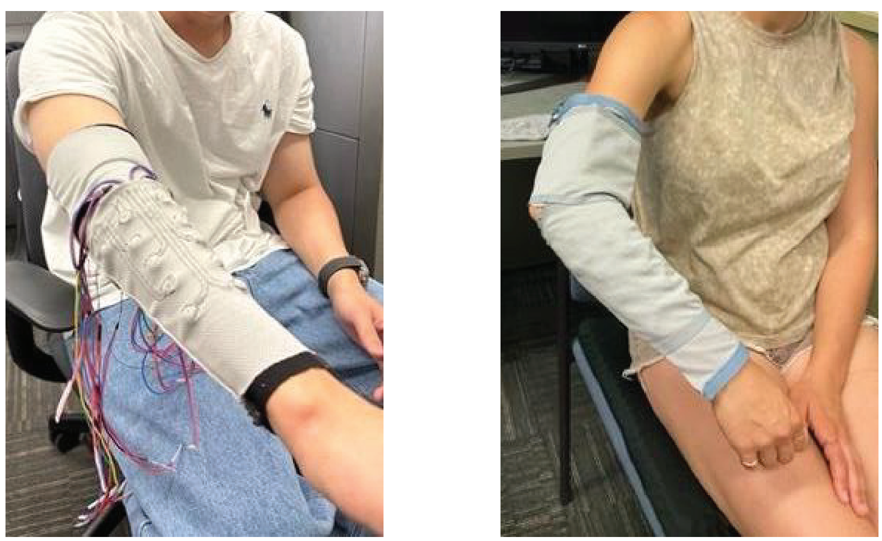

A B

FIGURE 5.2. (A) First prototype of haptic sleeve, (B) Second prototype of haptic sleeve with e-textile lines on the forearm

the dorsal side of the forearm using a combination of ATM and PS. For the Z-direction, movements were conveyed by ATM combined with PS illusions moving along both the medial and lateral portions of the forearm. Positive Z-direction movements were indicated by vibration traveling from the ventral to the dorsal part of the forearm, while negative Z-direction movements were represented by vibration traveling in the opposite direction.

The perceived velocity of tactile stroke illusions was manipulated at three levels by adjusting the duration time of individual vibrotactors and inter-stimulus onset asynchrony (SOA), which is the function of the individual actuator duration time [**37**] (Fig. 5.4).

To ensure wearability and comfort the haptic sleeve prototype underwent through 2 rounds of iteration. First, the sleeve was constructed from two layers of lightweight, breathable, and stretchable knit fabric to maintain secure contact with the skin. Vibrotactors and the connecting cables were embedded between the fabric layers within circular pockets and routing channels (Fig. 5.2A). In the second iteration, cables were eliminated and e-textile signal transmission lines were developed which allowed the use of a single layer of fabric (Fig. 5.2B). The e-textile signal transmission lines were stitched on the sleeve with Karl Grimm copper Silver plated High Flex 3981 conductive thread and attached to the vibrotactors with round metal crimps and looped stitches. The sleeve also prioritized ease of movement and thermal comfort with an elbow opening (Fig. 5.1C&D).

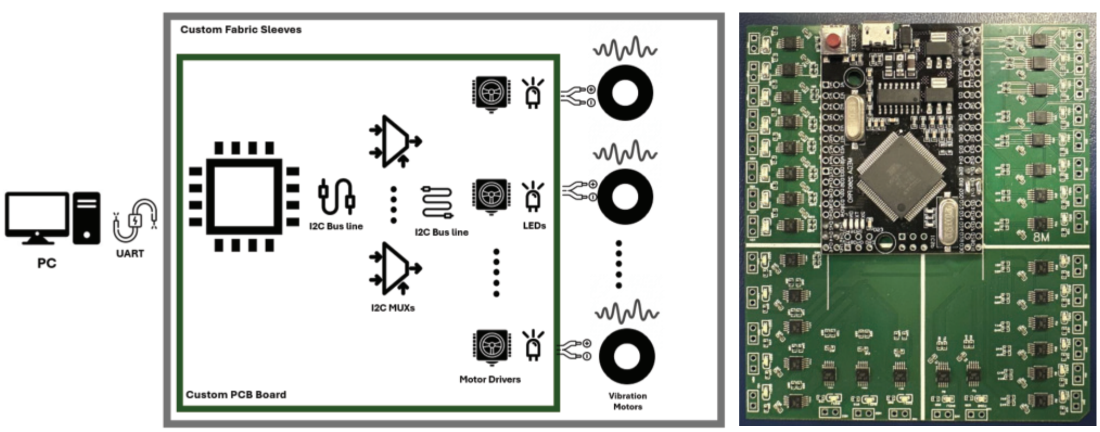

A B

FIGURE 5.3. (A) Schematic of PCB (B) actual picture of PCB.

We developed a specialized electronic hardware platform (shown in Fig. 5.3) centered on the ATmega2560 microcontroller(Microchip Technology Inc.) for managing precise vibrotactor actuation, where the microcontroller communicated directly with a computer via a UART protocol. To efficiently handle multiple control inputs and outputs, our system incorporated four TCA9548APWR I2C multiplexer chips (Texas Instruments Incorporated). These chips facilitate the distribution of I2C data from the microcontroller to 32 possible vibrotactor motor drivers, although we employed 16 vibrotactors in this study. The DRV2605LDGSR motor drivers were chosen for their ability to interpret a range of control signals such as voltage, frequency, and duration (Texas Instruments Incorporated), ensuring precise motor operation. This control unit housed in a dedicated upper-arm pocket independently regulated the frequency, amplitude, and timing of each vibrotactor.

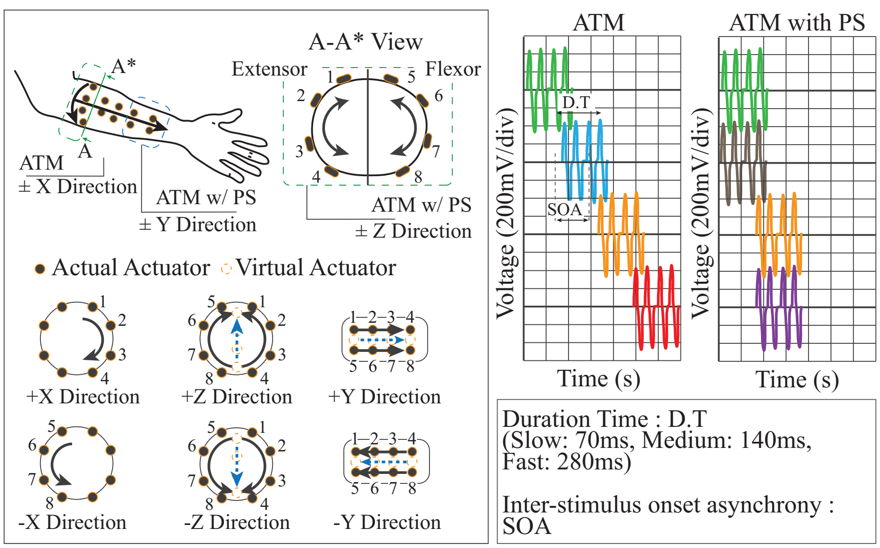

FIGURE 5.4. Schematic description for conveying directional and speed information through the sequential activation of vibrotactors arranged in a haptic sleeve.

5.3.3 Pilot User Testing

5.3.3.1 Design of the feasibility test

To evaluate the feasibility of using the haptic sleeve to encode robotic movement information, we recruited N=10 participants to perform testing. The experimental protocol was approved by the UC Davis Institutional Review Board (IRB), and participants provided written informed consent prior to participation.

Before testing, we measured the maximum circumference of each participant's self-reported dominant arm's forearm to ensure proper fit of the haptic sleeve. Participants then donned the haptic sleeve on their self-reported dominant arm. They were informed that the testing would involve patterns of vibrotactile stimulation displayed to the forearm via the haptic sleeve. These vibration patterns encoded directional information, which included orthogonal directions (±X, Y, or Z) at three possible velocity levels (slow, medium, or fast, as described in the design section above), totaling 18 combinations of direction and velocity.

Participants were informed that, for each vibration pattern presented, their task was to identify both the perceived movement direction and velocity. They were first provided with a familiarization period during which each combination of direction and velocity was sequentially displayed to the participant via the haptic sleeve, and they were informed of the direction and velocity each combination encoded. Following familiarization, testing then began with each combination of direction and velocity being randomized and repeated 3 times, resulting in a total of 54 vibration patterns presented to each participant.

Our primary outcome measure was the recognition accuracy with which participants could report the direction and velocity of vibration patterns. To identify significant differences in our data, we employed a multiple linear mixed-effects (LME) model. In this model, the accuracy of participants' responses was the dependent variable, with combinations of direction and speed serving as fixed effects and individual participants included as a random effect. Furthermore, we analyzed the comparison of individual fixed effects and their interactions using false discovery rate adjustment after obtaining estimated marginal means.

5.3.4 Findings and Discussion

Fig. 5.5 shows recognition accuracy for each type of encoded information individually (direction and velocity). Overall, participants correctly reported directional patterns with approximately 90% accuracy. Participants correctly identified the patterns in the negative X direction and the positive and negative Y directions with a median accuracy value of 100%. However, greater variability was observed for directional patterns in the positive X and positive Z directions, with a median accuracy value of 94.44% (Q1=88.89%, Q3=100%), as well as for the negative Z direction, which had a median accuracy of 100% (Q1=88.89%, Q3=100%). However, these differences were not statistically significant. These results may reflect the variability of vibration perception sensitivity across forearm dermatomes (lateral (C7) and medial (T1) portions of the forearm). This could be attributed to the difference in the extent of somatosensory cortical representation in the human brain or known differences in the density of mechanoreceptors across the forearm [**53**].

Velocity recognition accuracy differed more clearly across conditions. Participants reported fast speed pattern with significantly higher accuracy than both medium and slow velocities, with significant differences observed between fast and medium ($p < 0.001$) and between fast and slow speed ($p < 0.001$).

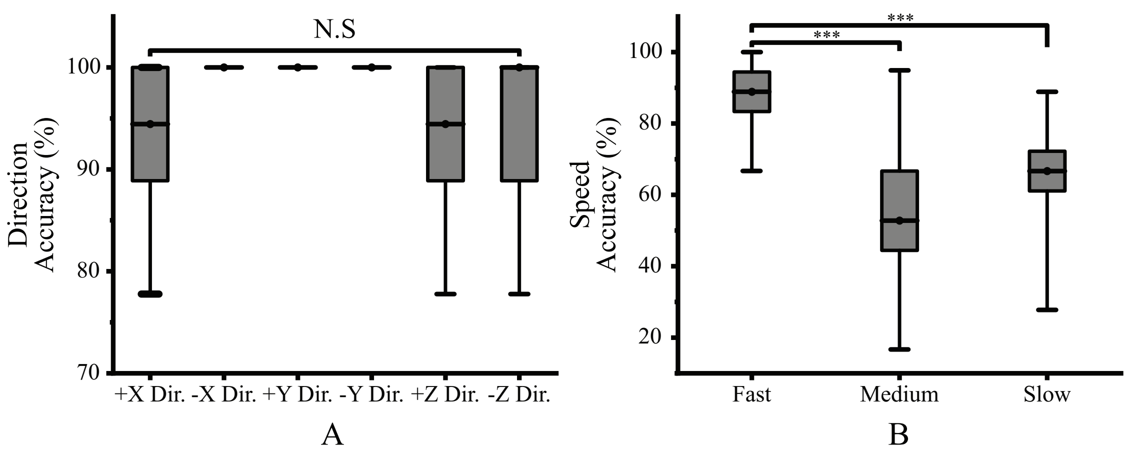

FIGURE 5.5. Recognition accuracy for each vibration pattern (A) direction and (B) speed, the median value indicated on the box as a black circle, and the whiskers extended from the minimum to the maximum. (* $p < 0.5$, ** $p < 0.01$, *** $p < 0.001$).

To further examine recognition accuracy across combined direction-velocity conditions, we created a confusion matrix to illustrate participants' recognition average accuracy across all 18 combinations. The confusion matrix illustrates that participants were readily able to identify Euclidean directional information, and that the fast velocity encoding consistently outperformed the medium and slow (Fig. 5.6).

Finally, to assess whether haptic sleeve fit influenced recognition accuracy, we performed a correlation analysis between forearm circumference and combined direction-velocity accuracy. Participants' forearm circumferences ranged from 25.4 cm to 30.2 cm (mean = 27.4 cm ± 2.0 cm). We found a very weak negative correlation (r = -0.036) between the combined direction-and-velocity results and forearm circumference. However, it should be noted that the goal of the human tests was to examine the feasibility of the haptic sleeve, and the range of forearm sizes tested does not necessarily represent the diversity anticipated across flight crew members. Thus, further testing to examine the effects of fit is warranted, as is the examination of sleeve sizing and adjustable features to accommodate varying forearm sizes.

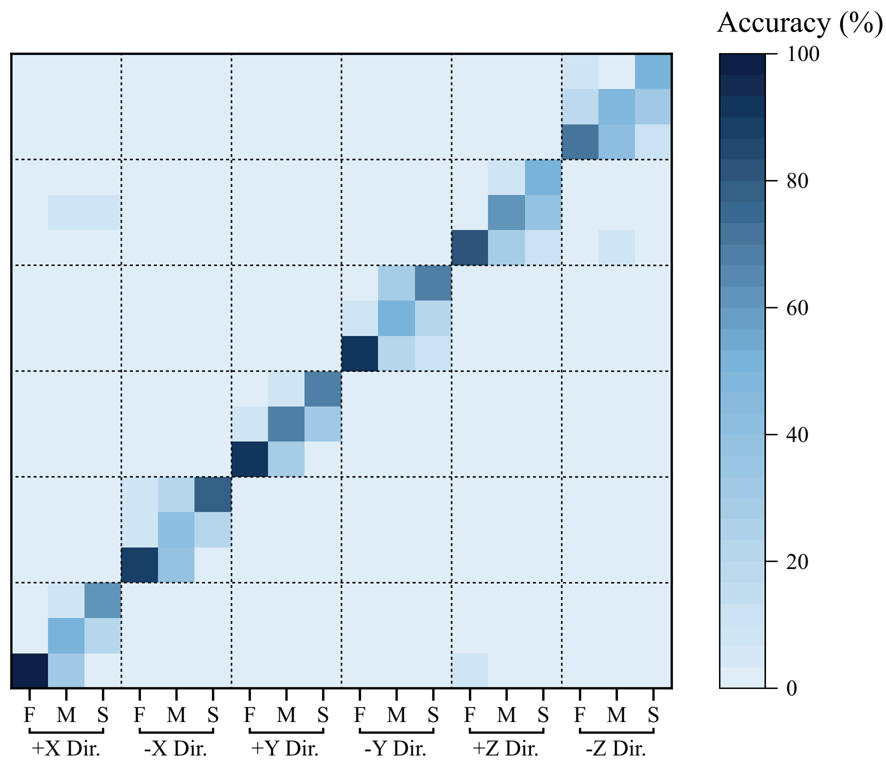

Figure 5.6. Confusion matrix of recognition accuracy for each vibration pattern combined with directions and speed

5.3.5 Conclusion and Future Directions

In this paper, we contributed to the development of a prototype wearable haptic sleeve that leverages tactile stroke illusions and feasibility testing with human subjects. Our feasibility test demonstrated its potential for conveying task-relevant directional and velocity cues relevant to robotic operation movements. Specifically, we arrived at two key findings: first, participants demonstrated an acute ability to use tactile stroke illusions to interpret Euclidean directional cues; second, participants were readily able to detect differences in velocity information; accurately identifying fast velocity separate from slow or medium. However, we noted that the medium and slow velocity patterns were less accurately perceived which opens new directions for future exploration. For example, future experiments may focus on how best to manipulate vibration profiles or the resolution to which we can detect velocity differences. This may help research identify strategies to maximize the amount of information that can be encoded through tactile stroke illusions. Collectively these results suggest that wearable haptic interfaces based on tactile stroke illusions offer a promising approach for augmenting or substituting cues relevant to robotic operations, particularly in environments where visual attention is highly taxed. By providing complementary movement information through the haptic channel, such interfaces may reduce reliance on vision and support more efficient and robust performance in teleoperations.

In addition, future research will focus on refining the prototype to enhance its reliability and user experience. We plan to conduct extensive testing by manipulating various physical characteristics of vibration to evaluate its effectiveness in conveying speed and complex robotic movements. To achieve these future directions, we will explore vibration perception across parts of the forearm to induce tactile stroke illusions and validate the methods for rendering tactile sensations using this sleeve with a much larger subject population. Moreover, since we now have this sleeve platform, we will also explore the simultaneous collection [**54**], [**55**], [**56**], [**57**] and analysis [**57**], [**58**], [**59**] of physiological signals during feedback. Additionally, we will assess the efficacy of haptic feedback in learning to control robotic operations. Ultimately, our goal is to develop a robust and intuitive haptic interface that significantly enhances the precision and efficiency of robotic operations.

5.4 Effect of haptic feedback on motor learning and visual dependence for a robotic teleoperation

5.4.1 Background

Teleoperation of robotic systems is inherently human-in-the-loop, in which operators must acquire, refine, and retain mappings between control inputs, sensory feedback, and robotic behavior. Because these mappings can be non-intuitive under inherent constraints in teleoperation such as delayed or degraded sensory information, effective teleoperation requires sensorimotor processes through which these mappings are gradually formed and refined through experience.

Many current tele-robotic systems are typically equipped with multiple active telepresence cameras to provide operators with sufficient visual access to the remote environment and task space [**60**], [**61**]. While vision provides rich spatial and predictive information, excessive reliance on visual feedback imposes substantial cognitive demands and can lead to slower response and reduced accuracy, particularly in complex or time constrained tasks. This visual dominance is especially pronounced during early stages of teleoperation learning, when operators depend heavily on visual monitoring to compensate for uncertainty in control mappings.

To address these limitations, haptic feedback can be introduced as a complementary sensory channel to support teleoperation skill acquisition [**62**], [**63**], [**64**]. By conveying robotic-task relevant information, haptic feedback can reduce the need for continuous visual monitoring and redistribute perceptual demands across sensory modalities. Rather than serving as a redundant signal, haptic feedback enables cross modal integration, in which information from haptic and vision is jointly incorporated to guide motor actions [**65**].

In natural motor behavior, learning involves forming and retaining associations between sensory cues and motor outcomes, along with adaptive redistribution of sensory modalities as skill develops. However, most existing teleoperation studies focuses primarily on the immediate effects of haptic feedback on task performance. Although some studies has demonstrated the role of artificial haptic feedback in skill acquisition, it still remains debatable [**66**] and largely limits to performance based metrics rather than integrating physiological measures that reflect operator state and visual demand. As a result, the mechanisms through which haptic feedback may support motor learning and reduce visual dependence in teleoperation remain poorly understood.

Building on these gaps, this chapter presents a feasibility study that develops and validates a visuo haptic behavioral assessment battery for teleoperation learning, integrated with a wearable haptic sleeve that encodes collision warning information. By combining performance based measures with eye gaze metrics that index visual demand, this framework enables systematic evaluation of how haptic feedback influences cross modal integration, motor learning, and shifts in sensory reliance. This approach allows assessment of whether haptic feedback supports not only immediate performance improvements, but also sustained learning outcomes, including skill retention over time and generalization across tasks.

5.4.2 Methods

5.4.2.1 Participants

A total of N = 6 able-bodied individuals with no known neurological or neuromuscular impairments participated in this study (50% male with a mean of 26.83 $\pm$ 2.27 years). All participants self-reported as right-handed. Participants were divided equally into two groups: a haptic feedback group (N = 3), who received vibrotactile feedback during this study, and a non-haptic control group (N = 3), who completed this study without haptic feedback.

The study was approved by the University of California Institutional Review Board, and all participants provided written informed consent prior to participating.

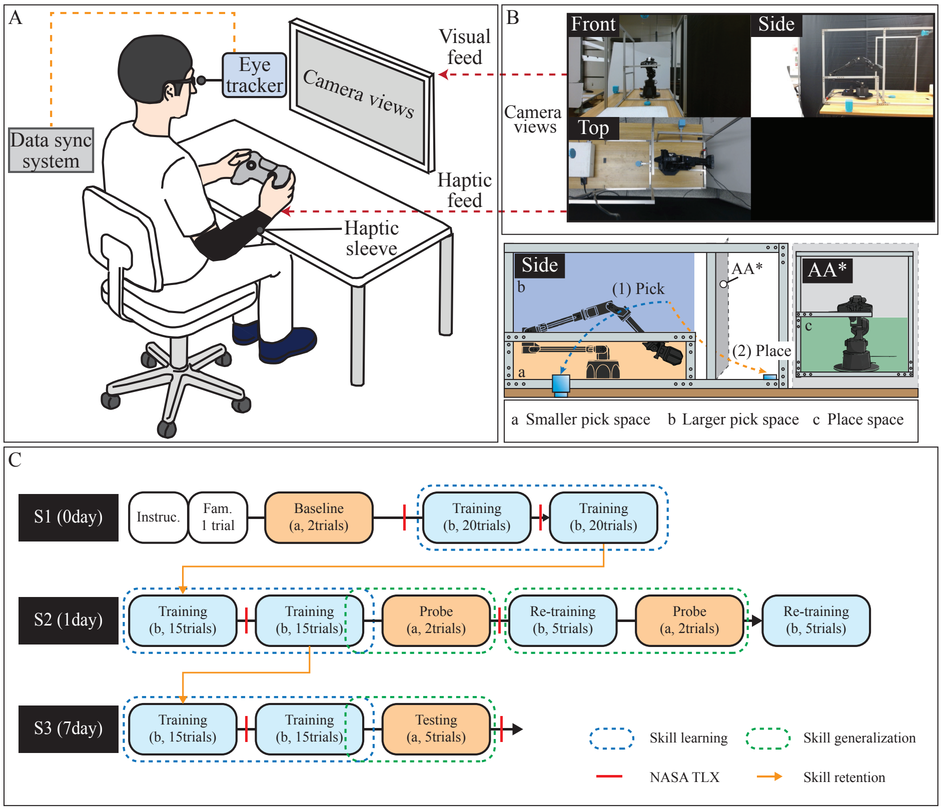

FIGURE 5.7. Experimental setup and procedure. (A) Schematic description of the participant-side setup, including an eye-tracker, a game controller used to control the teleoperated robot, a vibrotactile haptic sleeve (haptic group only), and a display presenting three different views of the robot workspace, (B) Workspace views and schematic of the pick-and-place task. Colored regions indicate the allowed workspace used to approach and grasp the object: blue denotes the larger pick space (pick over the bar), and orange denotes the smaller pick space (pick under the bar). In both tasks, the object is placed through the same green space to the target. (C) Schematic description of the experimental procedure, consisting of three sessions. Session 1 included a baseline phase (2 trials) followed by training (40 trials). Session 2 included training (30 trials), two retraining phases (5 trials each), and two probe phases (2 trials each). Session 3 included training (30 trials) and testing (5 trials). Colors in (C) indicate which task condition (blue: larger pick space; orange: smaller pick space) was performed in each phase, while dashed boxes mark the phases used to compute skill-related outcomes (skill learning, retention, and generalization) and red lines indicate when NASA Task Load Index (TLX) was measured.

5.4.2.2 Experimental description

1) Teleoperation Setup:

The hardware for the teleoperation environment comprised a Trossen ViperX 300s robotic arm, three 1080p webcams (Logitech) positioned to provide front, side, and top views, and a laptop computer with a 3.6 GHz Core i7-13620H CPU (Intel, Corp.) running a generic Linux kernel to execute the control loop. Participants sat facing an LCD monitor that displayed the three synchronized camera views and was instructed to hold a joystick controller (PlayStation, Sony) with both hand, as shown in Fig. 5.7A.

For participants assigned to the haptic group (in Fig. 5.7A), a haptic sleeve embedded with twelve linear resonant vibration actuators (Precision Mircodrives, C10-100) that we previously developed [**67**] was secured to the dominant forearm. All participants were also equipped with a wearable eye-tracking systems (Pupil Labs, Neon), which recorded binocular gaze data at a sampling rate of 120 Hz. This non-contact infrared based system captured real time gaze behavior throughout the experiment.

The software architecture of the setup was developed as a modular platform, with control functions developed as Robot Operating System (ROS) nodes. The collision environment was defined a priori and imported into the MoveIt planning scene as static collision objects, allowing the system to query collisions and separation distances against known workspace geometry. Collision and distance computations were performed using MoveIt's planning scene collision checking interface, which relies on a selectable collision detection backend. In our implementation, the planning scene was configured to use the Bullet collision detector to obtain nearest contact information, including penetration depth and contact normal direction, for the current robot state. These outputs were then published as ROS messages and used to generate directional haptic feedback commands [**68**].

2) Haptic Feedback Encoding:

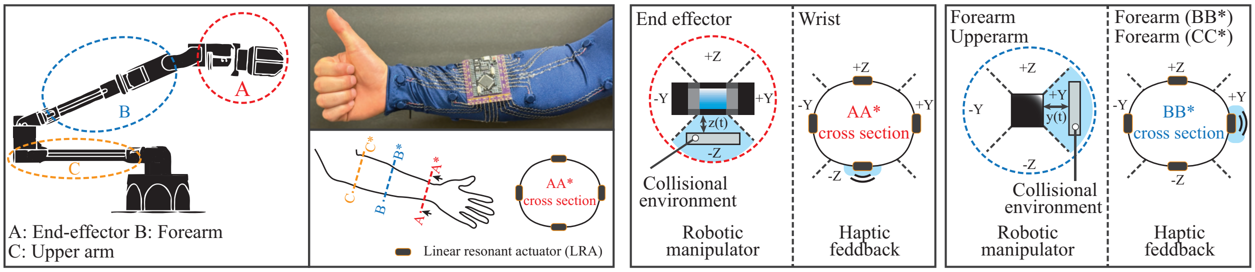

FIGURE 5.8. Haptic feedback mapping for collision avoidance. Schematic illustrating how the teleoperated robot is segmented into multiple body/link regions for haptic feedback. Each robot segment is assigned to a corresponding actuator (or actuator group) on the haptic sleeve, enabling localized vibration that indicates which part of the robot is approaching contact. Collision feedback also encodes collision direction: vibrations are delivered to actuators positioned to represent the contact normal (e.g., left vs right, upward vs downward), allowing participants to infer where and from which direction a collision is likely to occur. Example scenarios are shown to demonstrate how distinct vibration patterns are generated for different robot segments and approach directions when the robot nears an obstacle, providing real-time cues to support corrective motion before contact.

Haptic feedback was generated from the nearest robot-collisional environment contact information returned by the MoveIt planning scene, which was configured to use the Bullet collision detector. For each update, the collision checker produced a contact normal vector $\mathbf{n}(t) \in \mathbb{R}^3$ (unit length) and a penetration depth $d(t) \in \mathbb{R}^+$, along with the identities of the contacting bodies. To make the directional cue invariant to the robot base yaw, the contact normal was rotated by the negative yaw joint angle $\psi(t)$ about the world z axis, allowing a consistent operator-centered direction. The directional penetration vector was computed as $\mathbf{v}(t) = d(t)\mathbf{n}_{\text{yaw}}(t)$. Because the haptic sleeve was intended to make the operator perceive the robot arm as co-located with their own arm within the collision environment, we encoded direction on the operator's forearm plane. Accordingly, only the components corresponding to right-left and up-down on the forearm, $\Delta y(t) = v_y(t)$ and $\Delta z(t) = v_z(t)$, were transmitted. The forward–backward component $v_x(t)$ was not used because it does not map intuitively onto the forearm surface (it would require a depth-like cue relative to the arm) and can be perceptually ambiguous for rapid corrective responses.

$$\mathbf{n}_{\text{yaw}}(t) = \mathbf{R}_z(-\psi(t))\ \mathbf{n}(t), \tag{5.1}$$

where $\mathbf{R}_z(\cdot)$ denotes a rotation matrix about the z axis. A directional penetration vector was then computed as

$$\mathbf{v}(t) = d(t)\,\mathbf{n}_{\text{yaw}}(t) = \begin{bmatrix} v_x(t) & v_y(t) & v_z(t) \end{bmatrix}^{\mathsf{T}}. \tag{5.2}$$

Accordingly, we transmitted only the right-left and up-down components on the operator's forearm, $\Delta y(t) = v_y(t)$ and $\Delta z(t) = v_z(t)$. A discrete mode $M(t)$ selected the actuator group based on the robot link involved in the contact (end-effector, lower arm, upper forearm/upper arm), as described in Fig. 5.8. Feedback was transmitted only when the penetration depth exceeded depth threshold d_{th} of 0.02 (m). For near-contact events, the direction was discretized into four quadrants using the polar angle

$$\theta(t) = \operatorname{atan2}(\Delta z(t),\, \Delta y(t))\,, \tag{5.3}$$

and mapped to a binary directional cue $(\tilde{y}(t), \tilde{z}(t))$ for robust actuation. The resulting command was serialized and streamed to the microcontroller as an ASCII packet,

$$\mathbf{u}(t) = \langle M(t),\, \tilde{y}(t),\, \tilde{z}(t) \rangle \tag{5.4}$$

3) Task Procedure:

Each participant was randomly assigned, prior to any testing: non-haptic group and haptic group (N=3 in each group). The study comprised three experimental sessions. Session 2 was chosen to be 24 hours after session 1 to allow for overnight consolidation following initial practice [**69**], [**70**]. The retention interval was chosen to be significantly longer (7 days) to examine skill retention absent of daily practice (session 3). The experimental setup was identical across all sessions, with different training structure differed by session (see details below, Fig. 5.7C).

During the experimental sessions, participants performed repeated trials of a teleoperated pick-and-place task with two objectives: complete the required pick-and-place movement and avoid contacting the obstacle environment whenever possible. Trials were performed under two spatial constraint conditions. In the larger constraint condition, participants grasped a 3D printed cubic object by moving the end-effector over the bar (space b, the blue area in Fig. 5.7B.) and then transported the object to a target location by moving under the bar (space c, the green area in Fig. 5.7B.). In the smaller constraint condition (space a, the orange area in Fig. 5.7B.) , participants moved the end-effector through a narrower passage under the bar (space a, the orange area in Fig. 5.7B.) and then positioned it at the same target location using space c, as shown in Fig. 5.7B.

The experiment began with a short familiarization phase in session 1, during which participants learned to operate the joystick controls, for those in the haptic group, experienced how vibrotactile cues encoded collision related information. This familiarization ensured that all participants understood the control interface and, when applicable, the meaning of the haptic feedback before formal data collection. Following the familiarization phase, participants first made a baseline phase consisting of two trials of the pick-and-place task under the smaller spatial constraint (space a). This baseline assessment provided an initial measure of performance prior to training. After this baseline period, participants were trained with 40 trials of pick-and-place task performed under the larger spatial constraint (space b), as described in Fig. 5.7C.

To assess 1-day retention and learning generalization, participants first underwent 30 trials under the trained larger space condition(space b). They then performed two probe trials under the smaller spatial constraint (space a) to assess generalization to a less spacious task. These probe trials were followed by five retraining trials during which participants performed the task under the trained space (space b). This sequence of probe and retraining trials was repeated once more throughout the session 2, resulting in a total of 44 trials. After 7 days from the session 1 (session 3), to assess long-term retention and learning generalization, participants underwent 30 trials under the larger spatial constraint condition (space b), followed by five trials under the smaller spatial constraint (space a) to assess generalization after extended time without practice, as described in Fig. 5.7C.

Within each session, participants completed the NASA Task Load Index (TLX) questionnaires twice, as illustrated in the experimental timeline.

4) Outcome metrics:

The robot's end effector was recorded in accordance with the control loop frequency at 10 Hz and synchronized across all trials. Completion time, travel distance, smoothness, and number of collisions were computed from the end effector position data on a per trial basis. Trials in which participants failed to complete the task were excluded from these outcome metric computations to avoid confounds from premature termination and subsequent re attempts that introduce unequal practice and strategy changes during learning.

(1) Number of collisions: For each trial, the number of collisions was defined as the total count of robot–environment contact events that occurred from the moment the participant began controlling the robot until the object was placed at the target position.

(2) Completion time: Each trial's completion time was defined as the elapsed time from the moment the participants began controlling the robot to the moment the object was placed at the target position.

(3) Travel distance: Each trial's travel distance was computed as the cumulative Euclidean distance between consecutive position samples.

(4) Smoothness: Movement smoothness was quantified using spectral arc length [**71**], which uses a movement speed profile's Fourier magnitude spectrum. Higher values indicate smoother movements.

(5) Cognitive load: Participants reported the NASA Task Load Index (NASA-TLX, Appendix H, Supplementary Table 1) , which rates their perceived levels of mental, physical, and temporal demand subscales using 20-point rating scales [**72**], [**73**], [**74**]. As shown in 5.7B, participants reported their workload score twice per session: in session 1, after the baseline tasks and midway through the training tasks; in session 2, midway through the training tasks and after the first probe tasks; and in session 3, midway through the training tasks and after the probe tasks.

(6) Visual dependence: Visual dependence was quantified using an Area of Interest (AOI)–based approach. AOIs are spatially defined regions of the visual display that correspond to task-relevant objects and are defined based on the semantic structure of the interface. In this study, the task display was divided into three AOIs corresponding to the key visual elements required for task execution, as illustrated in Fig. 5.7B. Gaze fixation data were mapped onto these AOIs, and visual dependence was quantified as the proportion of valid gaze samples allocated to each AOI relative to the total viewing time. This metric captures the extent to which participants relied on task-relevant visual information during task performance.

(7) Skill learning: Skill learning was quantified as the ratio of performance in the last five trials of each training session to performance in the first five trials of the same session, capturing the extent of performance improvement within that session.

(8) Skill retention: Skill retention was quantified as the ratio of performance in the first five trials of the subsequent training session to performance in the last five trials of the preceding session, to assess how well skill gains were preserved across sessions. A retention ratio greater than 1 indicates improved performance at the start of the next session.

(9) Skill generalization: Skill generalization was quantified using a generalization ratio defined as the median performance on the early probe trials divided by the median performance on the final five training trials immediately preceding the probe. Values

near 1 indicate full generalization of training gains to the probe task, and values greater than 1 indicate probe performance exceeded the end-of-training level.

5.4.3 Results

5.4.3.1 Number of collisions

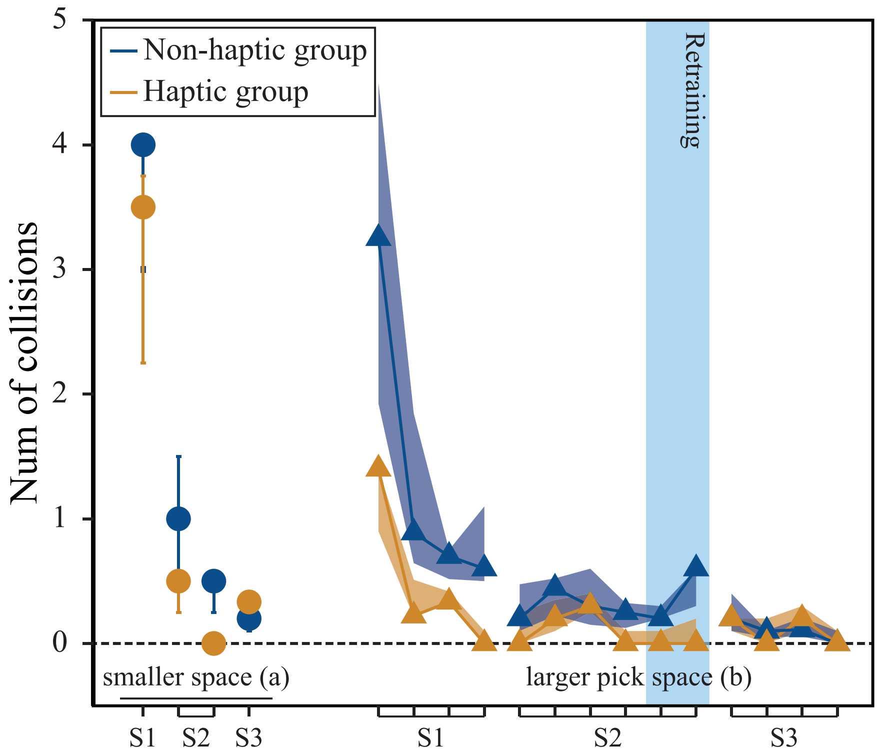

FIGURE 5.9. Collisions across sessions and phases. Number of collisions is summarized for the haptic and non-haptic groups across sessions and experimental phases using predefined trial windows. For each group and window, collisions are aggregated across participants and reported as the median with interquartile range (IQR; 25th–75th percentiles). Trial windows are aligned with the phase structure (baseline, training, retraining, probe, and testing) to enable comparisons of collision behavior within and across sessions.

Number of collisions was used to quantify how haptic feedback helped operators avoid collisions as shown in Fig. 5.9. Collisions were summarized within predefined trial windows for each session. Training and retraining phases were segmented into consecutive 5-trial windows, whereas baseline, probe, and testing phases were treated as phase-level segments, with all consecutive trials within the same phase aggregated into a single window. In the baseline phase, the haptic group showed a slightly lower median collision rate than the non-haptic group (3.5 [1.0 $\sim$ 4.0] for the haptic group and 4.0 [2.0 $\sim$ 4.0] for the non-haptic group). During the first training phase, both groups reduced collisions across windows (Haptic group: from 1.4 [0.9 $\sim$ 1.4] in the first window to 0.0 [0.0 $\sim$ 0.1] in the last window; Non-haptic group: from 3.3 [1.9 $\sim$ 4.5] to 0.6 [0.5 $\sim$ 1.1]). Across this phase, the haptic group generally exhibited fewer collisions than the non-haptic group across windows. During Session 2, the haptic group generally showed fewer collisions than the non-haptic group across the training and retraining phases. However, both groups maintained low collisions across those phases (Haptic group: 0.0 [0.0 $\sim$ 0.3] in the first window and 0.0 [0.0 $\sim$ 0.1] in the last window; Non-haptic group: 0.2 [0.1 $\sim$ 0.5] to 0.25 [0.1 $\sim$ 0.3]). During the probe phases, the haptic group also exhibited fewer collisions, indicating improved collision avoidance during the task. Finally, in the last session (7 days after Session 1), both groups exhibited fewer collisions than in the first window of the initial training phase, and collision levels were comparable to those observed in the last window of the second retraining phase. Across the phases of the final session, both groups maintained similarly low collision counts with little change over time.

5.4.3.2 Outcome metrics across trials

Each outcome metric (completion time, travel distance, and smoothness) was quantified to evaluate the feasibility of the experimental procedure and to confirm that these measures captured skill relevant changes across trials within each session, as shown in Fig. 5.10.

During the training phase of Session 1 (S1), completion time decreased across trials in both groups, indicating performance improvement. The non-haptic group showed a 76.8% reduction in completion time, decreasing from 246.8 s [218.0 $\sim$ 263.1] on the first trial to 57.4 s [56.1 $\sim$ 84.6] on the last trial. The haptic group showed a 64.2% reduction, decreasing from 128.1 s [119.4 $\sim$ 146.3] on the first trial to 45.8 s [44.5 $\sim$ 46.6] on the last trial. By the final trial, the haptic group completed the task faster than the non-haptic group, suggesting that haptic feedback supported more efficient task execution by the end of training. During the baseline phase of S1, the haptic group also showed a greater reduction in completion time (57.0%) than the non-haptic group (17.5%).

During the training phase of Session 2 (S2), completion time decreased across trials in both groups, but the reductions were smaller than in S1. In the haptic group, completion time was reduced by 36.5%, from 61.9 s [55.5 $\sim$ 68.2] on the first trial to 39.3 s [37.8 $\sim$ 48.7] on the last trial. In the non-haptic group, completion time was reduced by 57.2%, from 110.8 s [110.8 $\sim$ 110.8] on the first trial to 47.4 s [47.1 $\sim$ 47.6] on the last trial. During the retraining phases, despite the probe phase immediately beforehand, both groups maintained completion times comparable to the final trial of the preceding training phase, with only small changes across trials within each retraining phase. In the haptic group, completion time decreased

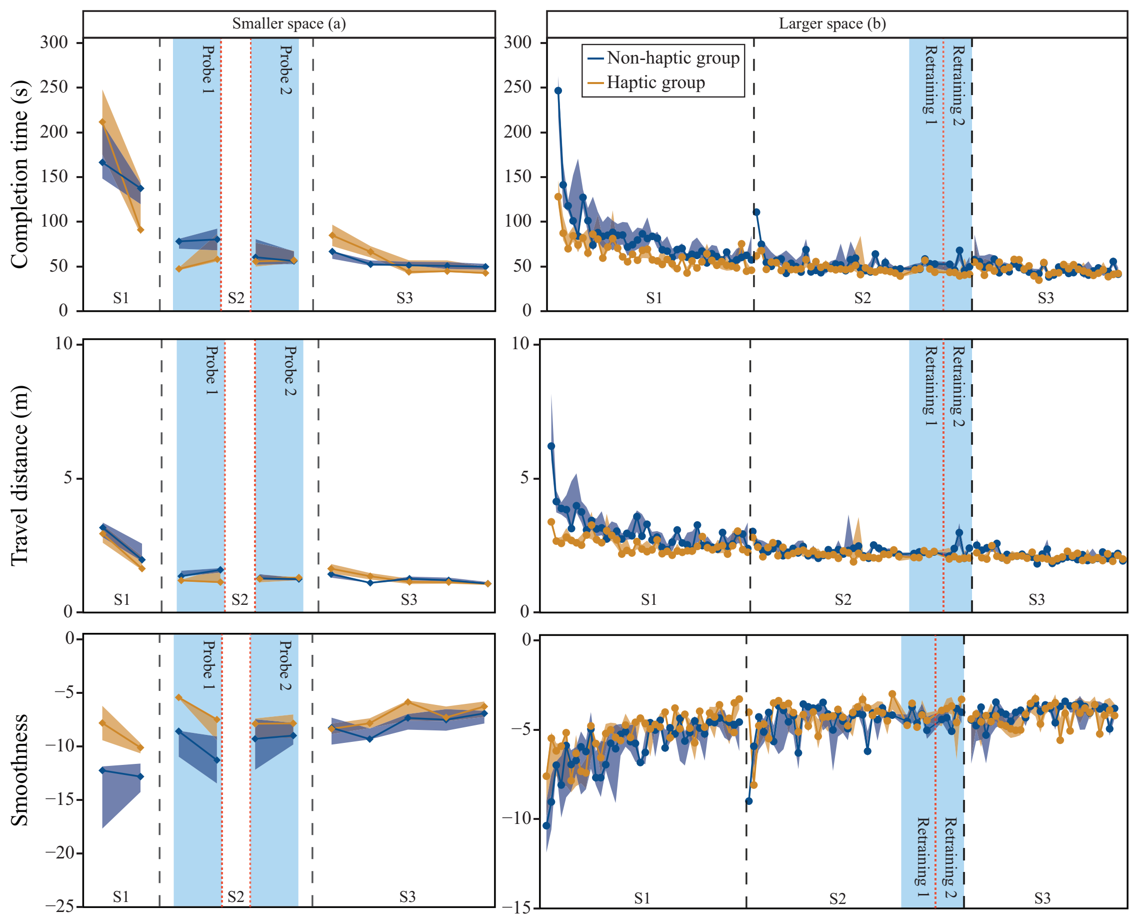

FIGURE 5.10. Each outcome metric (completion time, travel distance, and smoothness) across trials within each session. Dots denoted individual trial median values, and shaded bands indicate across participant variability over trials.

slightly from 46.2 s [42.0 $\sim$ 50.6] on the first trial of the first retraining phase to 43.5 s [42.7 $\sim$ 53.7] on the last trial, and from 43.4 s [42.1 $\sim$ 50.9] on the first trial of the second retraining phase to 41.2 s [40.4 $\sim$ 42.9] on the last trial. In the non-haptic group, completion time increased from 47.9 s [43.6 $\sim$ 53.0] to 52.8 s [48.1 $\sim$ 56.0] across the first retraining phase, and from 45.8 s [44.0 $\sim$ 50.9] to 49.7 s [48.3 $\sim$ 60.9] across the second retraining phase. During the probe phases of S2, the haptic group completed the pick-and-place task in the smaller workspace faster than the non-haptic group during the first probe phase, whereas both groups showed comparable completion times during the second probe phase.

Finally, during the last session (S3), both groups required more time to complete the task than on the last trial of the final retraining phase in S2. For the haptic group, completion time increased by 33.3%, from 41.2 s [40.4 $\sim$ 42.9] on the last trial of the final S2 retraining phase to 54.9 s [54.0 $\sim$ 82.6] on the first trial of the S3 training phase. For the non-haptic group, completion time increased by 16.3%, from 49.7 s [48.3 $\sim$ 60.9] to 57.8 s [56.5 $\sim$ 85.7]. However, by the last trial of the S3 training phase, both groups returned to completion times comparable to those on the last trial of the final S2 retraining phase, and the non-haptic group achieved completion times similar to those of the haptic group. A similar pattern was observed when participants performed the task in the smaller workspace (a).

A similar pattern was observed for travel distance, where decreases in travel distance indicated improved performance. A corresponding trend was also observed for movement smoothness, where increases in smoothness reflected improved performance. These results are summarized in Table 5.1

5.4.3.3 Skill learning

During the training phases across sessions, completion time was used as the primary metric of skill acquisition because it provides a direct, sensitive measure of how efficiently participants could complete the pick-and-place task while integrating perception, planning, and control.

As operators learn the task, they typically reduce unnecessary pauses, corrective motions,

TABLE 5.1. Summary of outcome metrics across each phase for each session

	Completion time (s)		Travel distance (m)		Smootheness	
	Haptic group	Non haptic group	Haptic group	Non haptic group	Haptic group	Non haptic group
Baseline	$91.0 \sim 211.8$	$137.4 \sim 166.4$	$1.6 \sim 2.9$	$2.0 \sim 3.2$	$-10.1 \sim -7.8$	$-12.8 \sim -12.3$
S1 training first trial	128.1	246.8	3.4	6.2	-7.6	-10.4
S1 training last trial	45.8	57.3	2.2	2.4	-3.3	-4.6
S2 training first trial	61.9	110.8	2.8	3.0	-4.0	-9.0
S2 training last trial	39.3	47.4	2.1	2.2	-3.0	-4.2
S2 1st probe	$47.3 \sim 58.0$	$68.0 \sim 69.9$	$1.1 \sim 1.2$	$1.4 \sim 1.6$	$-7.5 \sim -5.4$	$-11.3 \sim -8.6$
S2 1st retraining first trial	46.2	47.9	2.1	2.2	-4.8	-4.5
S2 1st retraining last trial	43.5	52.8	2.3	2.3	-4.5	-5.0
S2 2nd probe	$55.7 \sim 57.0$	$56.1 \sim 60.4$	$1.25 \sim 1.3$	$1.2 \sim 1.3$	-7.9	$-9.3 \sim -9.0$
S2 2nd retraining first trial	43.4	52.5	2.0	2.1	-3.9	-4.4
S2 2nd retraining last trial	41.2	49.7	2.0	2.4	-3.3	-4.0
S3 training first trial	54.9	57.8	2.2	2.5	-4.4	-3.7
S3 training last trial	42.1	41.4	2.0	1.9	-4.2	-3.8
S3 testing	$42.7 \sim 84.9$	$49.7 \sim 66.8$	$1.1 \sim 1.6$	$1.1 \sim 1.4$	$-8.4 \sim -5.9$	$-8.3 \sim -6.9$

and inefficient strategies, which appears as a faster completion time even when the task requirements are unchanged.

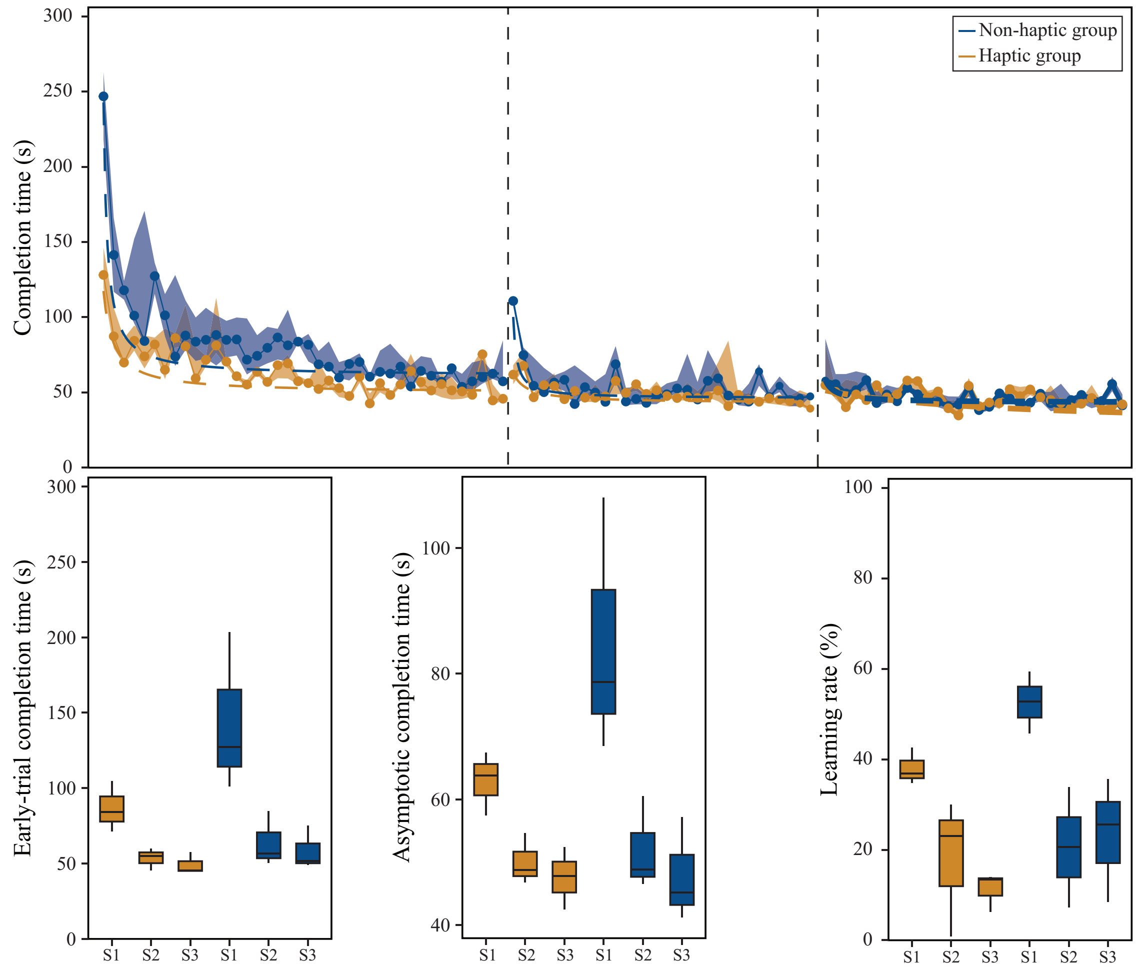

FIGURE 5.11. Skill learning in completion time. Completion time across training trials within each session is shown with the fitted curve. Dots denote individual trial median values, and shaded bands indicate across participant variability over trials. Early trial completion time was computed as the median completion time across the first five trials of each training phase within each session and is reported as the median with interquartile range (IQR; 25th–75th percentiles). Asymptotic completion time was defined from the fitted curve and is reported as the median with the same IQR. Learning rate was quantified as the percent change between the first five and last five trials of each training phase within each session and is reported as the median with the same IQR.

Before quantifying learning rate, participant-level completion time was summarized within each training phase. Specifically, for each participant and each training phase, we computed (i) **early-trial completion time** as the median completion time across the first five trials of that phase and (ii) **asymptotic completion time** as the median completion time across the final trials of that phase, as shown in Fig. 5.11. In Session 1 (S1), the haptic group completed the task more efficiently than the non-haptic group, as reflected by shorter completion times in both the early-trial and asymptotic completion times. However, in Sessions 2 (S2) and 3 (S3), the non-haptic group reached completion times comparable to those of the haptic group in both completion times. Specifically, early-trial completion time was 56.5 s [$53.5 \sim 70.6$] for the non-haptic group and 54.9 s [$50.2 \sim 57.4$] for the haptic group in S2, and 51.5 s [$50.2 \sim 63.3$] and 45.3 s [$45.1 \sim 51.5$] in S3, respectively. Similarly, asymptotic completion time was 47.7 s [$46.4 \sim 54.1$] for the non-haptic group and 47.6 s [$47.2 \sim 51.3$] for the haptic group in S2, and 44.0 s [$41.2 \sim 48.4$] and 45.9 s [$41.8 \sim 46.1$] in S3, respectively.

Learning rate was defined as the ratio of the median completion time in the first five trials to the median completion time in the last five trials of the same session, as shown in Fig. 5.11. Because the non-haptic group showed longer completion times in the early trials but reached asymptotic completion times that were comparable to those of the haptic group, the non-haptic group exhibited a higher learning rate than the haptic group in S1. Specifically, the haptic group showed a learning rate of 36.8% [$35.8\% \sim 39.7\%$], whereas the non-haptic group showed a learning rate of 52.7% [$49.2\% \sim 56.1\%$]. In contrast, in S3 the haptic group showed a smaller learning rate, suggesting less room for improvement within that session (13.5% [$9.9\% \sim 13.7\%$] for the haptic group vs. 25.6% [$17.1\% \sim 30.6\%$] for the non-haptic group).

5.4.3.4 Skill retention and generalization

As operators learned the task during the initial training phase, skill retention (how much of the trained skill was preserved) was quantified 1 day after S1 and 6 days after S2 as the ratio of completion time in the last five trials of the preceding training phase to the completion time in the first five trials of the subsequent training phase, with values closer to 1 indicating better retention (i.e., minimal loss of performance between sessions).

Skill generalization (how well the learned skill generalized to a novel task context) was quantified as the fraction of the training related performance change achieved during training that generalized to the probe task, relative to baseline performance. Values near 1 indicate full generalization of training gains to the probe task, and values greater than 1 indicate probe performance exceeded the end of training level.

Skill retention results indicated a dissociation between short term and long term retentions. The haptic group exhibited slightly greater long term performance retentions at the 6 day retention interval than the non haptic group (0.9 [0.8 $\sim$ 0.9] for the haptic group; 0.8

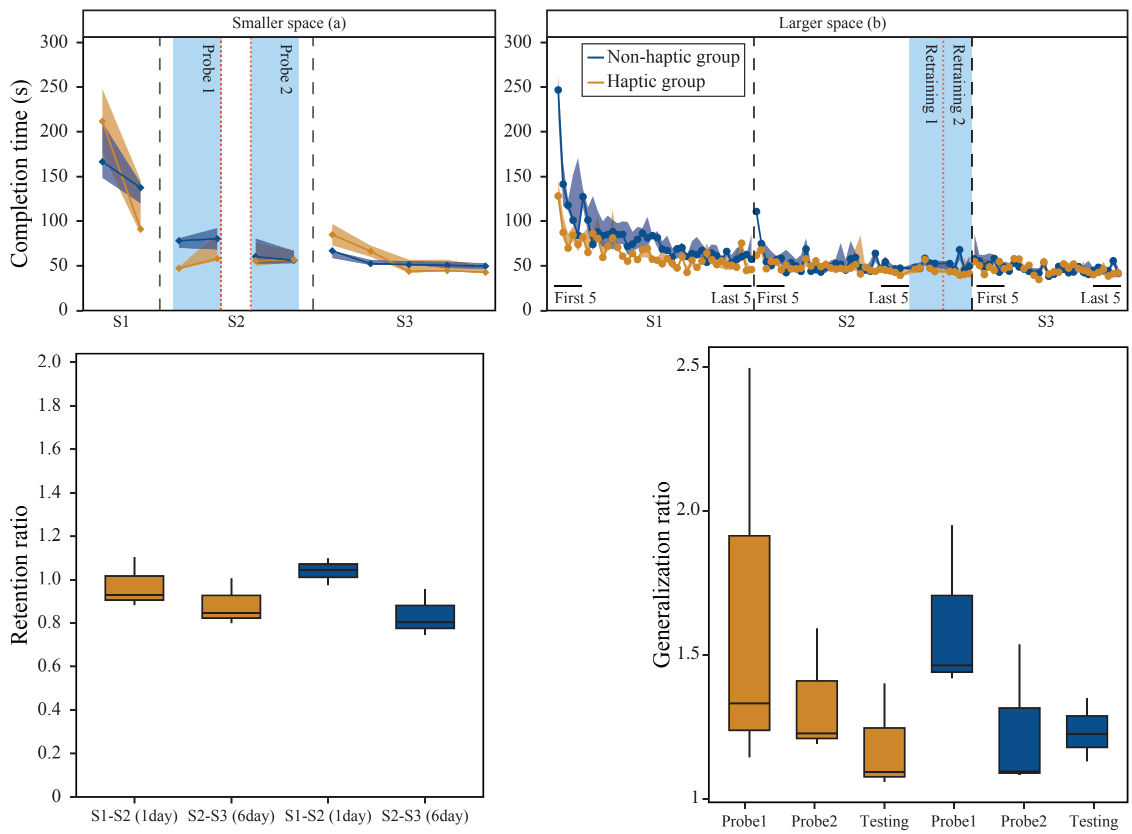

FIGURE 5.12. Skill retention and generalization in completion time. Completion time across training and probe trials within each session is shown. Dots denote individual trial median values, and shaded bands indicate across participant variability over trials. Skill retention was computed as the ratio of completion time in the last five trials of the preceding training phase to the completion time in the first five trials of the subsequent training phase. It was reported as the median with interquartile range (IQR; 25th–75th percentiles). Skill generalization was quantified as the fraction of the training related performance change achieved during training that generalized to the probe task, relative to baseline performance. It was reported as the median with the same IQR.

[0.8 $\sim$ 0.9] for the non haptic group), whereas the non haptic group showed slightly greater short term performance retentions at the 1 day retention interval (0.9 [0.9 $\sim$ 1.0] for the haptic group; 1.0 [1.0 $\sim$ 1.1] for the non haptic group), as shown in Fig. 5.12. Finally, skill generalization analyses showed that the haptic group exhibited a generalization ratio comparable to the non haptic group, indicating that trained performance carried over to the novel task to a similar extent in both groups. Specifically, the haptic group exhibited generalization ratios of 1.3 [1.2 $\sim$ 1.9] in the first probe phase, 1.2 [1.2 $\sim$ 1.4] in the second probe phase, and 1.1 [1.1 $\sim$ 1.2] in the final testing phase. The non haptic group showed similar ratios of 1.5 [1.4 $\sim$ 1.7], 1.1 [1.1 $\sim$ 1.3], and 1.2 [1.2 $\sim$ 1.3] across the same phases.

5.4.3.5 Visual dependence

Fig. 5.13 illustrates the spatial distribution of gaze fixations allocation across the three predefined Areas of Interest (AOIs) for the haptic and non-haptic groups during training sessions (S1 - S3). Across sessions, the haptic group predominantly allocated gaze to a single side view, with the density remaining concentrated within on AOI across all sessions. In contrast, the non-haptic group distributed gaze across two AOIs (front and side) throughout training phases. Gaze density revealed sustained allocation to both the front and side views across all sessions. This pattern remained stable during all sessions, indicating continued reliance on multiple visual perspectives during task performance.

5.4.4 Discussion and Conclusion

This work integrated a wearable haptic interface with a teleoperated robotic task and established a methodological framework to evaluate how haptic feedback shapes teleoperation learning and performance using a visuo haptic behavioral assessment battery. Using collision avoidance cues delivered through the haptic interface, we showed that haptic feedback measurably influenced task performance and altered the extent to which operators relied on vision to complete the task.

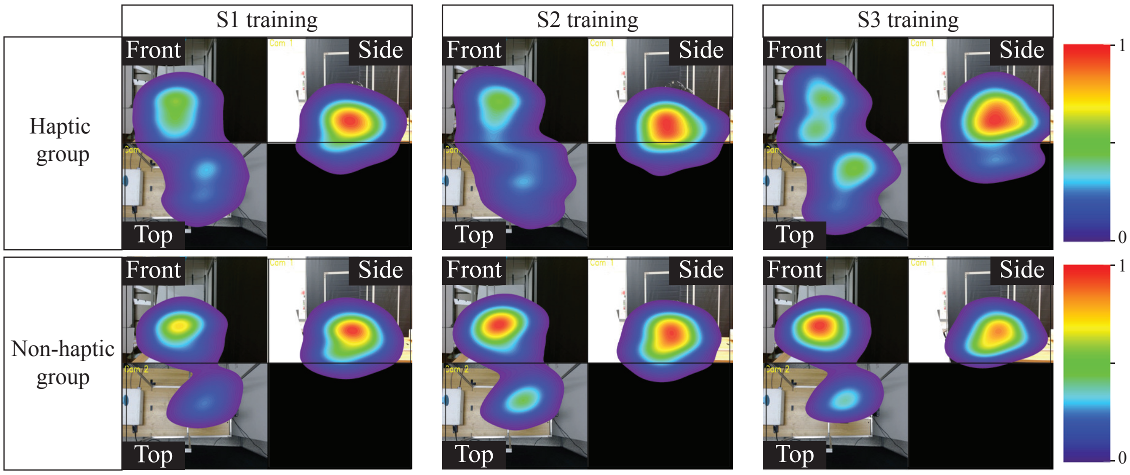

FIGURE 5.13. Spatial distribution of gaze fixation allocation across training sessions. For each session, gaze fixation distributions are shown for three predefined Areas of Interest (AOIs) corresponding to the front, side, and top views of the teleoperation task workspace. Heatmaps represent the normalized density of gaze fixation samples, with red colors indicating higher gaze concentration.

We found that haptic feedback potentiated task performance across outcome metrics, indicating an early advantage at the onset of learning. For example, during the S1 training phase, participants in the haptic group completed the task faster than those in the non haptic group, suggesting that collision cues supported more efficient control from the outset. Importantly, there was no difference between groups at the S1 baseline, indicating comparable initial ability before training. The performance advantage that emerged during S1 training is therefore consistent with haptic feedback supporting early learning by providing immediate collision related information that helped participants correct errors and execute the task more efficiently. These findings align with prior work showing that haptic feedback delivered early in training can facilitate skill acquisition in minimally invasive surgery tasks [**63**]. Across trials in the S1 training phase, participants assigned to the haptic group efficiently performed the task and avoided the collisions. This finding is aligned with previous researches that suggests augmented haptic feedback generally enhances the operator's performance [**75**], [**64**].

However, although both groups acquired skill across the training phases, the haptic group exhibited a lower learning rate than the non haptic group. This pattern is expected because haptic feedback provided an early performance advantage, leaving less room for improvement across subsequent trials. One possible explanation is the Guidance Hypothesis, which proposes that augmented or assistive feedback can improve immediate performance but encourage reliance on the feedback, thereby reducing learning gains when improvement is quantified over practice [**76**], [**77**]. A complementary explanation is that haptic guidance can reduce the opportunity for learners to make and correct errors [**78**]. Because error based learning may be a key driver of motor adaptation, attenuating error experience may limit the adaptation process and, in turn, yield smaller performance gains over practice despite better initial performance [**79**], [**80**], [**81**]. Notably, by the end of the final training phase, both groups converged to a similar performance level, indicating comparable asymptotic completion time. Taken together, these results suggest that haptic collision cues primarily accelerated early task execution rather than increasing the final performance ceiling, and that continued practice reduced the between group difference, yielding comparable asymptotic performance.

Our findings indicate that haptic feedback did not measurably affect generalization of the learned skill to the novel task, as generalization ratios were comparable between groups across probe and testing phases. This may reflect that the collision related haptic cues primarily acted as online guidance during training, improving early performance without producing a lasting change in the underlying control strategy that supports generalization. This interpretation aligns with prior studies reporting that guidance type haptic feedback can improve immediate performance yet provide limited benefits for generalization [**82**], [**83**].

The observed difference in gaze allocation suggests that haptic feedback changed how visual information was used during task execution. Participants in the haptic group relied primarily on a single dominant visual view, whereas participants in the non-haptic group consistently distributed gaze across multiple views. This pattern suggests that haptic feedback may have reduced the need to integrate visual information across views to support task performance. From a multisensory integration perspective, the shift toward a dominant single-view gaze pattern in the haptic group may reflect sensory reweighting, in which task-relevant information is redistributed across modalities based on their reliability. In this context, haptic feedback may have provided information that would otherwise require visual confirmation from multiple viewpoints, allowing participants to rely on one primary visual view while maintaining performance. While the density heatmaps suggest distinct gaze allocation strategies, further analysis may be needed to evaluate whether haptic feedback directly altered visual information requirements or whether the observed patterns arise from differences in movement dynamics and task events that shape where participants look.

Overall, these results suggest that wearable collision related haptic feedback can be an effective tool for improving early teleoperation performance and reducing visual dependence. However, the absence of a generalization advantage indicates that the benefits of this feedback were primarily expressed as immediate performance support rather than a persistent change in generalizable skill. From an application perspective, this distinction matters: haptic collision cues may be most valuable for accelerating early performance and improving safety during practice, whereas additional training strategies may be needed to enhance robustness when task demands or environments change. This still opens an important question: what haptic encoding and training design best promote robust, generalizable skill acquisition. One promising direction is error amplification, in which haptic cues exaggerate task relevant deviations or collisions to increase the salience of errors and drive stronger error based updating. In contrast to guidance type cues that reduce experienced error, error amplification aims to preserve and structure error information, which may improve adaptation and support broader generalization to novel task contexts [**84**].

When taken together, this work established a methodological framework and a visuo haptic assessment battery to evaluate not only whether haptic feedback supports teleoperation performance across learning, short term and long term retention, and generalization, but also how it changes visual reliance and learning dynamics over time. Using this framework, we showed that collision related haptic cues can meaningfully shape teleoperation behavior by improving early performance and reducing reliance on vision during initial skill acquisition. Together, these contributions offer a way to study how haptic information and vision interact during teleoperation training, and they establish a basis for developing haptic encoding methods that support robust skill acquisition while mitigating excessive visual dependence.

References

[1] R. Naik, A. Kogkas, H. Ashrafian, G. Mylonas, and A. Darzi, "The measurement of cognitive workload in surgery using pupil metrics: A systematic review and narrative analysis," *Journal of surgical research*, vol. 280, pp. 258–272, 2022.

[2] T. Bapna, J. Valles, S. Leng, M. Pacilli, and R. M. Nataraja, "Eye-tracking in surgery: a systematic review," *ANZ Journal of Surgery*, vol. 93, no. 11, pp. 2600–2608, 2023.

[3] M. R. Endsley, "Toward a theory of situation awareness in dynamic systems," in *Situational awareness*, pp. 32–64, Routledge, 2017.

[4] H. Alagi, S. E. Navarro, J. Hergenhan, S. Music, and B. Hein, "Teleoperation with tactile feedback based on a capacitive proximity sensor array," in *2020 IEEE International Instrumentation and Measurement Technology Conference (I2MTC)*, pp. 1–6, IEEE, 2020.

[5] J. D. Brown, A. Paek, M. Syed, M. K. O'Malley, P. A. Shewokis, J. L. Contreras-Vidal, A. J. Davis, and R. B. Gillespie, "Understanding the role of haptic feedback in a teleoperated/prosthetic grasp and lift task," in *2013 World Haptics Conference (WHC)*, pp. 271–276, IEEE, 2013.

[6] P. G. De Barros, R. W. Lindeman, and M. O. Ward, "Enhancing robot teleoperator situation awareness and performance using vibro-tactile and graphical feedback," in *2011 IEEE Symposium on 3D User Interfaces (3DUI)*, pp. 47–54, IEEE, 2011.

[7] K. Shamaei, L. H. Kim, and A. M. Okamura, "Design and evaluation of a trilateral shared-control architecture for teleoperated training robots," in *2015 37th Annual International Conference of the IEEE Engineering in Medicine and Biology Society (EMBC)*, pp. 4887–4893, IEEE, 2015.

[8] A. M. Okamura, "Haptic feedback in robot-assisted minimally invasive surgery," *Current Opinion in Urology*, vol. 19, no. 1, pp. 102–107, 2009.

[9] C. Pacchierotti and D. Prattichizzo, “Cutaneous/tactile haptic feedback in robotic teleoperation: Motivation, survey, and perspectives,” *IEEE Transactions on Robotics*, vol. 40, pp. 978–998, 2023.

[10] R. F. Friesen and Y. Vardar, “Perceived realism of virtual textures rendered by a vibrotactile wearable ring display,” *IEEE Transactions on Haptics*, vol. 17, no. 2, pp. 216–226, 2023.

[11] C. Gaudeni, L. Meli, L. A. Jones, and D. Prattichizzo, “Presenting surface features using a haptic ring: A psychophysical study on relocating vibrotactile feedback,” *IEEE Transactions on Haptics*, vol. 12, no. 4, pp. 428–437, 2019.

[12] J. Saint-Aubert, “Identifying tactors locations on the proximal phalanx of the finger for navigation,” in *International Conference on Human Haptic Sensing and Touch Enabled Computer Applications* (I. Nisky, J. Hartcher-O’Brien, M. Wiertlewski, and J. Smeets, eds.), vol. 12272, pp. 42–50, Springer International Publishing, 2020. Series Title: Lecture Notes in Computer Science.

[13] A. Talhan, H. Kim, and S. Jeon, “Tactile ring: Multi-mode finger-worn soft actuator for rich haptic feedback,” *IEEE Access*, vol. 8, pp. 957–966, 2020.

[14] C. De Paz, D. Travieso, J. Ibáñez-Gijón, M. Bravo, L. Lobo, and D. M. Jacobs, “Sensory substitution: The affordance of passability, body-scaled perception, and exploratory movements,” *PLOS ONE*, vol. 14, no. 3, p. e0213342, 2019.

[15] L. H. Favela, M. A. Riley, K. Shockley, and A. Chemero, “Perceptually equivalent judgments made visually and via haptic sensory-substitution devices,” *Ecological Psychology*, vol. 30, no. 4, pp. 326–345, 2018.

[16] G. Desmarais, M. Meade, T. Wells, and M. Nadeau, “Visuo-haptic integration in object identification using novel objects,” *Attention, Perception, & Psychophysics*, vol. 79, no. 8, pp. 2478–2498, 2017.

[17] T. L. Gibo, W. Mugge, and D. A. Abbink, “Trust in haptic assistance: weighting visual and haptic cues based on error history,” *Experimental Brain Research*, vol. 235, no. 8, pp. 2533–2546, 2017.

[18] C. Bozzacchi, R. Volcic, and F. Domini, “Grasping in absence of feedback: systematic biases endure extensive training,” *Experimental Brain Research*, vol. 234, no. 1, pp. 255–265, 2016.

[19] S. Grushko, A. Vysocký, D. Heczko, and Z. Bobovský, “Intuitive spatial tactile feedback for better awareness about robot trajectory during human–robot collaboration,” *Sensors*, vol. 21, no. 17, p. 5748, 2021.

[20] A. H. Rupert, B. D. Lawson, and J. E. Basso, “Tactile situation awareness system: Recent developments for aviation,” in *Proceedings of the Human Factors and Ergonomics Society Annual Meeting*, pp. 722–726, 2016.

[21] M. Zhu, A. H. Memar, A. Gupta, M. Samad, P. Agarwal, Y. Visell, S. J. Keller, and N. Colonnese, “PneuSleeve: In-fabric multimodal actuation and sensing in a soft, compact, and expressive haptic sleeve,” in *Proceedings of the 2020 CHI conference on human factors in computing systems*, pp. 1–12, ACM, 2020.

[22] T. Debus, T. Becker, P. Dupont, T.-J. Jang, and R. D. Howe, “Multichannel vibrotactile display for sensory substitution during teleoperation,” in *Telemanipulator and Telepresence Technologies VIII* (M. R. Stein, ed.), pp. 42–49, 2002.

[23] J. Bimbo, C. Pacchierotti, M. Aggravi, N. Tsagarakis, and D. Prattichizzo, “Teleoperation in cluttered environments using wearable haptic feedback,” in *2017 IEEE/RSJ International Conference on Intelligent Robots and Systems (IROS)*, pp. 3401–3408, IEEE, 2017.

[24] B. Huang, Z. Wang, Q. Cheng, S. Ren, H. Cai, A. A. Valdivia, K. Mahadevan, and D. Wigdor, “AeroHaptix: A wearable vibrotactile feedback system for enhancing collision avoidance in UAV teleoperation,” *IEEE Robotics and Automation Letters*, vol. 10, no. 5, pp. 4260–4267, 2025.

[25] A. Hein and M. Brell, "conTACT - a vibrotactile display for computer aided surgery," in *Second Joint EuroHaptics Conference and Symposium on Haptic Interfaces for Virtual Environment and Teleoperator Systems (WHC'07)*, pp. 531–536, IEEE, 2007.

[26] J. S. Zelek, S. Bromley, D. Asmar, and D. Thompson, "A haptic glove as a tactile-vision sensory substitution for wayfinding," *Journal of Visual Impairment & Blindness*, vol. 97, no. 10, pp. 621–632, 2003.

[27] J. Foottit, D. Brown, S. Marks, and A. M. Connor, "An intuitive tangible game controller," in *Proceedings of the 2014 Conference on Interactive Entertainment*, pp. 1–7, ACM, 2014.

[28] A. Mazzoni and N. Bryan-Kinns, "Mood glove: A haptic wearable prototype system to enhance mood music in film," *Entertainment Computing*, vol. 17, pp. 9–17, 2016.

[29] G. Essick, "Factors affecting direction discrimination of moving tactile stimuli," in *Advances in Psychology*, vol. 127, pp. 1–54, Elsevier, 1998.

[30] O. B. Kaul and M. Rohs, "HapticHead: A spherical vibrotactile grid around the head for 3d guidance in virtual and augmented reality," in *Proceedings of the 2017 CHI Conference on Human Factors in Computing Systems*, pp. 3729–3740, ACM, 2017.

[31] A. Withana, D. Groeger, and J. Steimle, "Tacttoo: A thin and feel-through tattoo for on-skin tactile output," in *Proceedings of the 31st Annual ACM Symposium on User Interface Software and Technology*, pp. 365–378, ACM, 2018.

[32] H. E. Burtt, "Tactual illusions of movement.," *Journal of Experimental Psychology*, vol. 2, no. 5, pp. 371–385, 1917.

[33] C. E. Sherrick and R. Rogers, "Apparent haptic movement," *Perception & Psychophysics*, vol. 1, no. 3, pp. 175–180, 1966.

[34] G. V. Békésy, "Sensations on the skin similar to directional hearing, beats, and harmonics of the ear," *The Journal of the Acoustical Society of America*, vol. 29, no. 4, pp. 489–501, 1957.

[35] G. A. Gescheider, "Cutaneous sound localization.," *Journal of Experimental Psychology*, vol. 70, no. 6, pp. 617–625, 1965.

[36] C. M. Nunez, B. N. Huerta, A. M. Okamura, and H. Culbertson, "Investigating social haptic illusions for tactile stroking (SHIFTS)," in *2020 IEEE Haptics Symposium (HAPTICS)*, pp. 629–636, IEEE, 2020.

[37] A. Israr and I. Poupyrev, "Tactile brush: drawing on skin with a tactile grid display," in *Proceedings of the SIGCHI Conference on Human Factors in Computing Systems*, pp. 2019–2028, ACM, 2011.

[38] J. Raisamo, R. Raisamo, and V. Surakka, "Comparison of saltation, amplitude modulation, and a hybrid method of vibrotactile stimulation," *IEEE Transactions on Haptics*, vol. 6, no. 4, pp. 517–521, 2013.

[39] F. Mancini, A. Bauleo, J. Cole, F. Lui, C. A. Porro, P. Haggard, and G. D. Iannetti, "Whole-body mapping of spatial acuity for pain and touch," *Annals of Neurology*, vol. 75, no. 6, pp. 917–924, 2014.

[40] K. Hale and K. Stanney, "Deriving haptic design guidelines from human physiological, psychophysical, and neurological foundations," *IEEE Computer Graphics and Applications*, vol. 24, no. 2, pp. 33–39, 2004.

[41] A. Gerald, J. Ye, R. Batliwala, P. Hsu, J. Pang, and S. Russo, "Soft optical sensor and haptic feedback system for remote and robot-assisted palpation," in *2023 IEEE/RSJ International Conference on Intelligent Robots and Systems (IROS)*, pp. 5107–5113, IEEE, 2023.

[42] J. Yin, R. Hinchet, H. Shea, and C. Majidi, "Wearable soft technologies for haptic sensing and feedback," *Advanced Functional Materials*, vol. 31, no. 39, p. 2007428, 2021.

[43] T. Maeda, S. Yoshida, T. Murakami, K. Matsuda, T. Tanikawa, and H. Sakai, "Fingeret: A wearable fingerpad-free haptic device for mixed reality," in *Proceedings of the 2022 ACM Symposium on Spatial User Interaction*, pp. 1–10, ACM, 2022.

[44] S. Weinstein, "Intensive and extensive aspects of tactile sensitivity as a function of body part, sex and laterality," in *the First Int'l symp. on the Skin Senses, 1968*, 1968.

[45] R. F. Becker, "The cerebral cortex of man. by wilder penfield and theodore rasmussen. the macmillan company, new york, n.y. 1950. 248 pp," *American Journal of Physical Anthropology*, vol. 11, no. 3, pp. 441–444, 1953.

[46] D. Purves, G. J. Augustine, D. Fitzpatrick, L. C. Katz, A.-S. LaMantia, J. O. McNamara, S. M. Williams, *et al.*, "Mechanoreceptors specialized to receive tactile information," *Neuroscience*, vol. 9, 2001.

[47] S. J. Bolanowski, G. A. Gescheider, R. T. Verrillo, and C. M. Checkosky, "Four channels mediate the mechanical aspects of touch," *The Journal of the Acoustical Society of America*, vol. 84, no. 5, pp. 1680–1694, 1988.

[48] L. A. Jones and N. B. Sarter, "Tactile displays: Guidance for their design and application," *Human Factors: The Journal of the Human Factors and Ergonomics Society*, vol. 50, no. 1, pp. 90–111, 2008.

[49] K. Hoechstetter, A. Rupp, A. Stančák, H.-M. Meinck, C. Stippich, P. Berg, and M. Scherg, "Interaction of tactile input in the human primary and secondary somatosensory cortex—a magnetoencephalographic study," *NeuroImage*, vol. 14, no. 3, pp. 759–767, 2001.

[50] R. O. Duncan and G. M. Boynton, "Tactile hyperacuity thresholds correlate with finger maps in primary somatosensory cortex (s1)," *Cerebral Cortex*, vol. 17, no. 12, pp. 2878–2891, 2007.

[51] J. C. Stevens and K. K. Choo, "Spatial acuity of the body surface over the life span," *Somatosensory & Motor Research*, vol. 13, no. 2, pp. 153–166, 1996.

[52] H. Elsayed, M. Weigel, F. Müller, M. Schmitz, K. Marky, S. Günther, J. Riemann, and M. Mühlhäuser, "VibroMap: Understanding the spacing of vibrotactile actuators across the body," *Proceedings of the ACM on Interactive, Mobile, Wearable and Ubiquitous Technologies*, vol. 4, no. 4, pp. 1–16, 2020.

[53] S. B. Eickhoff, C. Grefkes, K. Zilles, and G. R. Fink, "The somatotopic organization of cytoarchitectonic areas on the human parietal operculum," *Cerebral Cortex*, vol. 17, no. 8, pp. 1800–1811, 2007.

[54] E. Hosseini, R. Fang, R. Zhang, A. Parenteau, S. Hang, S. Rafatirad, C. Hostinar, M. Orooji, and H. Homayoun, "A low cost EDA-based stress detection using machine learning," in *2022 IEEE International Conference on Bioinformatics and Biomedicine (BIBM)*, pp. 2619–2623, IEEE, 2022.

[55] R. Fang, R. Zhang, E. Hosseini, A. M. Parenteau, S. Hang, S. Rafatirad, C. E. Hostinar, M. Orooji, and H. Homayoun, "Prevent over-fitting and redundancy in physiological signal analyses for stress detection," in *2022 IEEE International Conference on Bioinformatics and Biomedicine (BIBM)*, pp. 2585–2588, IEEE, 2022.

[56] J. Liu, H. Homayoun, C. Fang, N. Miao, and H. Wang, "Side channel-assisted inference attacks on machine learning-based ECG classification," in *2023 IEEE/ACM International Conference on Computer Aided Design (ICCAD)*, pp. 1–9, IEEE, 2023.

[57] R. Fang, R. Zhang, E. Hosseini, A. M. Parenteau, S. Hang, S. Rafatirad, C. E. Hostinar, M. Orooji, and H. Homayoun, "Towards generalized ML model in automated physiological arousal computing: A transfer learning-based domain generalization approach," in *2022 IEEE International Conference on Bioinformatics and Biomedicine (BIBM)*, pp. 2577–2584, IEEE, 2022.

[58] X. Guo, B. Zhou, X. Chen, C. Liu, and N. C. Dvornek, "MCP-net: Inter-frame motion correction with patlak regularization for whole-body dynamic PET," in *Medical Image Computing and Computer Assisted Intervention – MICCAI 2022* (L. Wang, Q. Dou, P. T. Fletcher, S. Speidel, and S. Li, eds.), vol. 13434, pp. 163–172, Springer Nature Switzerland, 2022. Series Title: Lecture Notes in Computer Science.

[59] X. Chen, B. Zhou, H. Xie, X. Guo, Q. Liu, A. J. Sinusas, and C. Liu, "Cross-domain iterative network for simultaneous denoising, limited-angle reconstruction, and attenuation correction of cardiac SPECT," in *International Workshop on Machine*

Learning in Medical Imaging (X. Cao, X. Xu, I. Rekik, Z. Cui, and X. Ouyang, eds.), vol. 14348, pp. 12–22, Springer Nature Switzerland, 2023. Series Title: Lecture Notes in Computer Science.

[60] I. El Rassi and J.-M. El Rassi, "A review of haptic feedback in tele-operated robotic surgery," *Journal of Medical Engineering & Technology*, vol. 44, no. 5, pp. 247–254, 2020.

[61] K. Hambuchen, J. Marquez, and T. Fong, "A review of NASA human-robot interaction in space," *Current Robotics Reports*, vol. 2, no. 3, pp. 265–272, 2021.

[62] M. K. Gale, K. Baker-Matsuoka, I. Nisky, and A. M. Okamura, "Effect of performance feedback timing on motor learning for a surgical training task," *IEEE Transactions on Biomedical Engineering*, pp. 1–10, 2025.

[63] M. Zhou, S. Tse, A. Derevianko, D. B. Jones, S. D. Schwaitzberg, and C. G. L. Cao, "Effect of haptic feedback in laparoscopic surgery skill acquisition," *Surgical Endoscopy*, vol. 26, no. 4, pp. 1128–1134, 2012.

[64] C. R. Tercero, Z. Najdovski, S. Ikeda, S. Nahavandi, and T. Fukuda, "Haptic feedback in endovascular tele-surgery simulation through vasculature phantom morphology changes," in *2013 World Haptics Conference (WHC)*, pp. 359–364, IEEE, 2013.

[65] F. K. Nahm, D. Tranel, H. Damasio, and A. R. Damasio, "Cross-modal associations and the human amygdala," *Neuropsychologia*, vol. 31, no. 8, pp. 727–744, 1993.

[66] B. Zheng and C. L. MacKenzie, "Kinematics of reaching and grasping with a tool," in *Proceedings of the Human Factors and Ergonomics Society Annual Meeting*, 2007.

[67] K. Hong, R. Zhang, K. G. Lee, P. R. Young, W. M. Joiner, S. K. Robinson, G. Goncu-Berk, and J. S. Schofield, "A wearable haptic sleeve interface for spaceflight robotic arm operations," in *Companion of the 2024 on ACM International Joint Conference on Pervasive and Ubiquitous Computing*, pp. 318–322, 2024.

[68] J. Pan, S. Chitta, and D. Manocha, "FCL: A general purpose library for collision and proximity queries," in *2012 IEEE International Conference on Robotics and Automation*, pp. 3859–3866, IEEE, 2012.

[69] W. Muellbacher, U. Ziemann, J. Wissel, N. Dang, M. Kofler, S. Facchini, B. Boroojerdi, W. Poewe, and M. Hallett, "Early consolidation in human primary motor cortex," *Nature*, vol. 415, no. 6872, pp. 640–644, 2002.

[70] A. Karni, G. Meyer, C. Rey-Hipolito, P. Jezzard, M. M. Adams, R. Turner, and L. G. Ungerleider, "The acquisition of skilled motor performance: Fast and slow experience-driven changes in primary motor cortex," *Proceedings of the National Academy of Sciences*, vol. 95, no. 3, pp. 861–868, 1998.

[71] S. Balasubramanian, A. Melendez-Calderon, and E. Burdet, "A robust and sensitive metric for quantifying movement smoothness," *IEEE Transactions on Biomedical Engineering*, vol. 59, no. 8, pp. 2126–2136, 2011.

[72] C. M. Carswell, D. Clarke, and W. B. Seales, "Assessing mental workload during laparoscopic surgery," *Surgical Innovation*, vol. 12, no. 1, pp. 80–90, 2005.

[73] D. Stefanidis, R. Haluck, T. Pham, J. B. Dunne, T. Reinke, S. Markley, J. R. Korndorffer, P. Arellano, D. B. Jones, and D. J. Scott, "Construct and face validity and task workload for laparoscopic camera navigation: virtual reality versus videotrainer systems at the SAGES learning center," *Surgical Endoscopy*, vol. 21, no. 7, pp. 1158–1164, 2007.

[74] R. Berguer and W. Smith, "An ergonomic comparison of robotic and laparoscopic technique: The influence of surgeon experience and task complexity," *Journal of Surgical Research*, vol. 134, no. 1, pp. 87–92, 2006.

[75] J. Konstantinova, M. Li, V. Aminzadeh, K. Althoefer, Thrishantha, and P. Dasgupta, "Evaluating manual palpation trajectory patterns in tele-manipulation for soft tissue examination," in *2013 IEEE International Conference on Systems, Man, and Cybernetics*, pp. 4190–4195, IEEE, 2013.

[76] R. A. Schmidt, D. E. Young, S. Swinnen, and D. C. Shapiro, "Summary knowledge of results for skill acquisition: Support for the guidance hypothesis.," *Journal of Experimental Psychology: Learning, Memory, and Cognition*, vol. 15, no. 2, pp. 352–359, 1989.

[77] D. Powell and M. K. O'Malley, "The task-dependent efficacy of shared-control haptic guidance paradigms," *IEEE Transactions on Haptics*, vol. 5, no. 3, pp. 208–219, 2012.

[78] R. Sigrist, G. Rauter, R. Riener, and P. Wolf, "Augmented visual, auditory, haptic, and multimodal feedback in motor learning: A review," *Psychonomic Bulletin & Review*, vol. 20, no. 1, pp. 21–53, 2013.

[79] K. A. Thoroughman and R. Shadmehr, "Learning of action through adaptive combination of motor primitives," *Nature*, vol. 407, no. 6805, pp. 742–747, 2000.

[80] J. L. Patton, M. E. Stoykov, M. Kovic, and F. A. Mussa-Ivaldi, "Evaluation of robotic training forces that either enhance or reduce error in chronic hemiparetic stroke survivors," *Experimental Brain Research*, vol. 168, no. 3, pp. 368–383, 2006.

[81] R. Shadmehr, M. A. Smith, and J. W. Krakauer, "Error correction, sensory prediction, and adaptation in motor control," *Annual Review of Neuroscience*, vol. 33, no. 1, pp. 89–108, 2010.

[82] L. Marchal-Crespo, J. Lopez-Oloriz, L. Jaeger, and R. Riener, "Optimizing learning of a locomotor task: Amplifying errors as needed," in *2014 36th Annual International Conference of the IEEE Engineering in Medicine and Biology Society*, pp. 5304–5307, IEEE, 2014.

[83] L. Marchal-Crespo, L. Michels, L. Jaeger, J. López-Olóriz, and R. Riener, "Effect of error augmentation on brain activation and motor learning of a complex locomotor task," *Frontiers in Neuroscience*, vol. 11, p. 526, 2017.

[84] M.-H. Milot, L. Marchal-Crespo, C. S. Green, S. C. Cramer, and D. J. Reinkensmeyer, "Comparison of error-amplification and haptic-guidance training techniques for learning of a timing-based motor task by healthy individuals," *Experimental Brain Research*, vol. 201, no. 2, pp. 119–131, 2010.

Conclusion and future directions

It has been well established that the dynamic integration of signals from different sensory modalities plays a key role in bodily self-perception [**1**], the movement of oneself in the environment [**2**], and human motor control. Yet there remains significant gaps in a cohesive understanding of how these multisensory processes adapt when sensory cues are degraded or when behavior is performed through human robot interfaces. Further, although haptic feedback can provide distinct yet complementary information to visual information in many of these contexts, it remains unclear how haptic cues should be structured and incorporated to support embodiment, spatial understanding, and skilled control when visual information is limited, unreliable, or cognitively demanding during interaction with the teleoperated robotic systems.

In this dissertation, we show that haptic information is not merely an auxiliary channel that adds sensation, but a functional source of task relevant information. Across chapters, haptic cues support embodiment over non biological limbs, promote spatial understanding through sensory substitution when vision is limited, facilitate complex movement coordination, and shape control strategies for seamless interaction with teleoperated robotic systems.

In **Chapter 2**, we demonstrated that key components of embodiment over an upper limb prosthesis simulator are shaped by sensorimotor conditions and can emerge as distinct yet coherent experiences. Because embodiment is not fixed but modifiable, understanding its dynamics matters for real world prosthesis use: it can influence how naturally a user controls the device, how strongly it is incorporated into the body schema, and whether it is ultimately accepted and used in daily life [**3**], [**4**], [**5**].

Moving forward, it is important to extend this work to cohorts of upper limb prosthesis users to determine how embodiment forms and changes when biological kinesthetic and proprioceptive feedback are absent or altered. Studying prosthesis users will allow us to test whether the relationships observed in controlled sensorimotor conditions generalize to real world prosthesis operation, where sensory uncertainty, compensatory strategies, and long term learning shape daily use. This direction can also clarify which types of supplemental feedback, such as vibrotactile or force related cues, most effectively support agency, ownership, and functional control for individuals with different amputation levels and experience.

In **Chapter 3**, we provided a deeper understanding of how tactile cues cognitively form the spatial representations during navigation task [**6**] and across levels of visual experience (**Chapter 3**). Together, these findings support that effective use of tactile cues depends not only on access to tactile information itself, but also on the user's ability to translate scale, stabilize heading, and update orientation during movement.

Future studies should validate these findings in more realistic navigation contexts more closely alighted with real-world tasks that include path planning, obstacle avoidance, and dynamic environments. A key direction is to test whether tactile cues support not only route following, but also flexible navigation behaviors such as detours and reorientation after disorientation. These studies can also quantify how tactile guidance influences cognitive load and confidence, particularly for visually impaired users, and determine how training improves the efficiency and reliability of tactile based spatial updating. Furthermore, future work should examine how individual factors, including visual history, tactile expertise, and spatial ability, relate to the formation of spatial representations and navigation performance when using tactile cues.

In **Chapter 4**, our investigations highlighted the integration of multiple sensory modalities, including haptic and visual information, and supported the coordinated multiple limb movements. This approach allowed us to characterize robust learning and adaptive multisensory integration effects across multiple sessions.

Future work can extend these findings by explicitly modeling how sensory information is weighted and updated over time using a Bayesian inference framework. Bayesian models would allow estimation of latent sensory weights that reflect the relative reliability of each modality and how these weights evolve with experience [**7**], [**8**]. Such an approach would enable quantitative testing of whether learning is driven by increased trust in haptic cues, reduced dependence on vision, or dynamic reweighting based on task demands and uncertainty. Applying Bayesian sensory integration models could also provide mechanistic insight into individual differences in learning rates and multisensory strategies, particularly in conditions where visual information is degraded or absent.

In **Chapter 5**, we developed wearable vibrotactile haptic interfaces for robotic operations. Using these interfaces, we investigated a structured framework to assess the effects of haptic feedback on teleoperation skill acquisition and validated a visuo-haptic assessment battery to characterize how haptic feedback influences visual allocation. This approach allowed us to elucidate how haptic information shapes skill acquisition and modulates visual dependency during teleoperated task performance.

Future studies should also investigate adaptive haptic feedback systems that modify feedback parameters in real time based on user performance, sensory uncertainty, or inferred cognitive state. Rather than providing static haptic cues, closed-loop systems could adjust intensity, timing, or spatial encoding to optimize learning efficiency and reduce cognitive load. These adaptive approaches may be particularly beneficial for novice users or in environments where visual information is unreliable or constrained. Furthermore, future studies should also incorporate physiological measures of cognitive load, such as pupillometry, to complement behavioral and performance-based metrics. Task-evoked pupil dilation provides a continuous, non-invasive index of cognitive effort and attentional demand, and can be used to assess how haptic feedback alters the cognitive resources required for teleoperation and multisensory coordination [**9**]. Integrating pupillometric measures with visuo-haptic assessment batteries would allow direct testing of whether haptic feedback reduces cognitive load by offloading visual processing, or whether increased performance arises despite elevated cognitive demands during early learning phases.

Taken together, this dissertation demonstrates that haptic information plays a fundamental and functional role in shaping human perception, action, and learning during interaction with both biological and artificial systems. Across multiple experimental contexts, we show that haptic cues are not merely supplemental to vision, but instead serve as a critical modality that can substitute for, complement, and dynamically reshape visual processing depending on task demands and sensory uncertainty. By systematically examining embodiment, spatial navigation, multi-limb coordination, and teleoperated skill acquisition, this work provides converging evidence that effective human–robot interaction depends on how sensory information is structured, integrated, and adapted over time.

References

[1] A. Guterstam, G. Gentile, and H. H. Ehrsson, "The invisible hand illusion: Multisensory integration leads to the embodiment of a discrete volume of empty space," *Journal of Cognitive Neuroscience*, vol. 25, no. 7, pp. 1078–1099, 2013.

[2] D. Mao and Y. Gu, "Multisensory coding of self-motion and its contribution to navigation," *Nature Reviews Neuroscience*, vol. 26, no. 11, pp. 715–732, 2025.

[3] J. Zbinden, E. Lendaro, and M. Ortiz-Catalan, "Prosthetic embodiment: systematic review on definitions, measures, and experimental paradigms," *Journal of NeuroEngineering and Rehabilitation*, vol. 19, no. 1, p. 37, 2022.

[4] J. Zbinden, E. Lendaro, and M. Ortiz-Catalan, "A multi-dimensional framework for prosthetic embodiment: a perspective for translational research," *Journal of NeuroEngineering and Rehabilitation*, vol. 19, no. 1, p. 122, 2022.

[5] J. L. Segil, L. M. Roldan, and E. L. Graczyk, "Measuring embodiment: A review of methods for prosthetic devices," *Frontiers in Neurorobotics*, vol. 16, p. 902162, 2022.

[6] L. Deuker, J. L. Bellmund, T. Navarro Schröder, and C. F. Doeller, "An event map of memory space in the hippocampus," *eLife*, vol. 5, p. e16534, 2016.

[7] D. E. Angelaki, Y. Gu, and G. C. DeAngelis, "Multisensory integration: psychophysics, neurophysiology, and computation," *Current Opinion in Neurobiology*, vol. 19, no. 4, pp. 452–458, 2009.

[8] M. O. Ernst and M. S. Banks, "Humans integrate visual and haptic information in a statistically optimal fashion," *Nature*, vol. 415, no. 6870, pp. 429–433, 2002.

[9] Y. Guo, D. Freer, F. Deligianni, and G.-Z. Yang, "Eye-tracking for performance evaluation and workload estimation in space telerobotic training," *IEEE Transactions on Human-Machine Systems*, vol. 52, no. 1, pp. 1–11, 2021.

Appendix A Embodiment questionnaires

Supplementary Table 1. Embodiment Questionnaires. Rate the following statements on a scale ranging from ”-3” (totally disagree) to ”+3” (totally agree), with ”0” indicating neither agreement nor disagreement (”uncertain”)

Questionnaire Type	Statement
Ownership Questionnaires	1. **I felt as if I was looking at my own hand.**
	2. **I felt as if the prosthetic hand was part of my body.**
	3. **It seemed as if I were sensing the movement of my finger in the location where the prosthetic finger moved.**
	4. **I felt as if the prosthetic hand was my hand.**
Ownership Control Questionnaires	5. **I felt as if my real hand were turning hard/plastic/robotic.**
	6. **It seems as if I had more than one right hand.**
	7. **It appeared as if the prosthetic hand were drifting towards my real hand.**
	8. **It felt as if I had no longer a right hand, as if my right hand had disappeared.**
Agency Questionnaires	9. **The prosthetic hand moved just like I wanted it to, as if it was obeying my will.**
	10. **I felt as if I was controlling the movements of the prosthetic hand.**
	11. **I felt as if I was causing the movement I saw.**
	12. **Whenever I moved my finger I expected the prosthetic finger to move in the same way.**
Agency Control Questionnaires	13. **I felt as if the prosthetic hand was controlling my will.**
	14. **I felt as if the prosthetic hand was controlling my movements.**
	15. **I could sense the movement from somewhere between my real hand and the prosthetic hand.**
	16. **It seemed as if the prosthetic hand had a will of its own.**

Appendix B Chapter 2 Statistical model coefficients

Supplementary Table 1. Estimated model coefficients for the agency response displayed in Figure 2.2 were generated by generalized mixed effect models (GLMMs). Link function between the linear predictor (η) and the expectation of the dependent variable (μ) is $\mu = \eta$ for each response.

Agency

Characteristic	Estimate Coefficient	Std.Error	z-value	p-value
Position				
C	—	—	—	
F	-0.293	0.028	-10.584	<0.001
M	-0.211	0.027	-7.963	<0.001
Activity				
1	—	—	—	
0	-2.374	0.042	-56.647	<0.001
Feedback				
1	—	—	—	
0	-0.344	0.027	-12.895	<0.001
Position * Activity				
F * 0	-0.678	0.054	-12.659	<0.001
M * 0	-1.901	0.067	-28.430	<0.001
Position * Feedback				
F * 0	0.362	0.039	9.294	<0.001
M * 0	0.359	0.038	9.413	<0.001
Fit Results (ANOVA)				
Log-likelihood	-4834.025	BIC	9766.728	
AIC	9692.051	marginal_R2	0.765	

Supplementary Table 2. Estimated model coefficients for the agency control response displayed in Figure 2.2 were generated by generalized mixed effect models (GLMMs). Link function between the linear predictor (η) and the expectation of the dependent variable (μ) is $\mu = \eta$ for each response.

Agency Control

Characteristic	Estimate Coefficient	Std.Error	z-value	p-value
Position				
C	—	—	—	
F	0.077	0.033	2.323	0.02
M	-0.023	0.033	-0.681	0.496
Activity				
1	—	—	—	
0	0.535	0.037	14.285	<0.001
Feedback				
1	—	—	—	
0	0.160	0.033	4.882	<0.001
Position * Activity				
F * 0	-0.233	0.052	-4.453	<0.001
M * 0	-0.264	0.052	-5.107	<0.001
Position * Feedback				
F * 0	-0.253	0.048	-5.291	<0.001
M * 0	-0.058	0.047	-1.232	0.218
Fit Results (ANOVA)				
Log-likelihood	-3025.968	BIC	6150.612	
AIC	6075.935	marginal_R2	0.046	

Supplementary Table 3. Estimated model coefficients for the ownership response displayed in Figure 2.3 were generated by generalized mixed effect models (GLMMs). Link function between the linear predictor (η) and the expectation of the dependent variable (μ) is $\mu = \eta$ for each response.

Ownership

Characteristic	Estimate Coefficient	Std.Error	z-value	p-value
Position				
C	—	—	—	
F	-0.571	0.060	-9.470	<0.001
M	-0.382	0.060	-6.421	<0.001
Activity				
1	—	—	—	
0	-1.321	0.060	-22.085	<0.001
Feedback				
1	—	—	—	
0	-0.265	0.060	-4.383	<0.001
Position * Activity				
F * 0	0.169	0.085	1.997	0.046
M * 0	0.419	0.085	4.934	<0.001
Position * Feedback				
F * 0	0.215	0.084	2.551	0.011
M * 0	0.037	0.087	0.426	0.670
Fit Results (ANOVA)				
Log-likelihood	-4777.620	BIC	9653.918	
AIC	9579.241	marginal_R2	0.208	

Supplementary Table 4. Estimated model coefficients for the ownership control response displayed in Figure 2.3 were generated by generalized mixed effect models (GLMMs). Link function between the linear predictor (η) and the expectation of the dependent variable (μ) is $\mu = \eta$ for each response.

Ownership Control

Characteristic	Estimate Coefficient	Std.Error	z-value	p-value
Position				
C	—	—	—	
F	0.074	0.034	2.190	0.029
M	-0.310	0.035	-8.769	<0.001
Activity				
1	—	—	—	
0	-0.235	0.036	-6.509	<0.001
Feedback				
1	—	—	—	
0	-0.034	0.034	-0.996	0.319
Position * Activity				
F * 0	-0.249	0.050	-4.947	<0.001
M * 0	-0.078	0.051	-1.531	0.126
Position * Feedback				
F * 0	-0.144	0.048	-3.004	0.003
M * 0	0.174	0.048	3.593	<0.001
Fit Results (ANOVA)				
Log-likelihood	-3025.968	BIC	6150.612	
AIC	6075.935	marginal_R2	0.046	

Supplementary Table 5. Estimated model coefficients for the intentional binding response displayed in Figure 2.4 were generated by generalized mixed effect models (GLMMs). Link function between the linear predictor (η) and the expectation of the dependent variable (μ) is $\mu = \eta$ for each response.

Characteristic	Estimate Coefficient	Std.Error	z-value	p-value
Position				
C	—	—	—	
F	15.217	13.024	1.168	0.243
M	-7.126	13.024	-0.547	0.584
Activity				
1	—	—	—	
0	-12.077	13.024	-0.927	0.354
Feedback				
1	—	—	—	
0	-59.058	13.024	-4.535	< 0.001
Position * Activity				
F * 0	-11.715	18.419	-0.636	0.525
M * 0	-1.208	18.419	-0.066	0.948
Position * Feedback				
F * 0	-8.575	18.419	-0.466	0.642
M * 0	8.937	18.419	0.485	0.628
Fit Results (ANOVA)				
Log-likelihood	-24827.710	BIC	49745.874	
AIC	49677.420	marginal_R2	0.024	

Supplementary Table 6. Estimated model coefficients for the peripersonal space response displayed in Figure 2.5 were generated by generalized mixed effect models (GLMMs). Link function between the linear predictor (η) and the expectation of the dependent variable (μ) is $\mu = \eta$ for each response.

Characteristic	Estimate Coefficient	Std.Error	z-value	p-value
Position				
C	—	—	—	
F	3.754	0.185	20.330	<0.001
M	3.230	0.187	17.260	<0.001
Activity				
1	—	—	—	
0	0.131	0.168	0.777	0.437
Feedback				
1	—	—	—	
0	-0.108	0.184	-0.586	0.558
Position * Activity				
F * 0	-0.344	0.263	-1.304	0.192
M * 0	-0.352	0.232	-1.517	0.129
Position * Feedback				
F * 0	-1.251	0.263	-4.757	<0.001
M * 0	-1.178	0.254	-4.645	<0.001
Fit Results (ANOVA)				
Log-likelihood	-9300.979	BIC	18700.635	
AIC	18625.958	marginal_R2	0.130	

Appendix C Modified Bedford Workload Questionnaires

Supplementary Fig 1. Modified Bedford Workload Questionnaires. Rate the following statements on a scale ranging from “1” (a piece of cake) to “10” (adequate performance was impossible).

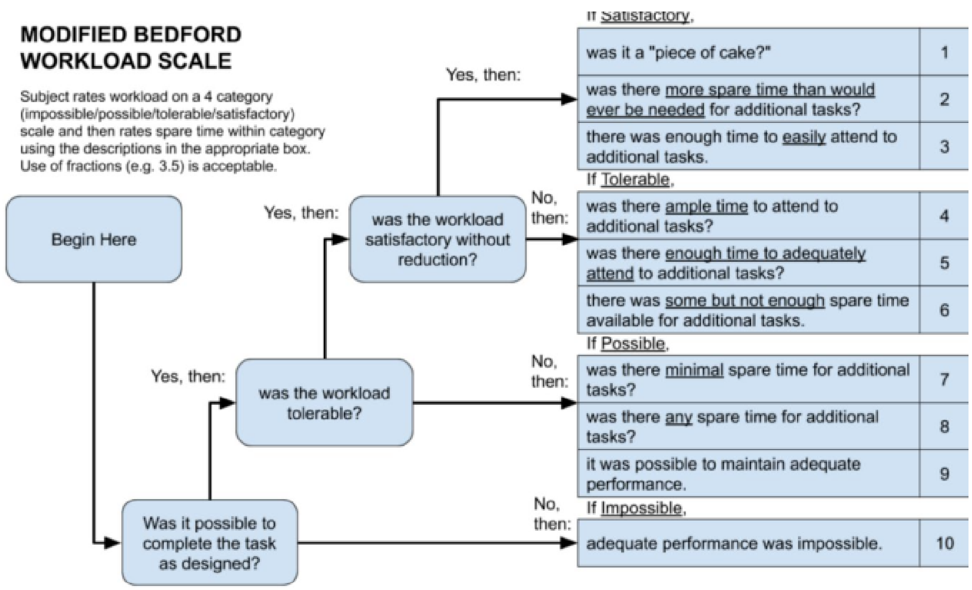

Appendix D Modified Bedford Workload scores

Supplementary Fig 1. Modified Bedford Workload score values across sensory feedback conditions and trials. Median values are plotted, and the whisker extends from the 25th percentile to the 75th percentile of the median Bedford score. Asterisks indicate statistical significance, where $p < 0.05$ (*), $p < 0.01$ (**), and $p < 0.001$ (***).

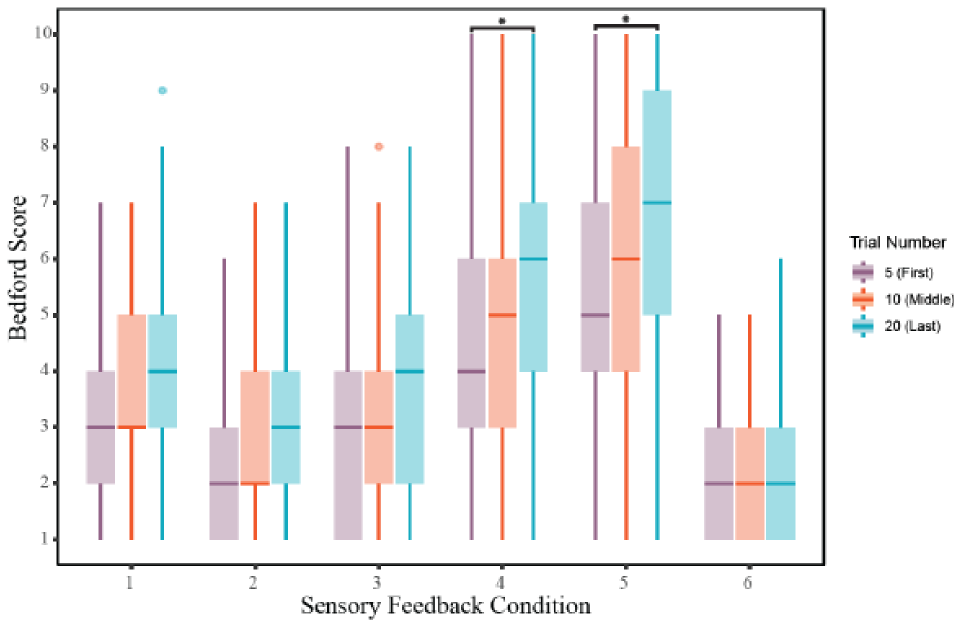

Appendix E Chapter 4 Statistical model coefficients

Supplementary Table 1. Generalized mixed effect models (GLMMs) fit statistics for each response variable (success rates, trial completion time, coordination score, and movement path efficiency)

	AIC	BIC	log Lik.	Degrees of Freedom
Success Rates	3107.1	3184.3	-1542.5	11
Trial Completion Time	80345.5	80593.6	-40136.7	36
Coordination Score	-6394.8	-5994.6	3254.4	57
Movement Path Efficiency	-6304.67	-6125.46	3178.34	26

Supplementary Table 2. Estimated model coefficients for the success response displayed in Figure 4.3 were generated by generalized mixed effect models (GLMMs). Link function between the linear predictor (η) and the expectation of the dependent variable (μ) is $\mu = \eta$ for each response.

Main Effect of Fixed Variables – Success Rate				
Variable	Estimate Coefficient	z-value	Std.Error	p-value
Sensory feedback condition ($\beta_{h=1,2,\ldots5}$)				
1 (β_0)	—			
2 (β_1)	0.70	0.989	0.712	0.3
3 (β_2)	-2.2	-4.86	0.443	<0.001
4 (β_3)	-5.3	-12.4	0.425	<0.001
5 (β_4)	-6.0	-14.2	0.426	<0.001
6 (β_5)	1.8	1.67	1.08	0.095
Session ($B_{s=8,9}$)				
1	—			
2 (β_8)	1.3	11.8	0.110	<0.001
3 (β_9)	2.2	17.8	0.126	<0.001
Control mapping ($\beta_{c=6,7}$)				
Control mapping 1	—			
Control mapping 2 (β_6)	-0.45	-3.80	0.118	<0.001
Control mapping 3 (β_7)	-0.45	-3.89	0.115	<0.001
SD of Random Effects	1.4			

Supplementary Table 3. Estimated model coefficients for the trial completion time response displayed in Figure 4.4 were generated by generalized mixed effect models (GLMMs). Link function between the linear predictor (η) and the expectation of the dependent variable (μ) is $\mu = \eta$ for each response.

Main Effect of Fixed Variables – Trial Completion Time				
Variable	**Estimate Coefficient**	**z-value**	**Std.Error**	**p-value**
Haptic condition ($\beta_{h=1,2,\dots 5}$)				
1	—			
2	-0.29	-9.21	0.032	<0.001
3	0.09	2.94	0.032	0.003
4	0.35	9.80	0.035	<0.001
5	0.58	14.9	0.039	<0.001
6	-0.38	-12.0	0.032	<0.001
Control mapping ($\beta_{c=6,7}$)				
Control mapping 1	—			
Control mapping 2 (β_6)	0.11	3.42	0.033	<0.001
Control mapping 3 (β_7)	0.45	13.8	0.033	<0.001
Session ($B_{s=8,9}$)				
1	—			
2 (β_8)	0.02	0.769	0.032	0.4
3 (β_9)	-0.19	-5.59	0.033	<0.001
Two-way Interaction of Fixed Variables				
Haptic Condition:Control Mapping				
2 * Control mapping 2 ($\beta_{1,6}$)	0.00	-0.118	0.035	>0.9
3 * Control mapping 2 ($\beta_{2,6}$)	-0.09	-2.53	0.035	0.011
4 * Control mapping 2 ($\beta_{3,6}$)	0.18	4.64	0.038	<0.001
5 * Control mapping 2 ($\beta_{4,6}$)	0.08	1.88	0.041	0.060
6 * Control mapping 2 ($\beta_{5,6}$)	-0.02	-0.590	0.035	0.6
2 * Control mapping 3 ($\beta_{1,7}$)	-0.08	-2.17	0.035	0.030
3 * Control mapping 3 ($\beta_{2,7}$)	-0.23	-6.57	0.035	<0.001
4 * Control mapping 3 ($\beta_{3,7}$)	-0.07	-1.71	0.038	0.087
5 * Control mapping 3 ($\beta_{4,7}$)	-0.19	-4.70	0.040	<0.001
6 * Control mapping 3 ($\beta_{5,7}$)	-0.09	-2.56	0.035	0.011
Haptic Condition:Session				
2 * 2 ($\beta_{1,8}$)	0.10	2.82	0.035	0.005
3 * 2 ($\beta_{2,8}$)	-0.05	-1.47	0.035	0.14
4 * 2 ($\beta_{3,8}$)	-0.14	-3.44	0.040	<0.001
5 * 2 ($\beta_{4,8}$)	-0.11	-2.45	0.043	0.014
6 * 2 ($\beta_{5,8}$)	0.09	2.48	0.035	0.013
Main Effect of Fixed Variables – Trial Completion Time				
2 * 3 ($\beta_{1,9}$)	0.16	4.63	0.035	<0.001
3 * 3 ($\beta_{2,9}$)	-0.08	-2.36	0.035	0.018
4 * 3 ($\beta_{3,9}$)	-0.08	-2.01	0.040	0.044
5 * 3 ($\beta_{4,9}$)	-0.03	-0.682	0.042	0.5
6 * 3 ($\beta_{5,9}$)	0.19	5.30	0.035	<0.001
Control Mapping:Session				
Control mapping 2 * 2 ($\beta_{6,8}$)	-0.15	-3.93	0.038	<0.001
Control mapping 3 * 2 ($\beta_{7,8}$)	-0.12	-3.23	0.037	0.001
Control mapping 2 * 3 ($\beta_{6,9}$)	-0.07	-1.78	0.038	0.076
Control mapping 3 * 3 ($\beta_{7,9}$)	-0.17	-4.48	0.037	<0.001
SD of Random Effects		0.18		

Supplementary Table 4. Estimated model coefficients for the coordination score response displayed in Figure 4.5 were generated by generalized mixed effect models (GLMMs). Link function between the linear predictor (η) and the expectation of the dependent variable (μ) is $\mu = \eta$ for each response.

Main Effect of Fixed Variables – Coordination Score				
Variable	**Estimate Coefficient**	**z-value**	**Std.Error**	**p-value**
Haptic condition ($\beta_{h=1,2,\ldots 5}$)				
1	—			
2	0.31	4.08	0.076	< 0.001
3	-0.14	-1.82	0.079	0.069
4	-0.85	-9.84	0.087	< 0.001
5	-1.05	-11.88	0.089	< 0.001
6	0.38	5.01	0.076	< 0.001
Control mapping ($\beta_{c=6,7}$)				
Control mapping 1	—			
Control mapping 2 (β_6)	-0.29	-3.30	0.088	< 0.001
Control mapping 3 (β_7)	-0.71	-8.32	0.086	< 0.001
Session ($B_{s=8,9}$)				
1	—			
2 (β_8)	-0.04	-0.51	0.082	0.609
3 (β_9)	0.10	1.20	0.083	0.229
Two-way Interaction of Fixed Variables				
Haptic Condition:Control Mapping				
2 * Control mapping 2 ($\beta_{1,6}$)	0.15	1.28	0.115	0.199
3 * Control mapping 2 ($\beta_{2,6}$)	0.15	1.26	0.119	0.208
4 * Control mapping 2 ($\beta_{3,6}$)	0.02	0.12	0.131	0.904
5 * Control mapping 2 ($\beta_{4,6}$)	0.15	1.10	0.135	0.27
6 * Control mapping 2 ($\beta_{5,6}$)	0.13	1.16	0.115	0.246
2 * Control mapping 3 ($\beta_{1,7}$)	-0.01	-0.12	0.113	0.905
3 * Control mapping 3 ($\beta_{2,7}$)	0.44	3.81	0.114	< 0.001
4 * Control mapping 3 ($\beta_{3,7}$)	0.42	3.36	0.125	< 0.001
5 * Control mapping 3 ($\beta_{4,7}$)	0.80	6.41	0.124	< 0.001
6 * Control mapping 3 ($\beta_{5,7}$)	0.18	1.59	0.112	0.113
Haptic Condition:Session				
2 * 2 ($\beta_{1,8}$)	-0.10	-0.90	0.109	0.368
3 * 2 ($\beta_{2,8}$)	0.17	1.55	0.111	0.12
4 * 2 ($\beta_{3,8}$)	0.39	3.29	0.120	< 0.001
5 * 2 ($\beta_{4,8}$)	0.38	3.04	0.124	0.002
6 * 2 ($\beta_{5,8}$)	-0.07	-0.62	0.110	0.535
2 * 3 ($\beta_{1,9}$)	-0.18	-1.64	0.110	0.1
3 * 3 ($\beta_{2,9}$)	0.09	0.81	0.112	0.418
4 * 3 ($\beta_{3,9}$)	0.53	4.44	0.119	< 0.001
5 * 3 ($\beta_{4,9}$)	0.54	4.49	0.121	< 0.001

Supplementary Table 4. Estimated model coefficients for the coordination score response displayed in Figure 4.5 were generated by generalized mixed effect models (GLMMs). Link function between the linear predictor (η) and the expectation of the dependent variable (μ) is $\mu = \eta$ for each response.

Main Effect of Fixed Variables – Coordination Score				
Variable	**Estimate Coefficient**	**z-value**	**Std.Error**	**p-value**
6 * 3 ($\beta_{5,9}$)	-0.20	-1.79	0.110	0.074
Control Mapping:Session				
Control mapping 2 * 2 ($\beta_{6,8}$)	0.19	1.52	0.124	0.128
Control mapping 3 * 2 ($\beta_{7,8}$)	0.27	2.18	0.126	0.029
Control mapping 2 * 3 ($\beta_{6,9}$)	0.12	0.98	0.124	0.326
Control mapping 3 * 3 ($\beta_{7,9}$)	0.36	2.91	0.125	0.004
Three-way Interaction of Fixed Variables				
Haptic Condition:Control Mapping:Session				
2 * Control mapping 2 * Session 2 ($\beta_{1,6,8}$)	-0.23	-1.46	0.159	0.144
3 * Control mapping 2 * Session 2 ($\beta_{2,6,8}$)	-0.01	-0.08	0.163	0.939
4 * Control mapping 2 * Session 2 ($\beta_{3,6,8}$)	-0.03	-0.17	0.175	0.864
5 * Control mapping 2 * Session 2 ($\beta_{4,6,8}$)	-0.17	-0.96	0.181	0.336
6 * Control mapping 2 * Session 2 ($\beta_{5,6,8}$)	-0.09	-0.59	0.159	0.552
2 * Control mapping 3 * Session 2 ($\beta_{1,7,8}$)	0.09	0.53	0.161	0.598
3 * Control mapping 3 * Session 2 ($\beta_{2,7,8}$)	-0.28	-1.69	0.163	0.092
4 * Control mapping 3 * Session 2 ($\beta_{3,7,8}$)	-0.62	-3.44	0.179	< 0.001
5 * Control mapping 3 * Session 2 ($\beta_{4,7,8}$)	-0.60	-3.34	0.179	< 0.001
6 * Control mapping 3 * Session 2 ($\beta_{5,7,8}$)	-0.11	-0.67	0.161	0.5
2 * Control mapping 2 * Session 3 ($\beta_{1,6,9}$)	-0.16	-1.02	0.159	0.306
3 * Control mapping 2 * Session 3 ($\beta_{2,6,9}$)	0.07	0.41	0.162	0.682
4 * Control mapping 2 * Session 3 ($\beta_{3,6,9}$)	-0.05	-0.29	0.173	0.769
5 * Control mapping 2 * Session 3 ($\beta_{4,6,9}$)	-0.10	-0.58	0.177	0.561
6 * Control mapping 2 * Session 3 ($\beta_{5,6,9}$)	-0.03	-0.19	0.159	0.853
2 * Control mapping 3 * Session 3 ($\beta_{1,7,9}$)	0.16	1.00	0.161	0.317
3 * Control mapping 3 * Session 3 ($\beta_{2,7,9}$)	-0.18	-1.13	0.162	0.26
4 * Control mapping 3 * Session 3 ($\beta_{3,7,9}$)	-0.47	-2.72	0.173	0.006
5 * Control mapping 3 * Session 3 ($\beta_{4,7,9}$)	-0.78	-4.49	0.174	< 0.001
6 * Control mapping 3 * Session 3 ($\beta_{5,7,9}$)	-0.16	-0.99	0.160	0.322
SD of Random Effects	0.341			

Supplementary Table 5. Estimated model coefficients for the movement path efficiency displayed in Figure 4.7 were generated by generalized mixed effect models (GLMMs). Link function between the linear predictor (η) and the expectation of the dependent variable (μ) is $\mu = \eta$ for each response.

Main Effect of Fixed Variables – Movement Efficiency				
Variable	**Estimate Coefficient**	**z-value**	**Std.Error**	**p-value**
Haptic condition ($\beta_{h=1,2,\dots5}$)				
1	—			
2	0.06	5.39	0.010	<0.001
3	0.05	4.74	0.010	<0.001
4	-0.06	-5.87	0.011	<0.001
5	-0.11	-9.21	0.012	<0.001
6	0.07	7.23	0.010	<0.001
Control mapping ($\beta_{c=6,7}$)				
Control mapping 1	—			
Control mapping 2 (β_6)	-0.06	-4.04	0.014	<0.001
Control mapping 3 (β_7)	-0.18	-13.1	0.013	<0.001
Session ($B_{s=8,9}$)				
1	—			
2 (β_8)	-0.01	-1.47	0.010	0.14
3 (β_9)	0.02	2.06	0.010	0.039
Two-way Interaction of Fixed Variables				
Haptic Condition:Control Mapping				
2 * Control mapping 2 ($\beta_{1,6}$)	-0.01	-0.876	0.015	0.4
3 * Control mapping 2 ($\beta_{2,6}$)	-0.01	-0.963	0.015	0.3
4 * Control mapping 2 ($\beta_{3,6}$)	-0.07	-4.66	0.016	<0.001
5 * Control mapping 2 ($\beta_{4,6}$)	-0.05	-3.17	0.017	0.002
6 * Control mapping 2 ($\beta_{5,6}$)	0.00	-0.084	0.015	>0.9
2 * Control mapping 3 ($\beta_{1,7}$)	0.03	2.13	0.015	0.034
3 * Control mapping 3 ($\beta_{2,7}$)	0.03	1.72	0.015	0.085
4 * Control mapping 3 ($\beta_{3,7}$)	0.04	2.34	0.016	0.019
5 * Control mapping 3 ($\beta_{4,7}$)	0.05	3.01	0.017	0.003
6 * Control mapping 3 ($\beta_{5,7}$)	0.05	3.20	0.015	0.001
Control Mapping:Session				
Control mapping 2 * 2 ($\beta_{6,8}$)	0.04	2.42	0.015	0.016
Control mapping 3 * 2 ($\beta_{7,8}$)	0.04	2.67	0.015	0.008
Control mapping 2 * 3 ($\beta_{6,9}$)	0.04	2.46	0.015	0.014
Control mapping 3 * 3 ($\beta_{7,9}$)	0.06	3.77	0.015	<0.001
SD of Random Effects		0.16		

Appendix F Movement path efficiency

Supplementary Table 1. Movement path efficiency raw statistics summary depending on each sensory feedback condition and each experiment session.

Haptic Condition	Session	Mean	Variance	SD	SE
1	1	0.754	0.033	0.181	0.008
1	2	0.774	0.031	0.177	0.008
1	3	0.829	0.025	0.159	0.007
2	1	0.838	0.021	0.145	0.007
2	2	0.830	0.021	0.146	0.007
2	3	0.871	0.020	0.142	0.007
3	1	0.811	0.023	0.151	0.007
3	2	0.835	0.020	0.143	0.007
3	3	0.867	0.020	0.142	0.007
4	1	0.702	0.053	0.230	0.015
4	2	0.716	0.055	0.235	0.013
4	3	0.745	0.057	0.238	0.012
5	1	0.659	0.051	0.225	0.017
5	2	0.694	0.046	0.213	0.013
5	3	0.710	0.057	0.240	0.013
6	1	0.870	0.018	0.134	0.006
6	2	0.861	0.016	0.125	0.006
6	3	0.892	0.016	0.126	0.006

Appendix G Chapter 4 Correlation matrix

Supplementary Fig 1. Correlation Matrix between Modified Bedford scores and other outcome metrics (Success rates, coordination score, trial completion time, and movement path efficiency). Positive correlation (shown in orange) is closer to +1.0 and negative correlation (shown in blue) is closer to -1.0.

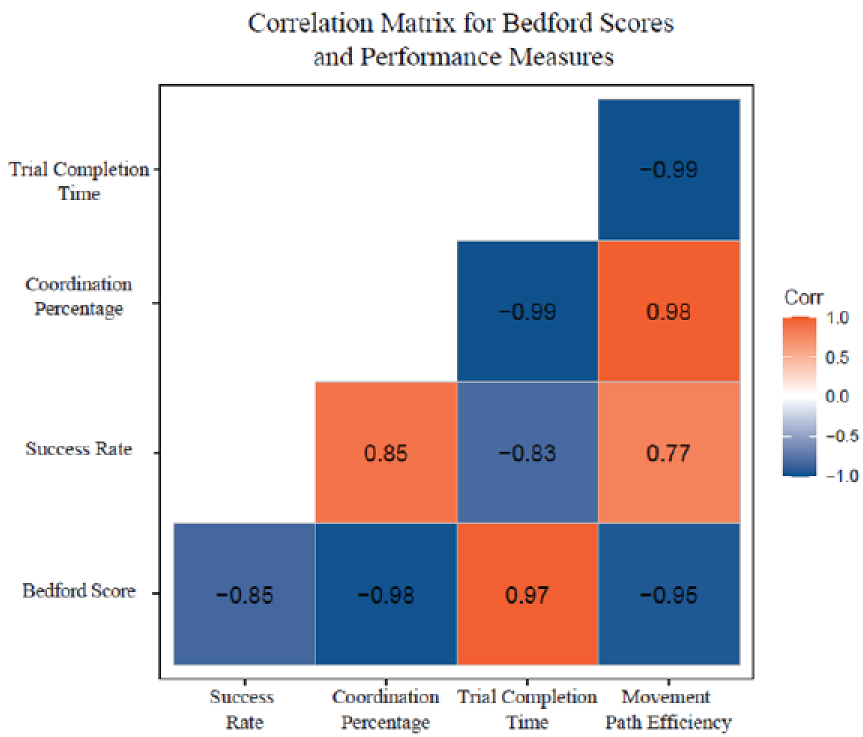

Appendix H NASA Task Load Index

Supplementary Table 1. NASA Task Load Index questionnaires.

NASA Task Load Index

Hart and Staveland's NASA Task Load Index (TLX) method assesses work load on five 7-point scales. Increments of high, medium and low estimates for each point result in 21 gradations on the scales.

Name	Task	Date

Mental Demand — How mentally demanding was the task?

Very Low — Very High

Physical Demand — How physically demanding was the task?

Very Low — Very High

Temporal Demand — How hurried or rushed was the pace of the task?

Very Low — Very High

Performance — How successful were you in accomplishing what you were asked to do?

Perfect — Failure

Effort — How hard did you have to work to accomplish your level of performance?

Very Low — Very High

Frustration — How insecure, discouraged, irritated, stressed, and annoyed wereyou?

Very Low — Very High